Performance recovery of rebar-corroded reinforced concrete beams repaired by cement mortar mixed with recycled nylon fibers from used fishing nets

廃棄漁網からのリサイクルナイロン繊維を混入したモルタル補修材料による鉄筋腐食コンクリートはりの性能回復効果

SRIMAHACHOTA Teeranai

A THESIS SUBMITTED IN PARTIAL FULFILLMENT OF THE REQUIREMENTS FOR THE DEGREE OF THE DOCTOR OF PHILOSOPHY

PhD's Thesis No. EG-xxx

Division of Engineering and Policy for Sustainable Environment

Graduate School of Engineering, Hokkaido University

December 2020

Abstract

Marine ecosystems are deteriorating due to derelict fishing gears (DFG) including fishing nets. Fishing nets that were discarded or lost in the ocean become traps, leading to the deaths to many of marine species especially sea lions, whales and turtles. It is estimated that 705,000 tons of DFG are lost in the ocean and kill more than 380,000 lives annually. It is also reported that entanglement of ships' propellers in DFG causes economic losses over 90 million USD in Korean Sea.

Fishing nets are usually made of very strong and durable materials, such as nylon, high-density polyethylene (HDPE) and polyamide, which are non-biodegradable. Even though many used fishing nets are recycled or utilized, applications of recycled fishing nets are still limited. In addition, recycling fishing nets, especially made of nylon, consumes lots of resources and energy, as well as emits greenhouse gases. Therefore, finding suitable solutions for collecting and recycling fishing nets is an urgent issue to mitigate environmental impact.

This research investigates the application of used fishing nets as reinforcement fibers in cement mortar from the viewpoints of mechanical properties and durability. Two main objectives were appointed, 1) application of recycled nylon fiber from used fishing nets (RN fiber) for the repair of corroded RC beams and 2) long-term durability of the mortar reinforced with the RN fibers subjected to the chloride ion ingress.

Four types of fiber were used as a reinforcing material in polymer cement mortar (PCM): two kinds of RN fiber from used fishing nets, manufactured fibrillated polyethylene (PE) microfiber, and manufactured polyvinyl alcohol (PVA) fiber. Reinforced concrete (RC) beams were placed in the tidal zone for 2 years to induce steel corrosion, then repairs were carried out by spraying PCM reinforced with those fibers on the repair section of the beams. The repairs were taken for the normal RC beams at the end of the exposure period. The upgraded RC beams underwent repair operations before starting the exposure and were not further repaired even after the exposure. Repairability of the RC beams was extensively investigated, such as load-carrying capacities after the repair, failure behavior, stain distributions, cracks formation, and chloride ion penetrability. The effectiveness of the reinforcement with RN fibers was compared with that of PE and PVA fibers. In addition, mechanical properties of the reinforced PCM as well as compatibility of RN fibers under high alkalinity in concrete were also studied.

Experimental results confirmed that RN fibers along with the manufactured PE microfiber and PVA fiber have great potential to be used as reinforcement in cement mortar and for the repair of lightly corroded RC beams. The addition of RN and PVA fibers seems to have no noticeable effect on the flowability of fresh PCM, but the addition of PE fiber results in a considerable reduction of flowability because of its geometry and the surface property.

Adding RN and PVA fibers does not show visible effect on the compressive strength, but the flexural capacity of the PCM is reduced. In contrast, adding PE fibers increases both the compressive and flexural strengths of PCM. It is concluded that fiber reinforcement contributes to post-peak flexural capacity and helps prevent abrupt failure. Flexural capacity of the RC beams that was deteriorated due to the corrosion of tensile rebar can be compensated with the sprayed PCM. The effectiveness of the RN fiber is comparable with that of the PVA fibers but inferior PE microfibers. Adding fibers helps distribute stresses throughout the beam under the bending load. RN fibers helps transfer stresses through wide cracks and spreads the cracks toward the support of the beams. PE fibers prevents severe damage of the beams by distributing damage from a wide crack to many small cracks. It is confirmed that RN fiber is stable under high alkalinity in mortar without any sign of deterioration; however, surface characteristics of RN fiber may cause poor bonding between fibers and mortar substrates.

For the long-term durability, mortar reinforced with RN and PE fibers subjected to chloride ion ingress were evaluated. RN fibers and PE fibers were mixed into ordinary Portland cement (OPC) mortar and PCM. Two groups of specimens were made: non-exposed specimens that were kept in laboratory and the specimens that were exposed to seawater for 3 months and 12 months. Chloride ion diffusion coefficients of non-exposed specimens were also evaluated using chloride migration tests. The spatial distribution of chloride ions, chloride penetration depth and the effective diffusion coefficient of exposed specimens were examined with electron probe microanalyzer (EPMA). Based on the chloride migration test, the effective diffusion coefficient of the reinforced mortar seems to be improved with the addition of RN and PE fibers, but the tendency is still unclear. The type of mortar mix (e.g. OPC or PCM) and water-to-binder ratio are still dominant factors to govern the effective diffusion coefficient of mortar. EPMA analysis results confirm that chloride ion penetration depth and chloride ion profile of exposed specimens are identical regardless of the type of fiber or fiber content. Changes in chloride ions ingress because of the addition of fiber seems to be negligible.

It is concluded that the recycled nylon fiber from used fishing nets tested in this study has been proven effective for reinforcing cementitious materials, and for repairing lightly corroded RC beams. RN fiber has comparable performance to that of the manufactured PVA and PR fibers. Application of recycled fiber for construction materials is a possible way to promote utilizing waste fishing nets.

Acknowledgement

I would like to express my deepest appreciation to Prof. Hiroshi Yokota, the supervisor of Lifetime Engineering laboratory, for his patience, kind supervision, valuable constructive suggestion, and guidance through my study. His supports are great contribution for accomplishing my PhD, also the inspiration for future achievements.

My sincere thanks go to research committee, Prof. Takashi Matsumoto and Prof. Takafumi Sugiyama for their constructive comments and viewpoints on this research. Their questions help pointing out research gaps which will lead to further improvements.

Special thanks go to Dr. Makoto Yamamoto of Sumitomo Osaka Cement Co., Ltd., Japan for supporting research materials. He is a key person for conducting repair operation of RC beams. His advises regarding to the PCM material are highly appreciated.

I would like to extend my sincere thanks to Assoc. Prof. Yoshikasu Akira as well as his students of Kagoshima university for their dedicate work on monitoring corrosion status of the exposed beams. They also support equipment for the on-site repair works.

Dr. Ema Kato and Dr. Yuichiro Kawabata from Port and Airport Research Institute (PARI) are highly appreciated for providing exposure site and consultation regarding to the research.

I very much appreciate supports from all of the Lifetime Engineering lab. members especially Mr. Haruka Matsuura and Mr. Shun Yamaguchi who always helping me conducting experiment as well as assisting my Japanese language in daily life. Thanks to all participants helping me cutting fishing nets for the experiment.

I would like to acknowledge the support from Japan Society for the Promotion of Science (JSPS), Mitsubishi UFJ Trust Bank and Hokkaido University in term of research fundings, scholarships and financial aids during my study.

Last but not least, I would like to thank my family for their support through their hard work back in Thailand. They gave me determination and strength in achieving this success. Finally, there are my friends who gave me sympathy and recognized difficulties in perusing PhD. Their friendships make me having good memories and enjoying life in Sapporo.

List of publications

1. International Journal (Doctoral course)

   (1) Srimahachota, T., Yokota, H. and Akira, Y. Recycled nylon fiber from waste fishing nets as reinforcement in polymer cement mortar for the repair of corroded RC beam, MDPI Materials, issue, page, 2020 (doi:).

   (2) Srimahachota, T., Matsuura, H., Yamaguchi, S. and Yokota, H. Influences of fiber geometries on mechanical behavior of recycled nylon short fiber reinforced mortar, Journal of Asian Concrete Federation, 6(2), 2020. (under review)

2. International Journal (Others)

   (1) Srimahachota, T., Zheng, H., Sato, M., Kanie, S. and Shima, H. Dynamics of washboard road formation driven by a harmonic oscillator, Physical Review E, 96, 062904, 2017 (doi: https://doi.org/10.1103/PhysRevE.96.062904).

3. Conferences (Doctoral course)

   (1) Srimahachota, T., Matsuura, H., Orasutthikul, S. and Yokota, H. Mechanical properties of mortar reinforced with recycled nylon fiber from waste fishing nets, Proceedings of the 7th HU International Doctoral Symposium, Sapporo, Japan, 19-21 November 2018, 2A-06.

   (2) Srimahachota, T., Matsuura, H. and Yokota, H. Mechanical properties of polymer cement mortar reinforced with polyethylene and recycled nylon fibers, Proceeding of the 3rd ACF Symposium on Assessment and Intervention of Existing Structures, Sapporo, Japan, 10-11 September 2019, S3-2-5.

   (3) Yokota, H., Srimahachota, T., Matsuura, H. and Yamaguchi, S. Recycling of waste fishing net as short fibers to reinforce cement mortar, Proceedings of International Conference on Building Materials (ICBM 2019), Hanoi, 31 October - 2 November 2019, 374-381.

   (4) Srimahachota, T., Matsuura, H. and Yokota, H. Mechanical properties of mortar reinforced with recycled nylon fiber from waste fishing nets, Proceeding of the 16th East Asia-Pacific Conference on Structural Engineering and Construction (EASEC 16), Brisbane, Australia, 3-6 December 2019, P035.

   (5) Srimahachota, T., Matsuura, H. and Yokota, H. Effectiveness of recycled nylon short fiber as a reinforcing material for repair of RC beams. Proceeding of the 6th International Conference on Construction Materials (ConMat'20), Fukuoka, Japan, 27-29 August 2020, 858-867.

4. Conferences (Others)

   (1) Ikeda, A., Hashimoto, K., Srimahachota, T., Zheng, H. and Kanie, S. Fundamental study on spontaneous corrugation pattern on dry sand due to moving vehicle. MATEC Web Conf., 258, 05020, 2019 (doi: https://doi.org/10.1051/matecconf/201925805020).

Table of Contents

List of figures

List of tables

CHAPTER 1

INTRODUCTION

1.1 BACKGROUND

Marine ecosystem is suffering from the marinade debris. Derelict fishing gears (DFG) particularly fishing nets that were discarded or lost in the ocean become traps and cause deaths to many of marine species especially sea lions, whales and sea turtles. It is estimated that more than 705,000 tons of DFG were lost in the ocean [1, 2] and more than 380,000 marine lives were killed by DFG annually (Figure 1.1) [3]. Recent studied found that DFG accounts more than 35,000 ton or accounts more than 46% of the plastic wastes in the Great Pacific Garbage Patch [4]. DFG that are dragged along the seafloor by ocean current cause damage to coral reef by tearing their tissues and causing fragmentation [5, 6]. In addition, it was reported that DFG can be navigational thread by causing entanglement to ship's propeller. More than 58,000 cases of entanglement by DFG were reported in Korean seas causing economic losses over 90 million USD [7]. Therefore, collecting and recycling projects for DFG are being implement in many countries.

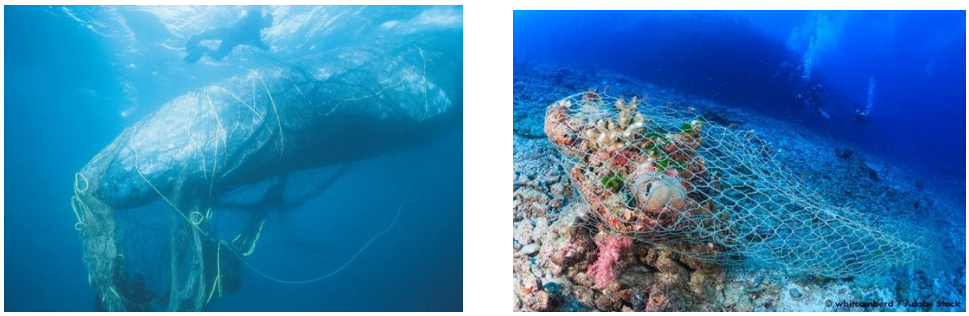

Figure 1.1 (Left) Sperm whale trapped in fishing nets and (Right) fishing nets on coral reef. (source: World Animal Protection)

Fishing nets are usually made of high-density polyethylene (HDPE) or polyamide such as nylon which are very strong and durable materials; therefore, fishing nets are basically non-biodegradable. Waste fishing nets are being recycled in to many product such as textiles, carpets, clothes, sunglasses frame, shoes and accessories (Figure 1.2) [8, 9, 10, 1, 11]. However, recycling those nets, especially nylon, consumed lots of resources and energy, and the recycling processes also emitting greenhouse gases (Figure 1.3) [12, 13]. Therefore, finding suitable recycling solutions for DFG is an urgent issue to mitigate environmental impacts.

Figure 1.2 Adidas's sneaker made from recycled fishing nets.

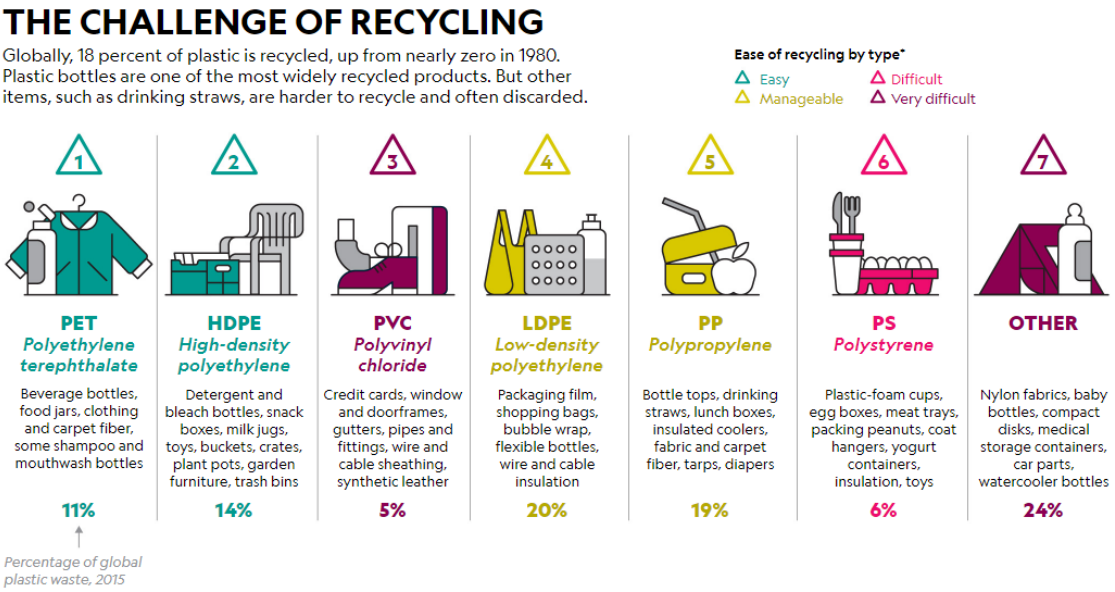

Figure 1.3 Ease of recycling plastics.

1.2 LITERATURE REVIEW

Synthetic fibers along with recycled fibers have long been studied for applying in cementitious materials. Mixing fibers in cementitious materials were found to improve mechanical properties and durability of concrete structures. This section summarized research on the usage of synthetic fibers and recycled fibers in civil engineering applications.

1.2.1 Usage of synthetic fibers in cementitious material

With the growing demand of the synthetic fiber reinforced concrete, several studies were conducted to verify its performance. Zheng and Feldman reviewed the performance of concrete reinforced with several kinds of fibers such as polyethylene (PE), polypropylene (PP), acrylics (PAN), polyviny1 alcohol (PVA), polyamides (PA), aramid, polyester (PES) and carbon reinforcements [14]. They found that those fibers improve water resistance as well as thermal resistance of concrete structures; furthermore, most fibers are durable under high alkaline environment in concrete as shown in Table 1.1.

Zhang and Li studied effect of polypropylene fiber on the durability of concrete composite containing fly ash and silica fume. They found that polypropylene fiber slightly reduced workability of fresh concrete. The freeze-thaw resistance, however, improved with the addition of fiber up to 0.08% by volume since fibers prevent bleeding and trap air inside the mixture [15]. This behavior was confirmed by Ramezanianpour et al. that workability of fresh concrete reduced due to the air trapped into the inner pore. In addition, polypropylene fiber reduced permeability and capillary porosity by pore blocking effect. This pore blocking effect causes less capillary porosity as well as decrease inner conductivity of pores, thus it reduces total charge passed in rapid chloride penetration tests [16]. However, adding too much fiber may increase porosity and lower resistance to ion penetration. Shrinkage cracks in concrete were reduced with the addition of polypropylene fiber especially when longer fiber and smaller diameter of fiber were used [17]. It was also concluded that fibrillated fiber gave better shrinkage control because of better mechanical anchorage between fiber and matrix.

Table 1.1 Durability of fibers for fiber reinforced concrete.

Fiber type	Environmental Durability		Thermal resistance	
	Water resistance	Alkali resistance	Behavior at high temperature	Temp. at which all strength is lost (℃)
Aramid	Good	Good	Progressive loss in tensile strength at 200℃ or higher	400-500
Nylon	Good	Good	Progressive loss in tensile strength at 100℃ or higher	180-200
Polyethylene	Good	Good	Progressive loss in tensile strength at 100℃ or higher	100-130
Polypropylene	Good to fair	Good	Progressive loss in tensile strength at 100℃ or higher	120-150
Polyvinyl Alcohol	Good	Good	Progressive loss in tensile strength at 100℃ or higher	200-240
Pitch-based carbon	Good	Good	Progressive loss in tensile strength at 300-350℃	500-600
PAN-based carbon	Good	Good	Progressive loss in tensile strength at 300-350℃	500-600

PVA fibers were also found to effectively enhance durability of concrete, in particular, the freeze-thaw resistance. The experiment of PVA fibers incorporate with metakaolin concrete showed improvement in compressive strength, splitting tensile strength and toughness, and PVA with the aspect ratio of 45 at 2% volume fraction gave outstanding performance [18]. However, using fiber with higher aspect ratio (e.g. more than 90) may increase micro void in the concrete and reduce compressive strength. It was also reported by Jang et al. that PVA fibers reinforcement enhances the flexural fatigue strength of the concrete under freeze-thaw cycles [19]. The study on the chloride penetration and rebar corrosion confirmed that both PVA and PE reinforcement give a comparable chloride corrosion protection performance in strain-hardening cement composite [20].

Readon et al. performed single fiber pull-out tests on the PVA fiber in mortar composites [21]. They described the pull out mechanism in 3 stages: 1) fiber debonding process where the fiber is stable under the tensile load, 2) the breakage of chemical bond between fiber and matrix where the load suddenly drops, and 3) slippage stage where fiber is hold only by frictional force as described in Figure 1.4 Fiber pull out curve. They concluded that, for PVA fiber, fiber did not rupture during the chemical debonding process but during pull-out due to delamination. Post-cracking response model were constructed for the PVA fibers reinforced concrete subjected to direct tensile strength [22]. The model valid within the fiber fraction up to 3.0% by volume.

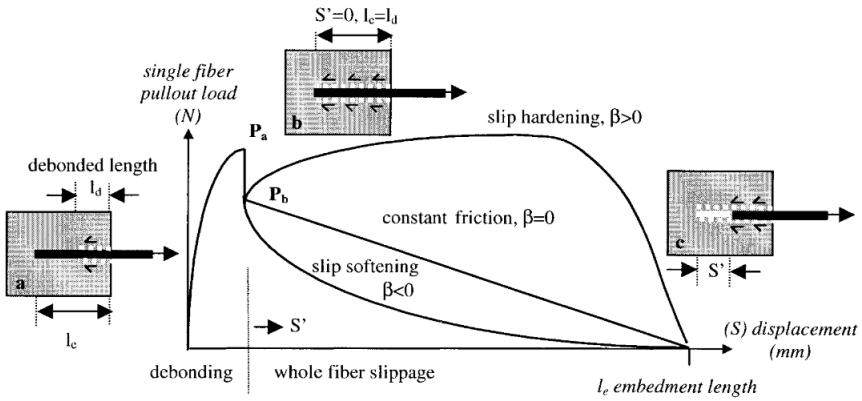

Figure 1.4 Fiber pull out curve.

There are many research conducted on the usage of nylon fibers in cementitious materials. Adding nylon fibers were found to improve both mechanical properties of concrete structures; for instance, compressive strength, splitting tensile strength, toughness. Durability were also improved particularly the reduction of permeability and chloride ion penetrability. The combination of nylon fibers and polypropylene fibers also improved spalling protection for the high-strength concrete under fire since adding fibers provides pore connectivity, so that the melted fibers provide pathway for vapor to escape from the concrete [23]. Adding polypropylene fibers slightly reduced workability which can compensate by adding nylon fibers. In addition, the compressive strength was found to decrease due to the increasing in void in matrix.

On the contrary, some studied found that compressive strength increased with the addition of polypropylene fibers. Lee S. Studied the effect of nylon fibers addition on the recycled aggregate concrete. He concluded that nylon fibers form a network that act as a bridge in cement matrix resulting in the reduction of micro cracks [24]. This crack bridging effect improves compressive strength and the splitting tensile strength of concrete. Nylon fibers also showed superior mechanical performance over the polypropylene fibers in term of compressive strength, splitting tensile strengths, modulus of rupture, and impact resistance due to better fiber distribution. The improvement in compressive strength was due to the fact that fiber prevent further propagation of the microcracks when load applied. During the load application, tensile stresses developed, and fibers tended to debonding. This debonding cracks change the crack propagation path by blunting it. This blunting process reduces crack-tip stress concentration, thus prevent further advance of cracks [25].

1.2.2 Recycled fiber as reinforcing material in cement mortar

The use of waste material in concrete application is being paid attention due to the raising awareness on the environmental issues and the waste management problems, especially plastic waste. Plastic waste such as waste plastic aggregate, Polyethylene terephthalate (PET) bottles light weight aggregate, recycled nylon from waste carpet, plastic fiber from waste PET bottle, manufactured PVA, and recycled HDPE fibers have been studied for applying in cementitious materials. Applying those recycled plastics were found to improve ductility of concrete and provide impact resistance as well as reduce shrinkage cracking. However, there are some reports indicated that bulk density and the compressive strength can be reduced [26].

The study on the mechanical properties of concrete reinforced with recycled HDPE revealed that fibers response to the post-cracking flexural ductility of the concrete [27]. With the addition of recycled HDPE fibers, tensile strength and flexural modulus were improved; moreover, plastic shrinkage cracking, drying shrinkage and water permeability were also reduced. It was proved, through SEM image of the fiber, that recycled HDPE fiber show no sign of chemical depredation in concrete as shown in Figure 1.5.

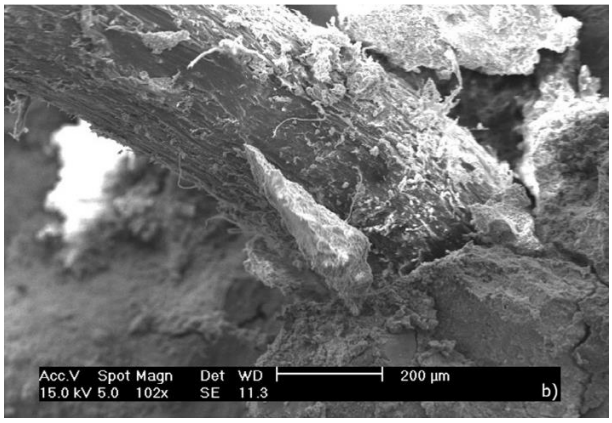

Figure 1.5 SEM image of HDPE fibers after 90 days in concrete.

Yin et al. study reinforcing performance of virgin polypropylene fiber and the recycled polypropylene fiber from the by-product of fiber manufacturing process. Recycled polypropylene fiber expressed a comparable efficiency for reinforcing concrete as a virgin fiber. Polypropylene fibers significantly improved flexural tensile strength and showed excellent post-cracking performance as well as expressed good bonding in concrete. Recycled polypropylene fibers also had good alkaline resistance in concrete environment [28].

Recycled polyethylene terephthalate (R-PET) fibers reinforcement was reported to have high potential usage for reinforcing cementitious materials. Forti Dora studied the R-PET reinforcement in concrete from the recycled PET bottle with 3 types of reinforcement: 1) circular-shapes R-PET (Figure 1.6), half-bottle R-PET (Figure 1.7), and R-PET strips (Figure 1.8). Results showed that, with the addition of fiber, bending capacity was improved. Moreover, R-PET fibers responded to a post-peak capacity of the beam [29]. Adding R-PET fiber seems to have no noticeable effect on the density of concrete as well as the compressive strength, however, fibers may change mortar porosity especially at the interface between fiber and cement matrix [30]. The study of the degradation in R-PET fiber reported a slight degradation on the surface of R-PET fiber in high alkaline environment as seen in Figure 1.9 [31]. Although this degradation had negligible effect on the mechanical properties except the toughness that was decreased with time. This study also confirmed in accordance with [29, 30] that compressive strength as well as modulus of elasticity have negligible affect from the addition of R-PET fiber. Overall, R-PET fibers showed good alkali resistance comparable to other type of fibers such as polypropylene and PVA fibers [32].

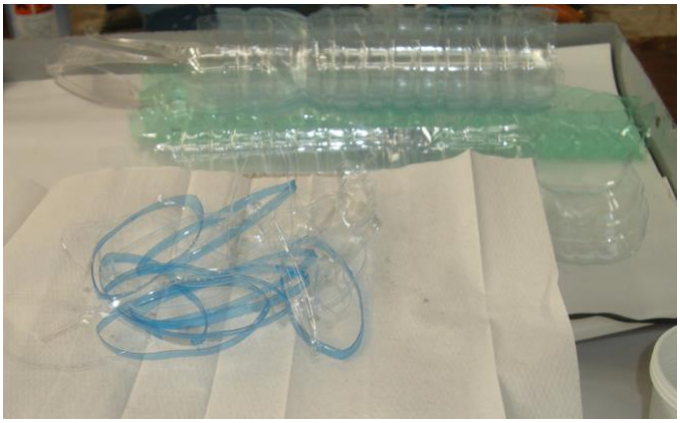

Figure 1.6 Circular R-PET fibers.

Figure 1.7 Half-bottle reinforcement.

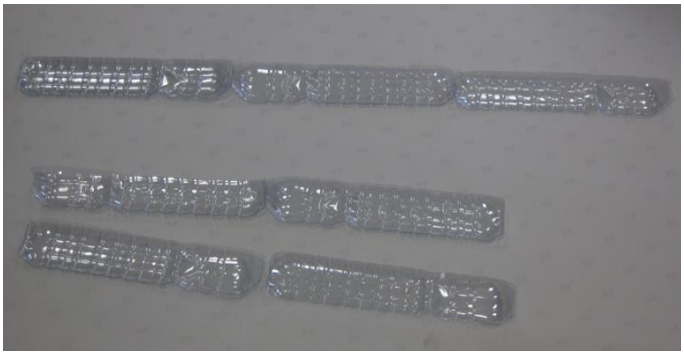

Figure 1.8 R-PET strips.

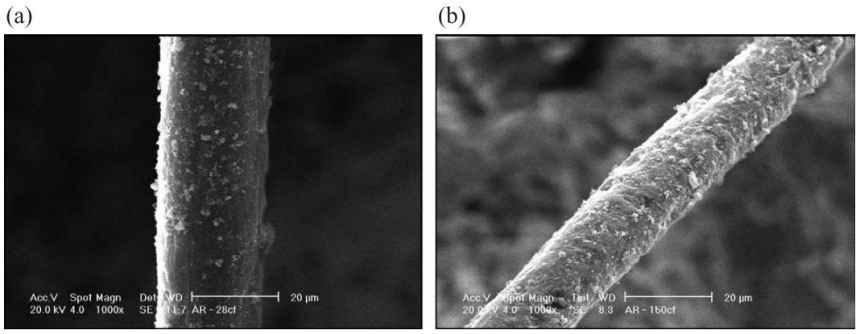

Figure 1.9 SEM image of R-PET fiber under (a) 42 days and (b) 164 days of hydration.

The usage of recycled nylon fibers in cementitious materials are being interested among other recycled fibers due to its excellent durability and abundancy. Ozger et al. conducted experimental studies on the mechanical and thermal properties of recycled nylon fiber from waste carpet. They concluded that fibers played important roles in providing lateral tensile strength and helped postpone or even prevent the enlargement of cracks. Adding fibers seem not to significantly affect the compressive strength and elastic modulus of concrete. They also reported that nylon fibers prevented the spalling of concrete under fire because the glass transition in fiber channels improved thermal strain and became escape part for water vapor [33]. Qin et al. compared the damage performance and compressive behavior of manufactured nylon fibers (NF) and the recycled nylon fabrics fibers (NFF). The recycled nylon fibers were processed by shredding from nylon fabric (Figure 1.10). Experimental results revealed that adding fibers improved integrity of concrete and provide higher compressive energy absorption capacity [34]. They concluded that using recycled fiber gave a comparable damage performance as manufactured fiber; therefore, it is possible to apply recycled nylon fiber in some of engineering applications.

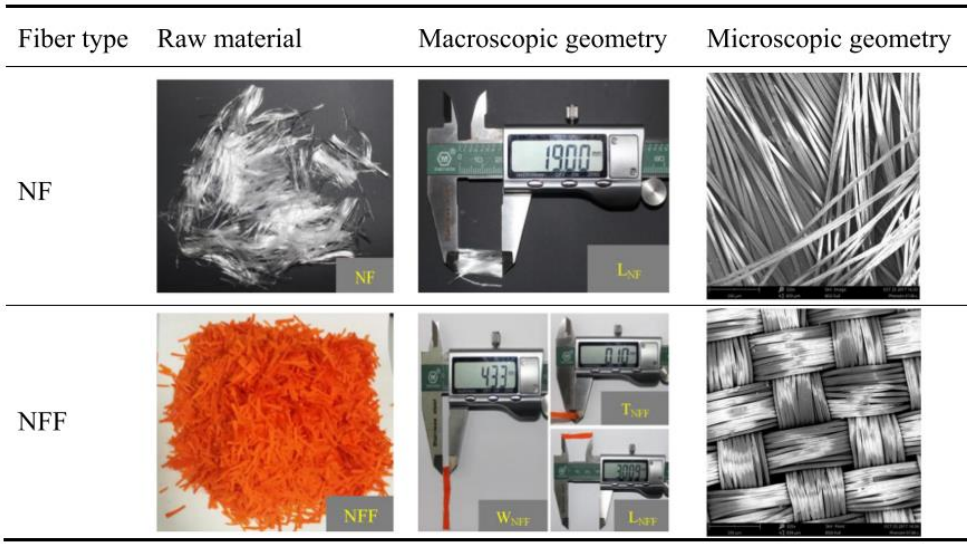

Figure 1.10 Manufactured nylon fiber (NF) and recycled nylon fabric fibers (NFF).

1.2.3 Recycled fiber from waste fishing nets for reinforcing cementitious materials

The expanding in fishery industries and the growing concern of the waste pollution in the ocean make fishing nets are being interested in civil engineering applications. The research conducted on the engineering properties of HDPE fibers between the new and waste fishing nets (Figure 1.11) guaranteed that young's modulus and the ultimate elongation strain remain unchanged; however, tensile strength slightly reduced compared to new HDPE fibers. Alkaline resistivity of the HDPE fibers from waste fishing nets was found to inferior to those of new nets [35, 36].

Figure 1.11 Recycled HDPE fiber from waste fishing nets.

Another type of fishing nets that are widely used is the nylon fishing nets. Orsutthikul et al. conducted experimental studies on the recycled nylon fiber from waste fishing nets for reinforcing cement mortar [37, 38]. They also compared the effectiveness of reinforcement with different fiber geometries and with other types of fiber such as knotted nylon fibers, PVA fibers, recycled embossed PET fibers as shown in Figure 1.12. Results indicated that adding fibers caused the increasing in flexural strength and toughness; however, the reduction in compressive strength was found due to the low Young's modulus of the fibers. Adding fibers also worsen the workability of fresh mortar especially at higher fiber content. They concluded that fibers contribute to ductile failure and respond for the post-peak capacity that the beam can carry some loads after the first crack.

Spadea et al. studied the recycled nylon fibers reinforced cement mortar. The nylon fibers were also obtained from waste fishing nets. Their results confirmed the corresponding mechanical behavior as Orsutthikul et al. [37, 38]. They performed leaching test and alkaline conditioned test, and results confirmed that recycled nylon fibers did not have adverse effect to human or environment according to the limit specified by UNI 10802:2013. The limit values are given in Table1.2. In addition, there is no sign of deterioration of fibers under high alkaline environment in concrete [39]. As a result, recycled nylon fiber from waste fishing nets showed a comparable effectiveness in reinforcing cementitious material to other types of synthetic or recycled fibers.

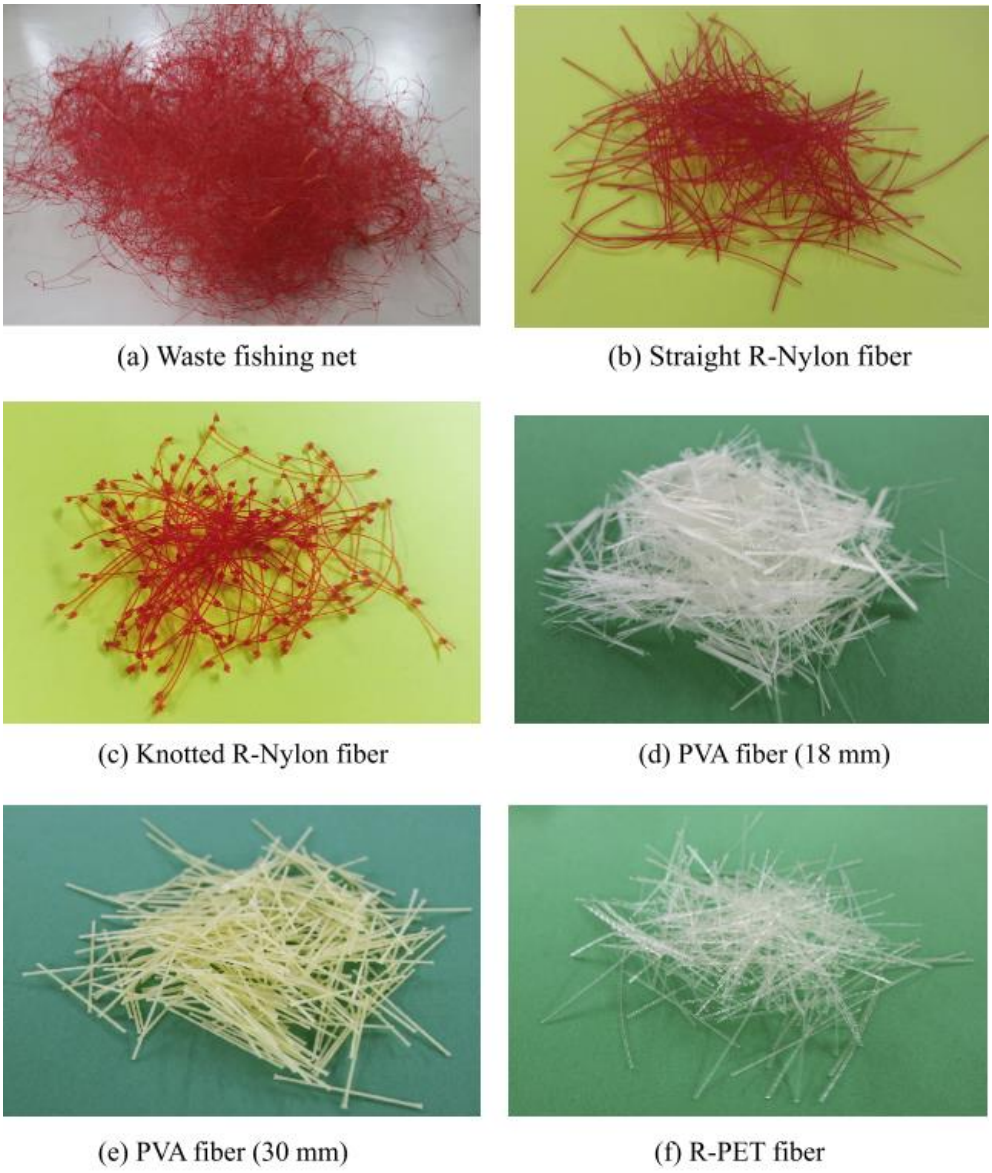

(a) Waste fishing net

(b) Straight R-Nylon fiber

(c) Knotted R-Nylon fiber

(d) PVA fiber (18 mm)

(e) PVA fiber (30 mm)

(f) R-PET fiber

Figure 1.12 Types of fiber.

Table1.2 Leaching test results.

Compound		Current value	Limit value
Nitrate	mg/l	5.9	50
Fluoride Sulfate	mg/l	<0.1	1.5
Sulfate	mg/l	3.6	250
Chloride	mg/l	2.2	100
Cyanide	mg/l	<0.1	50
Barium	mg/l	<0.1	1
Copper	mg/l	<0.01	0.05
Zinc	mg/l	<0.1	3
Beryllium	µg/l	<0.1	10
Cobalt	µg/l	<0.1	250
Nickel	µg/l	0.3	10
Vanadium	µg/l	<0.1	250
Arsenic	µg/l	<0.1	50
Cadmium	µg/l	<0.1	5
Chromium	µg/l	0.3	50
Lead	µg/l	0.2	50
Selenium	µg/l	<0.1	10
Mercury	µg/l	<0.1	1
Asbestos	mg/l	<0.01	30
COD	mg/l	12.6	30
PH	-	8.2	>5.5 < 12.0

1.3 PROBLEM STATEMENTS

The study on the recycled nylon fiber from waste fishing nets for reinforcing cement mortar comes from various issues:

1. There is a strong call for finding suitable recycling solutions for the waste fishing nets to mitigate environmental impacts.
2. The mechanical behavior of the recycled fiber reinforced concrete is still unclear, especially recycled fiber from waste fishing nets.
3. Most researched conducted on the mechanical properties of the fiber reinforced concrete. Only a few studies focus on long-term durability.
4. The increasing in deteriorated concrete structures provides a strong interest in the application of recycled fiber for the repair of concrete structure.

1.4 RESEARCH OBJECTIVES

This research provides extensive studies on the used recycled nylon fiber from waste fishing nets as a reinforcing material in cementitious materials. Application of fibers for the repair of corroded RC beams and durability are studied. There are 2 main objectives for this research as described below:

1. To study the application of recycled nylon fiber from waste fishing nets as reinforcement in polymer cement mortar for the repair of corroded reinforced concrete (RC) beams.

   In this study, recycled nylon short fibers (RN) from waste fishing nets were added into polymer cement mortar (PCM). RC beams were placed in tidal current for the duration of 1 and 2 years to induce steel corrosion. The PCM mixed with RN was used for spraying on the repair section of the steel corroded RC beams. The effectiveness of the reinforced PCM was extensively investigated; for instance, load-carrying capacity of the beams before and after the repair, failure behavior, stain distributions, cracks formations, and the chloride ion penetrability. The effectiveness of the reinforcement with RN fibers were compared with the manufactured polyethylene (PE) microfibers and polyvinyl alcohol (PVA) short fibers. In addition, deterioration of RN fibers was examined after the experiment to verify compatibility of RN fibers under high alkalinity in concrete.

2. To study the durability of the mortar reinforced with the RN fibers subjected to the chloride ion ingression.

   In this study, RN fibers and PE fibers were mixed into cement mortar and the PCM to study long-term durability focusing on the chloride ion ingression. This study aims to examine particularly, the chloride ion diffusion coefficient, chloride ion penetration depth after the exposure and spatial distribution of chloride ion in matrix. Two analysis were conducted, 1) effective diffusion coefficient by migration and 2) chloride ion penetrability under seawater exposure by electron probe micro analyzer (EPMA). Chloride ion resistivity of mortar reinforced with RN fiber were then compared with that of the manufactured PE.

1.5 THESIS STRUCTURE

This thesis divided into 6 chapters. Starting from introduction as the first chapter, then following by chapter two to five for the experimental woks, and the final chapter, chapter six, for the conclusions. Outline of the research are shown in Figure 1.13. Details of each chapter are described below:

Chapter 1 gives the background of the research which state the environmental issues and describe the importance of utilizing waste fishing nets. Literature review section summarizes past research based on synthetic fiber reinforced concrete, recycled fiber reinforced concrete, and the usage of recycled fibers from waste fishing nets. Problem statements and research objectives are described here.

Chapter 2 provides comprehensive studies on the application of the recycled nylon fiber from waste fishing nets as reinforcement in polymer cement mortar (PCM) for the repair of corroded RC beams. This chapter explains experimental works on the repair of corroded RC beams subjected to natural corrosion. This chapter mainly focusing on the tested RC beams having 1 year of neural exposure. Fibers used in this test are RN fibers and PE fibers which is added into PCM for the reinforcement. Mechanical performance of the PCM material and the repaired RC beams are examined. Effectiveness of the repair with respect to different fiber reinforcements are evaluated and discussed.

Chapter 3 used the same experimental procedure as that in Chapter 2 with some modification. However, Chapter 3 focuses on the tested beams having 2 years of natural exposure. Four kinds of fiber were used as a reinforcement in PCM which are RN fibers having diameter of 0.24 mm, RN fibers having diameter of 0.52 mm, manufactured polyvinyl alcohol (PVA) fibers and PE fibers. Flowability, compressive and flexural strength as well as cracks propagation of reinforced PCM were investigated. The RC beams were repaired in the same manner as in Chapter 2, but only the load-carrying capacity of the repaired beams were evaluated.

Chapter 4 investigates the effective diffusion coefficient of chloride ion in mortar and PCM that were reinforced with RN and PE fibers by chloride migration test. Effective diffusion coefficient of chloride ion is calculated and compared between different mixes. In addition, this chapter also discusses the characteristics of the reinforced mortar such as flowability and compressive strength.

Chapter 5 studies the chloride ion penetrability of mortar reinforced with RN and PE fibers. Testing cube specimens were sprayed with seawater for 3 months and 1 years. Chloride ion penetrability of the reinforced mortar subjected to seawater exposure are examined and discussed, for instance, spatial distribution of chloride ion, and chloride ion profile. Electron probe micro-analyzer (EPMA) technique was used in this study.

Chapter 6 summarizes findings from this research. Conclusions were drawn according to each experimental works as well as recommendations and future potentials for future works.

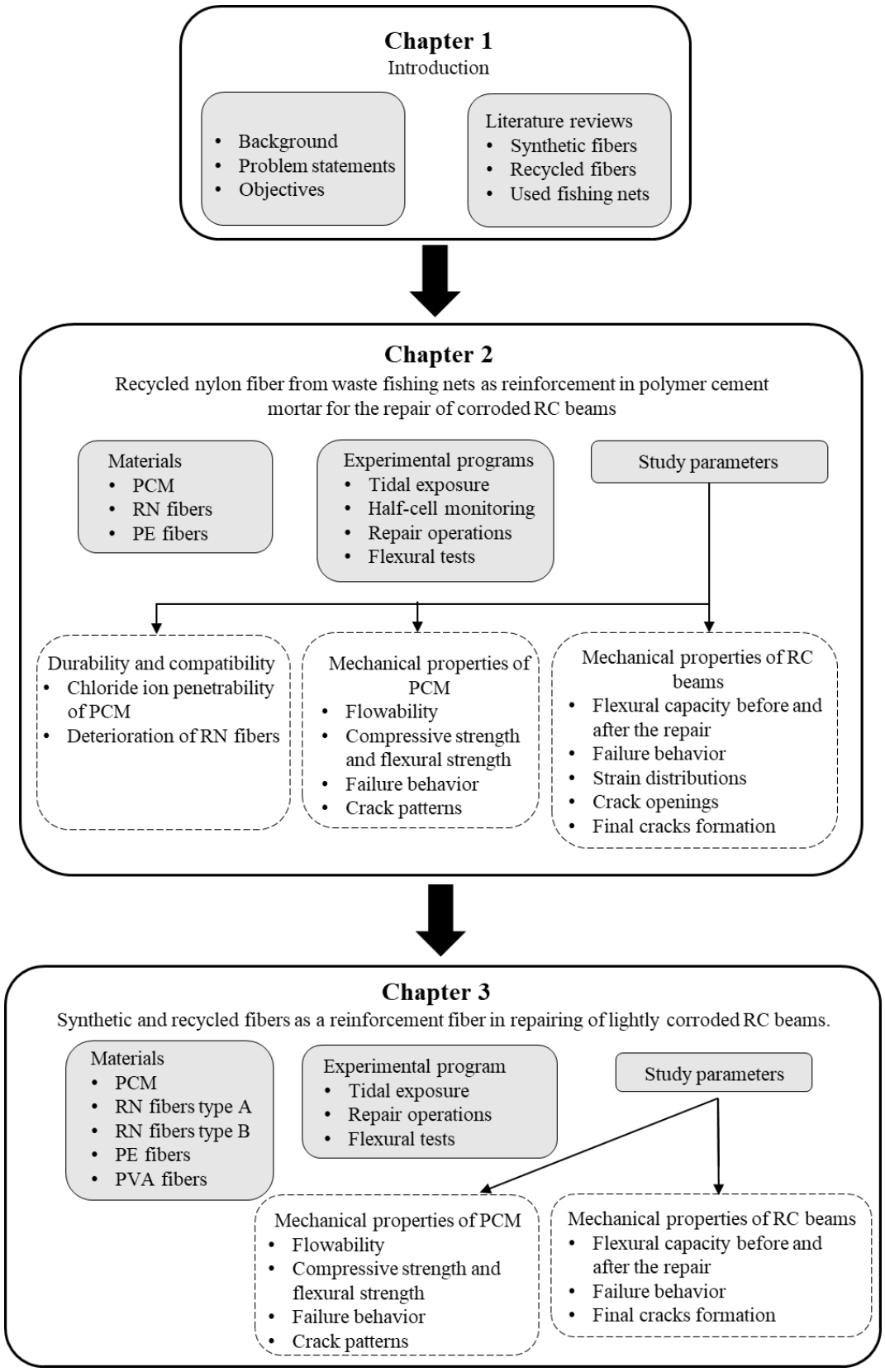

Figure 1.13 Outline of the research.

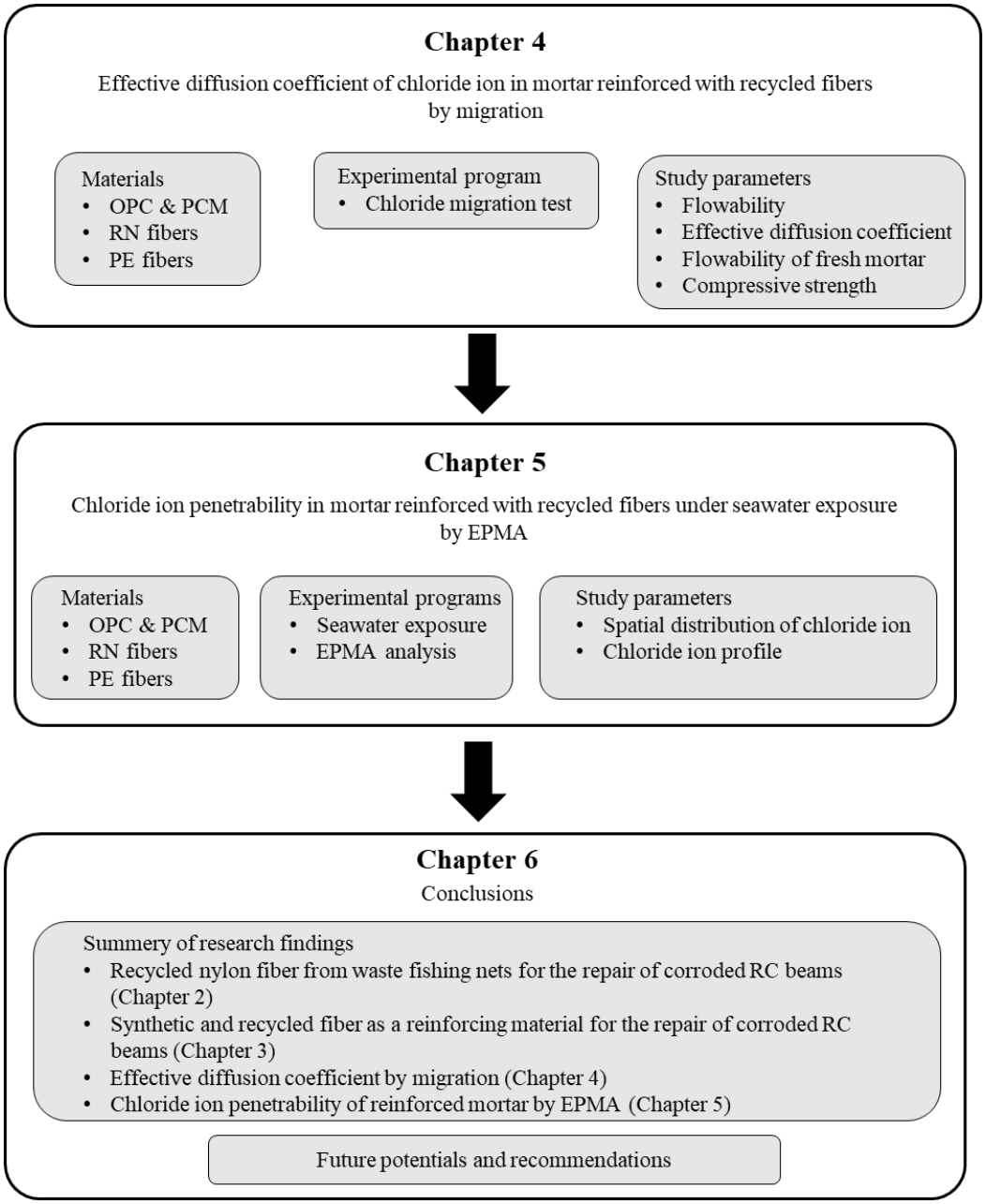

Figure 1.13 Outline of the research (Cont.).

1.6 REFERENCES

[1] L. Parker, "National Geographics," 2018. [Online]. Available: https://www.nationalgeographic.com/news/2018/06/heather-koldeway-explorer-nets-plastic-philippines-ocean-culture/. [Accessed 29 April 2020].

[2] E. Gilman, F. Chopin, P. Suuronen and B. Kuemlagen, "Abandoned, lost or otherwise discarded fishing gear: Methods to estimate ghost fishing mortality, and the status of regional monitoring and management," Food and Agriculture Organization of the United Nations, Rome, 2016.

[3] "Ocean Voyages Institute," 25 June 2019. [Online]. Available: https://www.oceanvoyagesinstitute.org/. [Accessed 29 April 2020].

[4] L. Lebreton, B. Slat, F. Ferrari, B. Sainte-Rose, J. Aitken, R. Marthouse, S. Hajbane, S. Cunsolo, A. Schwarz, A. Levivier, K. Noble, P. Debeljak, H. Maral, R. Schoeneich-Argent, R. Brambini and J. Reisser, "Evidence that the Great Pacific Garbage Patch is rapidly accumulating plastic," *Scientific Reports,* vol. 8, no. 1, pp. 1-15, 2018.

[5] "Waste Wise Products inc.," 30 July 2019. [Online]. Available: https://www.wastewiseproductsinc.com/blog/plastic-pollution/recycling-developments-in-the-fishing-industry/. [Accessed 29 April 2020].

[6] L. Valderrama Ballesteros, J. . L. Matthews and B. W. Hoeksema, "Pollution and coral damage caused by derelict fishing gear on coral reefs around Koh Tao, Gulf of Thailand," *Marine Pollution Bulletin,* vol. 135, no. March, pp. 1107-1116, 2018.

[7] S. Hong, J. Lee and S. Lim, "Navigational threats by derelict fishing gear to navy ships in the Korean seas," *Marine Pollution Bulletin,* vol. 119, no. 2, pp. 100-105, 2017.

[8] M. Charter, R. Carruthers and S. Femmer Jensen, "Products from Waste Fishing Nets Accessories, Clothing, Footwear, Home Ware, Recreation," Circular Ocean, 2018.

[9] Dovas, "Bored Panda," 2016. [Online]. Available: https://www.boredpanda.com/recycled-fish-net-ocean-trash-sneakers-adidas/?utm_source=google&utm_medium=organic&utm_campaign=organic. [Accessed 29 april 2020].

[10] "Patagonia," [Online]. Available: https://www.patagonia.com/our-footprint/recycled-nylon.html. [Accessed 29 April 2020].

[11] Y. Wang, "Fiber and textile waste Utilization," *Waste and Biomass Valorization,* vol. 1, no. 1, pp. 135-143, 2010.

[12] A. Stolte and F. Schneider, "Recycling options for Derelict Fishing Gear," MARELITT Baltic project, 2018.

[13] L. Parker, "National Geographics," June 2018. [Online]. Available: https://www.nationalgeographic.com/magazine/2018/06/plastic-planet-waste-pollution-trash-crisis/. [Accessed 29 April 2020].

[14] Z. Zheng and D. Feldman, "Synthetic Fibre-reinforced Concrete," *Progress in Polymer Science,* vol. 20, pp. 185-210, 1992.

[15] P. Zhang and Q. F. Li, "Effect of polypropylene fiber on durability of concrete composite containing fly ash and silica fume," *Composites Part B: Engineering,* vol. 45, no. 1, pp. 1587-1594, 2013.

[16] A. A. Ramezanianpour, M. Esmaeili, S. A. Ghahari and M. H. Najafi, "Laboratory study on the effect of polypropylene fiber on durability, and physical and mechanical characteristic of concrete for application in sleepers," *Construction and Building Materials,* vol. 44, pp. 411-418, 2013.

[17] N. Banthia and R. Gupta, "Influence of polypropylene fiber geometry on plastic shrinkage cracking in concrete," *Cement and Concrete Research,* vol. 36, no. 7, pp. 1263-1267, 2006.

[18] M. F. Nuruddin, S. U. Khan, N. Shafiq and A. Tehmina, "Strength development of concrete incorporating metakaolin and PVA fibres," *Applied Mechanics and Materials,* vol. 567, pp. 505-510, 2014.

[19] J. G. Jang, H. K. Kim, T. S. Kim, B. J. Min and H. K. Lee, "Improved flexural fatigue resistance of PVA fiber-reinforced concrete subjected to freezing and thawing cycles," *Construction and Building Materials,* vol. 59, pp. 129-135, 2014.

[20] K. Kobayashi, M. Suzuki, L. A. Dung, H. d. Yun and K. Rokugo, "The effects of PE and PVA fiber and water cement ratio on chloride penetration and rebar corrosion protection performance of cracked SHCC," *Construction and Building Materials,* vol. 178, pp. 372-383, 2018.

[21] C. Redon, V. C. Li, C. Wu, H. Hoshiro, T. Saito and A. Ogawa, "Measuring and modifying interface properties of PVA fibers in ECC matrix," *Journal of Materials in Civil Engineering,* vol. 13, no. 6, pp. 399-406, 2001.

[22] S. U. Khan and T. Ayub, "Modelling of the pre and post-cracking response of the PVA fibre reinforced concrete subjected to direct tension," *Construction and Building Materials,* vol. 120, pp. 540-577, 2016.

[23] G. Lee, D. Han, M. C. Han, C. G. Han and H. J. Son, "Combining polypropylene and nylon fibers to optimize fiber addition for spalling protection of high-strength concrete," *Construction and Building Materials,* vol. 34, pp. 313-320, 2012.

[24] S. Lee, "Effect of Nylon Fiber Addition on the Performance of Recycled Aggregate Concrete," *Applied Sciences,* vol. 9, no. 4, p. 767, 2019.

[25] P. S. Song, S. Hwang and B. C. Sheu, "Strength properties of nylon- and polypropylene-fiber-reinforced concretes," *Cement and Concrete Research,* vol. 35, no. 8, pp. 1546-1550, 2005.

[26] R. Siddique, J. Khatib and I. Kaur, "Use of recycled plastic in concrete: A review," *Waste Management,* vol. 28, no. 10, pp. 1835-1852, 2008.

[27] N. Pešić, S. Živanović, R. Garcia and P. Papastergiou, "Mechanical properties of concrete reinforced with recycled HDPE plastic fibres," *Construction and Building Materials,* vol. 115, pp. 362-370, 2016.

[28] S. Yin, R. Tuladhar, J. Riella, D. Chung, T. Collister, M. Combe and N. Sivakugan, "Comparative evaluation of virgin and recycled polypropylene fibre reinforced concrete," *Construction and Building Materials,* vol. 114, pp. 134-141, 2016.

[29] D. Foti, "Use of recycled waste pet bottles fibers for the reinforcement of concrete," *Composite Structures*, vol. 96, pp. 396-404, 2013.

[30] L. A. Pereira De Oliveira and J. P. Castro-Gomes, "Physical and mechanical behaviour of recycled PET fibre reinforced mortar," *Construction and Building Materials*, vol. 25, no. 4, pp. 1712-1717, 2011.

[31] D. A. Silva, A. M. Betioli, P. J. Gleize, H. R. Roman, L. A. Gómez and J. L. Ribeiro, "Degradation of recycled PET fibers in Portland cement-based materials," *Cement and Concrete Research*, vol. 35, no. 9, pp. 1741-1746, 2005.

[32] F. Fraternali, I. Farina, C. Polzone, E. Pagliuca and L. Feo, "On the use of R-PET strips for the reinforcement of cement mortars," *Composites Part B: Engineering*, vol. 46, pp. 207-210, 2013.

[33] O. B. Ozger, F. Girardi, G. M. Giannuzzi, V. A. Salomoni, C. E. Majorana, L. Fambri, N. Baldassino and R. Di Maggio, "Effect of nylon fibres on mechanical and thermal properties of hardened concrete for energy storage systems," *Materials and Design*, vol. 51, pp. 989-997, 2013.

[34] Y. Qin, X. Zhang and J. Chai, "Damage performance and compressive behavior of early-age green concrete with recycled nylon fiber fabric under an axial load," *Construction and Building Materials*, vol. 209, pp. 105-114, 2019.

[35] I. Maria, G. Bertelsen and L. M. Ottosen, "Engineering properties of fibres from waste fishing nets Materials, Systems and Structures in Civil Engineering Circular Ocean," in *International RILEM Conference on Materials*, Lyngby, 2016.

[36] I. Bertelsen and L. M. Ottosen, "Reuse of Waste Fishing Nets in Construction Materials," in *Circular Ocean Conference*, Ålesund, 2016.

[37] S. Orasutthikul, D. Unno and H. Yokota, "Effectiveness of recycled nylon fiber from waste fishing net with respect to fiber reinforced mortar," *Construction and Building Materials*, vol. 146, pp. 594-602, 2017.

[38] S. Orasutthikul, D. Unno, H. Yokota and K. Hashimoto, "Effectiveness of recycled nylon fibers as reinforcing material in mortar," *Journal of Asian Concrete Federation*, vol. 2, no. 2, p. 102, 2017.

[39] S. Spadea, I. Farina, A. Carrafiello and F. Fraternali, "Recycled nylon fibers as cement mortar reinforcement," *Construction and Building Materials*, vol. 80, pp. 200-209, 2015.

CHAPTER 2

RECYCLED NYLON FIBER FROM USED FISHING NETS AS REINFORCEMENT IN POLYMER CEMENT MORTAR FOR THE REPAIR OF CORRODED RC BEAMS

2.1 OUTLINE

This chapter provides a comprehensive investigation on the application of recycled nylon fiber from waste fishing nets for the repair of corroded RC beams. Waste fishing nets were utilized as recycled nylon (RN) short fibers for strengthening polymer cement mortar (PCM). Manufactured polyethylene (PE) microfiber were also applied for comparing the effectiveness to RN. Reinforced concrete (RC) beams were exposed to the marine tide for one year to induce rebar corrosion. Half-cell potential was applied for the monitoring of rebar corrosion. After the test beams were collected from the sea, repair operation was conducted accordingly. RC beams were repaired by removal of concrete cover, then sprayed with PCM reinforced with fibers. Mechanical properties such as flexural capacity, failure behavior, crack openings and final crack formation of the tested beams were extensively investigated to evaluate the effectiveness of the repair. Moreover, chloride ion penetrability of the PCM were examined to evaluate durability of repair material. This study focuses on the restorability of the flexural capacity of the RC beams that were exposed to the natural deterioration.

2.2 TESTING MATERIALS

2.2.1 Fibers

Two types of fiber were introduced in this study which are recycled nylon (RN) short fibers and polyethylene (PE) microfibers. RN fibers are the waste fishing nets that were collected by fishermen in Hokkaido. The fishing nets were washed by soaking in water for 72 hours, dried naturally, then manually cut into specified shape and length. Only the straight part of the net was used to prevent formation of fiber cluster during the mix [1]. Tensile strength and Young's modulus of RN fiber were calculated according to ASTM C1557-03 [2]. In addition to RN fibers, the manufactured PE microfiber receiving from the supplier in Japan were also introduced as shown in Figure 2.1. Properties of fiber are given in

Table **2.1**.

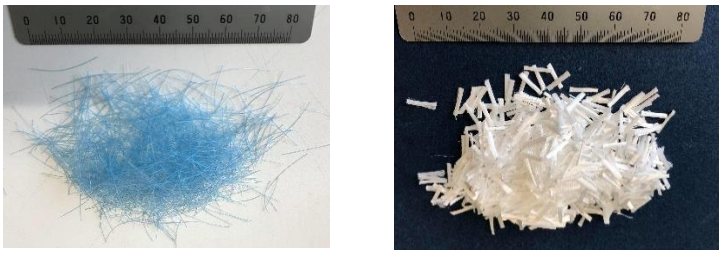

(a) RN fiber (b) PE fiber

Figure 2.1 Fibers used for reinforcing PCM.

Table 2.1 Properties of the RN and PE fibers.

Fiber	Diameter (mm)	Length (mm)	Density (kg/m^3)	Tensile strength (MPa)
Recycled nylon (RN)	0.24	20	1.13	334
Polyethylene (PE)	0.01-0.1	9	1.05	n/a

2.2.2 RC beams

The RC beams measuring 900 mm in length, 100 mm in width, and 150 mm in height were casted. Ordinary Portland cement (OPC) was used for making RC beams and the design strength was 33 MPa. The beams had water-to-cement ratio (w/c) of 0.5, and the sand-to-aggregate (s/a) ratio was 0.45. Mix proportion of the RC beams is given in Table 2.2. Galvanized coated steel rebars were used for making stirrups so that the corrosion concentrated on the tensile rebar. In addition, an electrical wire were connected to the tensile rebar for monitoring steel corrosion during the exposure (Figure 2.2). The beams were wrapped by wet towel for 7 days after the casting, then transported to the exposure site in Kagoshima. Figure 2.3 shows the geometry and reinforcement details of the RC beams.

Table 2.2 Mix proportion of RC beams per cubic meter.

Water (kg)	Cement (kg)	Sand (kg)	Gravel (kg)	W/C	s/a
175	350	871	1076	0.5	0.45

Figure 2.2 Test RC beams.

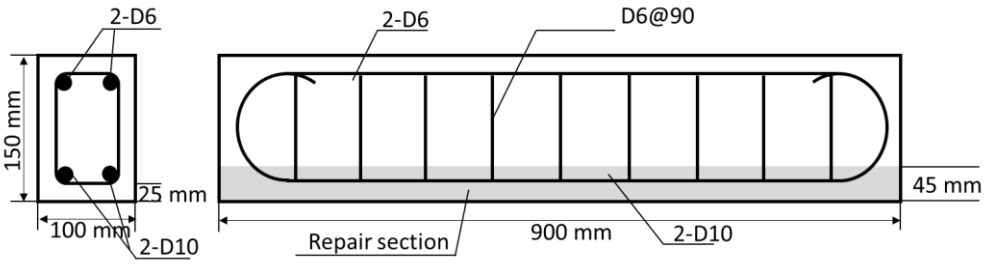

Figure 2.3 Geometry and reinforcement detail of the test beam.

2.2.3 Polymer cement mortar

The acrylic type polymer cement mortar (PCM) received from supplier in Japan was used for the repair of the RC beams. The water-to-binder ratio of PCM was 0.2 and the density was 1,677 kg/m^3. Three mixes of PCM were introduced for spraying on the repair section: 1) plain PCM with no fiber added (PCM-NF), 2) PCM reinforced with RN fiber (PCM-RN), and 3) PCM reinforced with PE fiber (PCM-PE). In addition, PCM specimens were casted in the 40×40×160 mm prism mold and the 50×100 mm cylinder mold for studying material properties. Some of PCM-PE cylinders were exposed to the same environment simultaneously as the beams to investigate the chloride ion penetrability.

During the repair operation, PCM was prepared by mixing with water for 1 minute. Air remover was added subsequently and continued mixing for 2 minutes. Without stopping the mixing operation, fibers were slowly added with the volume fraction of 1.0% and 1.1% for RN and PE respectively. Mix proportion of PCM was specified from the manufacturer as given in Table 2.3. The mixing was then continued for another 2 minutes; however, further mixing may extend to ensure uniform fiber distribution and there is no formation of fiber cluster. After finish mixing, PCM was pumped and sprayed through a nozzle on the removed section of RC beams.

Table 2.3 Mix proportion of PCM for 25 kg batch.

Fiber	PCM (kg)	Water (kg)	Fiber (kg)	Fiber content by volume (%)
PCM-NF	25	4.93	-	
PCM-RN	25	4.93	0.164	1.0
PCM-PE	25	4.93	0.160	1.1

2.3 EXPERIMENTAL PROGRAM

2.3.1 Exposure tests

RC beams were transported to exposure site located in Kagoshima. RC beams were experience tidal exposure to induce steel corrosion. The duration of the exposure was 1 year. Exposed beams were installed in the docking and placed at the seawater level (Figure 2.4) so that the test beams experienced sea tide. In addition, PCM-PE cylinders (100 mm in diameter and 200 mm in height) were casted and exposed to the same environment simultaneously as the beams to investigate the chloride ion penetrability of PCM itself. Figure 2.5 illustrates installation layout of the exposed beams.

Figure 2.4 Exposure site.

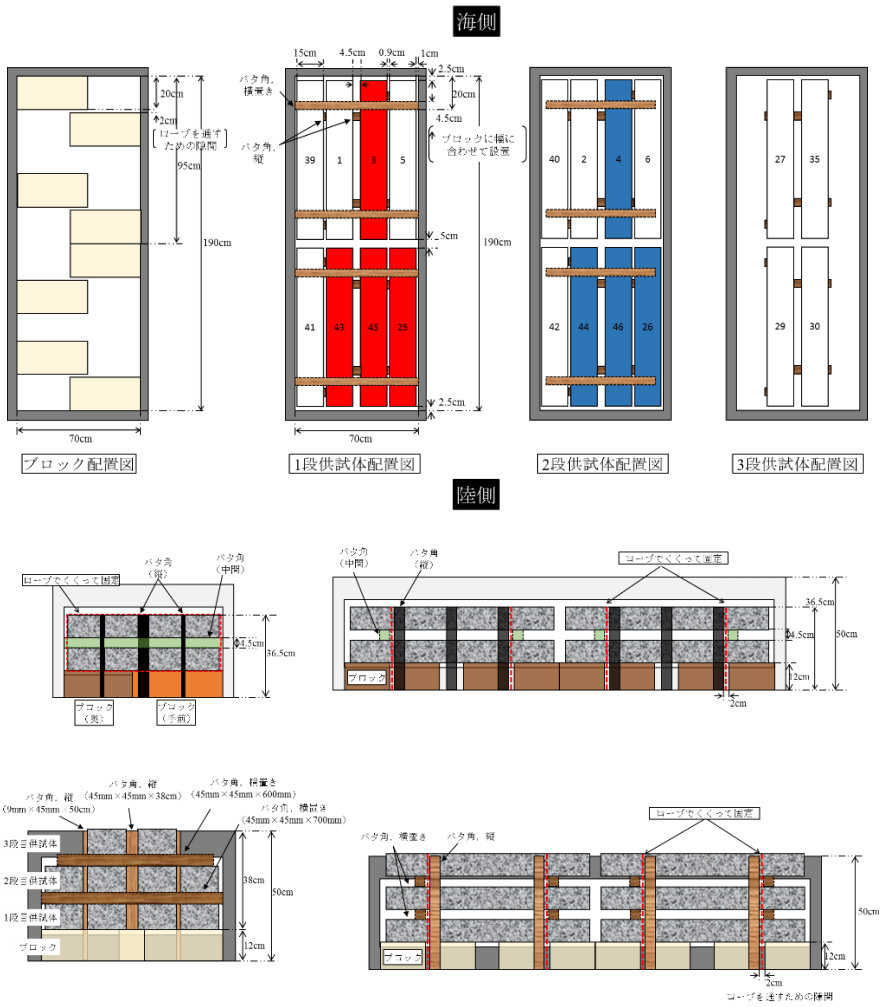

Figure 2.5 Specimen installation layout.

2.3.2 Monitoring RC beams

Steel corrosion in RC beams were monitored periodically using half-cell potential methods specified by Public Work Research Institute of Japan [3]. Corrosion of the rebar can be estimated by measuring the potential differences between rebar and the wet concrete surface with respected to the standard electrode. Figure 2.6 (a) shows measurement procedure and the Table 2.4 shows standard electrode reference values. In this study, five measuring points located in each side of the tensile rebar were measured as shown in Figure 2.7. It should be noted that due to difficulties in measurement on site, the measurement procedure was modified as shown in Figure 2.6 (b). At the site, seawater silver chloride electrode (SSE[sw]) was selected as reference electrode. A sponge was attached at the tip of the hose to reduce electrical resistivity. After the measurement, electrical potentials were then converted to the saturated copper sulfate electrode standard (CSE) for evaluating corrosion level. Rebar corrosion in beams can be estimated according to Table 2.5. However, in the case of using galvanized coated stirrups, it is expected that the corrosion is likely to be occurred when the measured potential was lower than -800 mV vs. CSE.

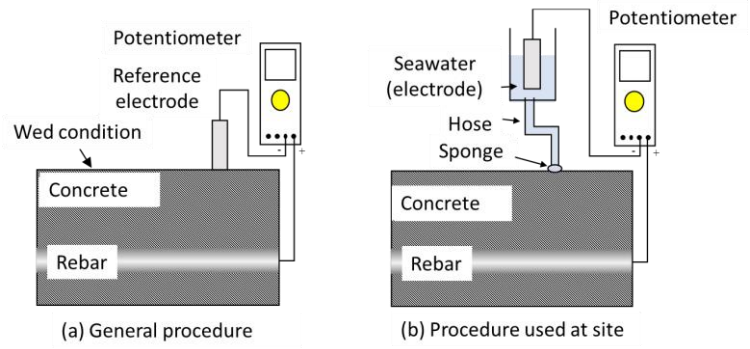

Figure 2.6 Measurement procedure of half-cell potential.

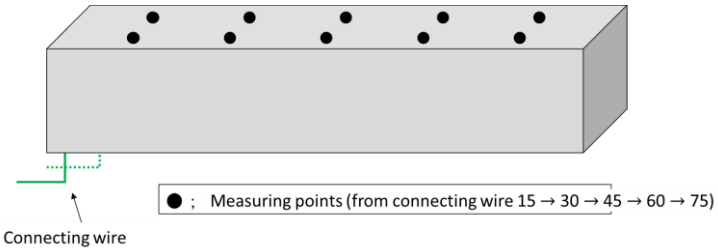

Figure 2.7 Measuring points on RC beams.

Table 2.4 Typical reference electrode for half-cell potential.

Reference electrode	Electrolyte	Potential (V vs. SHE, 25℃)
Copper sulfate electrode (CSE)	Saturated $CuSO_4$ Solution	+0.316
Lead electrode (PRE)	$Ca(OH)_2$+$CaSO_4$ (solid)	-0.483
Manganese dioxide electrode (MNO)	Saturated $Ca(OH)_2$ Solution	+0.120
Silver chloride electrode (SSE)	Saturated KCl Solution	+0.196
Seawater silver chloride electrode (SSE [sw])	Seawater	+0.250
Standard calomel electrode (SCE)	Saturated KCl Solution	+0.242

Table 2.5 Corrosion criteria for half-cell potential method.

Natural potential	Rebar corrosion
E > -150	No
-150 ≥ E > -250	Slightly
-250 ≥ E > -350	Moderate
E ≤ -350	Heavily

2.3.3 Repair operations

Exposed beams were lifted-up from the exposure side after completing exposed duration. Thereafter, repair operation of RC beams was conducted by removal of bottom surface cover up to 20 mm over the tensile rebar. After that, the removed section was then sprayed with different mixes of PCM as shown in Figure 2.8.

The tested RC beams were divided into 3 groups: group A beams were stored in the laboratory room for 10 months and then tested; group B beams (normal and upgraded RC beams) were exposed to the tidal zone for 1year; and group C beams (normal RC beams only) were repaired after the 1 year tidal exposure. The normal RC beam was directly exposed to the tide, and the repair was taken place after completing the exposure. The upgraded RC beams went through the repair operation before starting the exposure and was not further repaired even after the exposure. The details of the tested beams are listed in Table 2.6.

Figure 2.8 Removal of concrete cover and spraying PCM on RC beam.

Table 2.6 Name and conditions of the tested RC beams.

Specimen name	Condition	Exposure	Sprayed material
Group A			
RC0	Normal RC	No	
RN0	PCM sprayed before exposure	No	PCM-RN
PE0	PCM sprayed before exposure	No	PCM-PE
Group B			
RC1	Normal RC	1 year	
RN1	PCM sprayed before exposure	1 year	PCM-RN
PE1	PCM sprayed before exposure	1 year	PCM-PE
Group C			
RC1-NF	Repair after exposure	1 year	PCM-NF
RC1-RN	Repair after exposure	1 year	PCM-RN
RC1-PE	Repair after exposure	1 year	PCM-PE

2.3.4 Loading tests

Four-point flexural tests were conducted on the RC beams following the JIS A1106 standard [4]. There were four linear variable differential transformers (LVDTs) measuring vertical deflection of the beams; two at the mid-span, another two at the end supports. Eight strain gauges having 30 mm gauge length were glued on the beam; 6 gauges attached at the midspan at 30 mm interval, 1 gauge on the top surface at the midspan, and 1 gauge on the bottom surface. Crack openings were measured using a series of pi-type gauge with 50 mm gauge length installed at the bottom surface of the beam. In addition, gypsum was used for leveling the beam and filling the gap between beams and loading points to ensure homogeneous loads transfer. Universal testing machine (UTM) was used, and the load speed was set as 0.02 N/mm^2/sec. the loading was paused at every 10 kN increment to observe cracks. Experimental setup is shown in Figure 2.9.

For PCM specimens, compressive strength tests as per JIS A 1108 [5] and flexural strength tests following the JIS R 5201 [6] were conducted. Specimens were cure in water condition at 28 days before the tests. Autograph loading machine was used for the flexural strength tests and the load speed was set at 0.05 mm/min. Experimental setup of PCM is shown in Figure 2.10. Photographs show actual setting during the loading tests are given in Figure 2.11 and Figure 2.12.

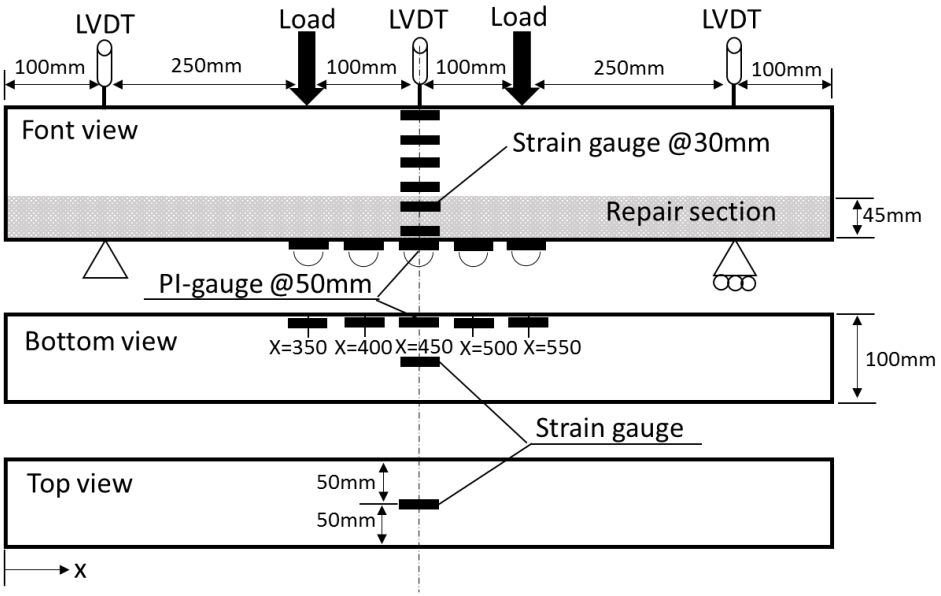

Figure 2.9 Experimental setup for RC beams.

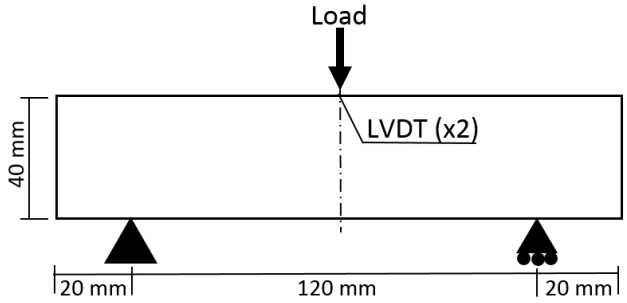

Figure 2.10 Experimental setup for PCM specimens.

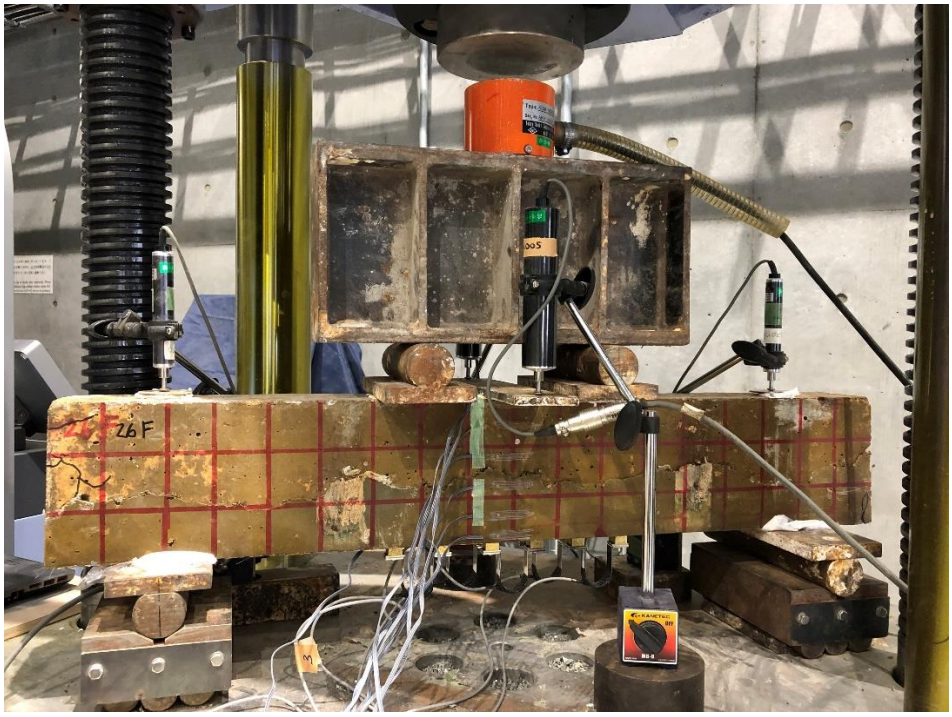

Figure 2.11 Four-point flexural test for RC beams.

Figure 2.12 Flexural strength tests for PCM specimens.

2.4 RESULTS AND DISCUSSIONS: MECHANICAL PROPERTIES OF THE REINFORCED PCM

This section discusses the material performance of the PCM reinforced with fibers. Test results obtained from the PCM specimens were summarized and discussed such as flowability of fresh mortar, compressive strength, flexural strength, failure behavior and the final cracks pattern.

2.4.1 Flow ability

Flowability of fresh PCM was measured following the JIS R 5210 [6]. Flow diameter and the %Δflow which is the difference in flow diameter compared to PCM-NF are summarized in Table 2.7. Adding fiber had an adverse effect on the flowability of PCM especially when PE fibers were used. PCM-PE showed considerable reduction in flow diameter up to 28.6%, but PCM-RN showed slightly reduction at 1.8% only. This was probably due to the small diameter of the PE fibers which account more surface area at a given amount. PE fibers also have lower density comparing to RN fibers; therefore, more fibers are needed at the same volume fraction. RN fibers showed slight reduction of flowability of PCM. This behavior was probably from the smooth surface of the RN. The reduction in flowability of fresh mortar when adding fibers were also found in the case of polypropylene and nylon fibers [7, 8, 9].

Table 2.7 Flow diameters of PCM specimens

Specimen name	Flow diameter (mm)	%Δflow
PCM-NF	179.6	-
PCM-RN	176.4	-1.8
PCM-PE	128.3	-28.6

2.4.2 Compressive and flexural strengths

Compressive strength and flexural strength tests were performed according to JIS A 1108 [5] and JIS R 5201 [6] respectively. Table 2.8 showed results from the compressive and flexural strength tests. It should be noted that results in each test are the averaged of three samples. With the addition of RN fibers, a considerable reduction in compressive strength was observed. Slight reduction in flexural strength was also found. This behavior was suggested by Orasutthikul et al. and Spadea et al. that RN fiber can increase void inside cement matrix and reduce the modulus of elasticity [1, 10]. In contrast, the addition of PE fibers seemed to increase both compressive strength and flexural strength at 24.3% and 39.2% respectively. It can be considered that PE fibers uniformly dispersed in the cement matrix and played an important role in enhancing lateral tensile strength of mortar during the load [11, 12, 13]. The PCM-PE having one-year tidal exposure gained compressive strength at approximately 50% comparing to PCM-PE without exposure.

Table 2.8 Compressive strength tests and flexural strength tests results.

	Compressive strength tests			Flexural strength tests			
	f'_c (MPa)	*SD*	%Δ f'_c	P_{cr} (kN)	f_b (MPa)	*SD*	%Δ f_b
PCM-NF	32.7	3.65		1.69	4.77	0.14	
PCM-RN	24.0[1]	3.53	-31.4	1.56	4.37	0.72	-8.4
PCM-PE	43.5	1.41	24.3	2.36	6.64	0.82	39.2
PCM-PE[2]	66.7	7.90	90.6	-	-	-	-

Note: f'_c is the compressive strength, *SD* is the standard deviation, %Δ f'_c is the percent difference in compressive strength compared to PCM-NF, P_{cr} is the maximum load, f_b is the flexural strength, and %Δ f_b is the percent difference in flexural strength compared to PCM-NF.

[1] Obtained with 40 mm cube specimens taken out from the beam.

[2] Specimen after 1-year of tidal exposure

2.4.3 Failure behavior

Three-point flexural tests were conducted on the PCM specimens. Figure 2.13 showed load-midspan curves of the PCM specimens during the loading test. With the addition of fiber, whether the RN or PE fibers, it was observed that the beams able to retain some loads after the yield point. On the contrary, PCM-NF expressed brittle failure since load suddenly decreased to zero after the peak. PCM-PE exhibited ductile failure as seen from the slope of the graph that it tends to be gradual than those of PCM-NF. PCM-PE showed the highest peak load followed by PCM-RN and PCM-NF. A hardening stage was found in PCM-PE in which the load increased after the peak. This behavior indicated that PE fiber shows better stress distribution and able to transfers stresses after the cracks occurred.

For PCM-RN, the load suddenly dropped after the yield point, but still sustain small residual load at approximately 0.3 kN until the end of the experiment. The lower post-peak load of PCM-RN was probably due to weak bonding of RN fiber since it has smooth surface. Even though the post-peak load of PCM-RN was rather low compared to PCM-PE, the beam did not fail completely after the cracks occurred. It is concluded that RN fiber prevented abrupt failure of the beam, and RN fibers can transfer some stresses through the cracks. This behavior was discussed by Lee, Seungtae and Qin et al. that the crack bridging effect of fiber improves strengths and integrity of the concrete [8, 12] The failure behavior of PCM-RN and PCM-PE are corresponding to the recycled fibers reinforced mortar conducted by Orasutthikul et al. [1].

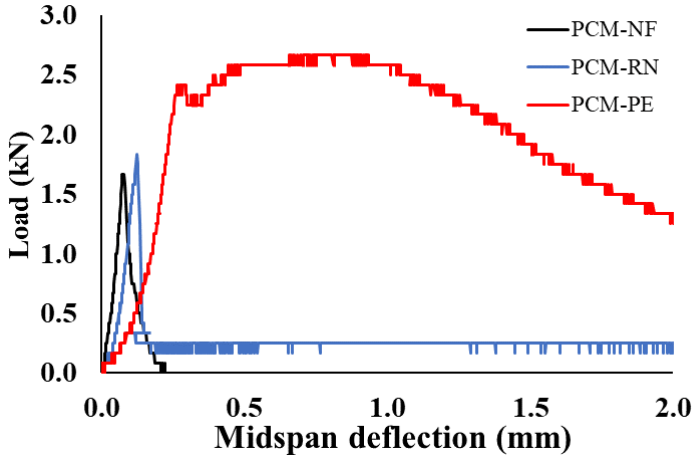

Figure 2.13 Load-midspan deflection curves of PCM-NF, PCM-RN and PCM-PE.

2.4.4 Final cracks pattern

The final cracks at the bottom face of the beam after the experiment are shown in Figure 2.14. PCM-RN had a wide single crack while PCM-PE had many small cracks aside the main crack at the center. This phenomenon confirmed that PE fiber transfers stresses by dispersing damage from a wide single crack into many small cracks. No breakage of RN fiber was observed; therefore, RN fibers were rather pulled-out than rupture during crack openings. Since the fiber did not break, the strength of reinforcement was rather depended on the bonding and pull-put strength of fiber. This behavior was also confirmed by Readon et al. that embedded fiber in matrix does not rupture but pulled-put during the loading test [14]. For the case of PE fibers, breakage of fiber was clearly observed at the main crack. Contrary to RN fibers, PE fiber breaks rather than pulled-out. It is concluded that RN fiber transfers stresses through wide cracks while PE fiber bridges small or micro cracks.

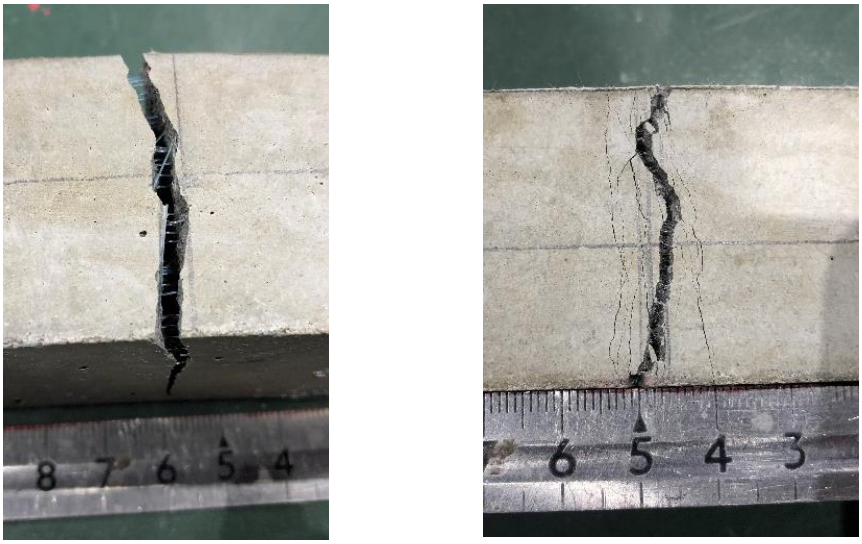

(a) PCM-RN (b) PCM-PE

Figure 2.14 Crack pattern at the bottom face of the beam.

2.5 RESULTS AND DISCUSSIONS: MECHANICAL PERFORMANCE OF THE REPAIRED RC BEAMS

This section discusses mechanical performance of the tested RC beams. Restorability of the repaired beams were compared with different repair materials such as PCM-RN and PCM-PE. Corrosion of the tensile rebar during and after the exposure was examined. Test results of the repaired RC beams, for instance flexural capacity, failure behavior, strain distribution, crack openings, cracks formation, and the rebar mass loss were summarized and discussed.

A total of 12 RC beams were divided into 3 groups: group A beams were stored in the laboratory room for 10 months and then tested; group B beams (normal and upgraded RC beams) were exposed to the tidal zone for 1year; and group C beams (normal RC beams only) were repaired after the 1 year tidal exposure. The normal RC beam was directly exposed to the tide, and the repair was taken place after completing the exposure. The upgraded RC beams went through the repair operation before starting the exposure and was not further repaired even after the exposure.

2.5.1 Half-cell potential

Half-cell potential of the exposed RC beams were measured periodically to monitor steel corrosion. Measured data from the RC beams were converted to CSE electrode references and plotted against the exposure duration. When half-cell potential is lower than -800 mV vs. CSE, the steel corrosion is likely to occurred. Half-cell potential results are shown in Figure 2.15.

The exposed beams showed a stable half-cell potential up to approximately at 250th day of exposure, then started to decrease. After 1 year, RC1, RN1, and PE1 had the half-cell potential of -473, -598, -356 mV respectively. RC1-NF and RC1-PE had half-cell potential of -779 and -902 mV indicating that the steel corrosion is likely to be occurred.

It should be noted that the effect of galvanized stirrups might delay the corrosion process. In addition, since the tested beams were stacked at the exposure site, the difficulties in reaching measuring point as well as uneven measuring surface (e.g. dirt, algae and shells) may affect to the accuracy of measurement. Based on the measurement results, adding fibers show no noticeable effect on the half-cell potential of the test beams.

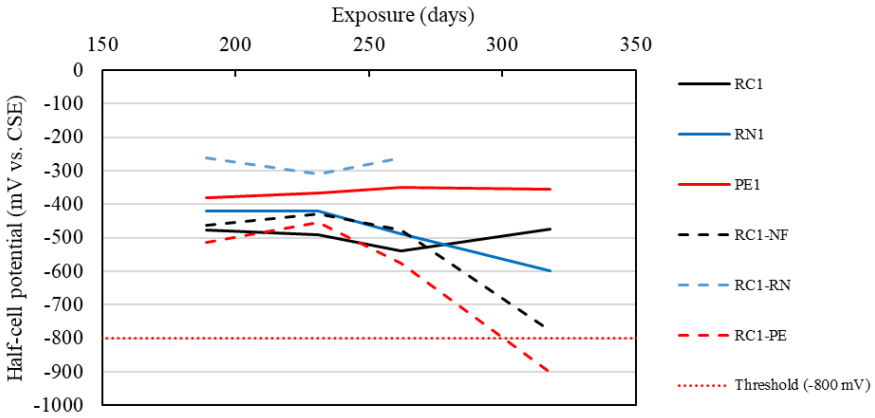

Figure 2.15 Changes in half-cell potential over time.

2.5.2 Flexural capacity

Test results from the four-points flexural tests of the RC beams are summarized in Table 2.9. RN0 showed slightly lower yield and ultimate loads comparing to RC0 probably due to the fact that PCM have not gain enough strength yet. However, PE0 gave higher flexural capacity and showed higher flexural strength up to 7%. The effect of spraying PCM-PE caused improvement in flexural capacity in the range of 20-24% for the yielding load and 1-7% for the ultimate load respectively.

For group B, the beams that were repaired prior the exposure, RN1 and PE1, showed increasing in flexural capacity up to 10% and 34% respectively. Even though RN1 did not show high flexural capacity as PE1, adding RN fiber contributed to the improvement in flexural capacity comparing to normal RC beams. Moreover, the relatively low flexural capacity of RC1 may indicate that steel corrosion might have occurred. The beams sprayed with PCM-RN (RN0 and RN1) tend to express flexural-shear failure mode probably from the fact that RN fiber reduces shear capacity by adding voids in the PCM matrix.

Normal RC beams that experienced 1-year tidal exposure and subsequent repair operation are arranged in group C. For all of the repaired beams, RC1-NF, RC1-RN and RC1-PE showed improvement in flexural capacities at the range of 15-17%. RC1-PE showed highest yield load (P_y), while RC1-RN and RC1-NF gave similar yield capacities. This behavior was due to the higher compressive and flexural strengths of PCM-PE. Test results confirmed that flexural capacity of the beams can be restored or even improved by spraying PCM reinforced with fiber. The results of tested RC beams with respect to the sprayed PCM are corresponding to the mechanical properties of PCM reinforced with fiber in section 2.4.2.

Table 2.9 Four-points flexural test results.

Specimen name	P_y (kN)	P_u (kN)	$\%\Delta P_y$	$\%\Delta P_u$	Failure type	Mass loss of each tensile bar (%)	
Group A							
RC0 (1)	49.1	59.6			Flexural		
RC0 (2)	48.1	60.9			Flexural		
RN0 (1)	41.4	55.4	-14.8	-8.0	Flexural-shear		
RN0 (2)	45.1	58.0	-7.2	-3.7	Flexural-shear		
PE0 (1)	58.5	61.0	20.4	1.2	Flexural		
PE0 (2)	60.7	64.2	24.9	6.6	Flexural-shear		
Group B							
RC1	45.2	56.2	-7.0	-6.7	Flexural	0.9	1.8
RN1	48.3	66.5	-0.6	10.4	Flexural-shear	0.8	0.7
PE1	64.6	81.1	32.9	34.6	Flexural	0.6	0.7
Group C							
RC1-NF	49.1	70.8	1.0	17.5	Flexural-shear	0.6	0.5
RC1-RN	50.2	69.9	3.3	16.0	Flexural	0.6	0.5
RC1-PE	62.0	69.7	27.6	15.7	Flexural	0.8	0.9

Note) P_y is the yield load and P_u is the ultimate load and $\%\Delta P_y$ and $\%\Delta P_u$ are the percent difference in P_y and P_u compared to the average of RC0 (1) and RC0 (2), respectively.

2.5.3 Failure behavior

Load-midspan deflection curves of the RC beams are shown in Figure 2.16. The results of group A beams are shown in Figure 2.16(a). PE0 gave higher yield and ultimate load capacities among group A beams, but RN0 showed lower flexural capacity comparing to RC0. RN0 beams showed lower stiffness which can be seen from the slope of the figure. A possible reason of having lower stiffness and lower flexural capacity of RN0 is that RN fiber has poor bonding between PCM substrates. However, using PE fiber as reinforcement could improve flexural performance of structure.

Figure **2.16** (b) shows the results from group B which are normal RC and upgraded RC beams having 1-year of tidal exposure. RC1 gave slightly lower flexural capacity, indicates that steel corrosion might have taken place. RN1 expressed similar loading behavior to RC1 with slightly higher yield and ultimate loads. The slight increase in the load-carrying capacity was provided by the addition of RN fibers. PE1 showed the highest yield and ultimate loads in which the load can be carried after the yield of tensile rebar. PE1 seems to be more ductile as indicated from the slopes of load-deflection curves shown in

Figure **2.16** (b). Furthermore, both RN1 and PE1 had slightly higher flexural capacity than RN0 and PE0. It is possible that PCM gain strength from the tidal exposure as indicated in Table 2.9. The upgraded beams expressed higher flexural capacity than RC0, which means that using sprayed PCM reinforced with fibers has a high potential in improving bending capacity structure.

RC beams in group C were repaired after completing 1-year exposure duration. Bottom covers of the beam were removed, then sprayed by three kinds of sprayed materials which are non-fiber PCM (RC1-NF), PCM reinforced with RN fiber (RC1-RN) and PCM reinforced with PE fiber (RC1-PE), and the results from flexural tests are shown in

Figure **2.16** (c). Load-deflection curves of RN1 are also shown to compare the changes in flexural capacity. The experimental results indicate that all the repaired beams show better performance in terms of yield and ultimate loads than non-repaired RC1. Flexural capacity among those beams were similar with RC1-PE that had the highest yield load followed by RC1-RN and RC1-NF. In addition, RC1-NF, RC1-RN and RC1-PE have slightly higher stiffness comparing to RC1. The results conclude that spraying PCM reinforced with RN and PE fibers can restore the flexural capacity of the beams to their original performance.

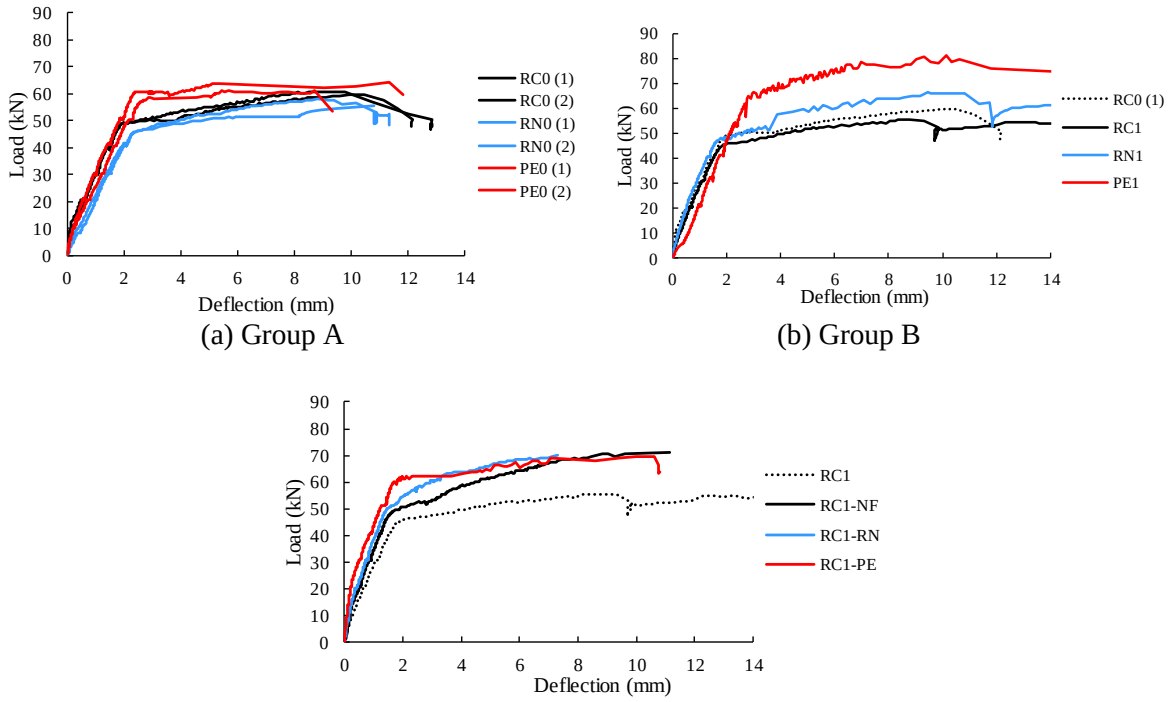

(a) Group A

(b) Group B

(c) Group C

Figure 2.16 Load-midspan deflection curves of RC beams.

In general, a section repair was conducted by removal of deteriorated concrete section and corroded reinforcing rebars; however, using sprayed PCM reinforced with fiber can be done without the removal of rebars because early repair for slightly rebar-corroded beams was intended. It is concluded that fibers can compensate the tensile stresses that had been carried by corroded tensile rebars. Beams sprayed with PCM-RN showed higher loading capacity than normal RC beams but inferior to PCM-PE. Therefore, recycled nylon fibers from fishing nets have a high potential to be used as a reinforcing material of concrete and for the repair of lightly corroded RC beams.

2.5.4 Strain distribution

Concrete strain was measured on the side surfaces of the beams at the midspan with the spacing of 30 mm. Strains measured in group A beams are plotted in Figure . RC beams sprayed with PCM seems to have linearly strain distribution, while RN0, RN1, RC1-NF showed imbalance strain distribution. The strain almost increased linearly for the case of PE0 as the load increased. Furthermore, RC beams that were sprayed with PCM-RN and PCM-PE showed higher strain during the load application compared to RC0 and RC1. Therefore, ductility of the RC beams can be improved with the addition of fibers. On the contrary, RC1-NF expressed similar strain distribution as RC0 and RC1 imply that PCM alone did not improve ductility of the RC beams. The equally strain distribution confirmed that there was no delamination between PCM and the substrate concrete. It can be concluded that adding fibers, whether RN of PE, helps in distributing strains throughout the concrete and improve ductility of the structures.

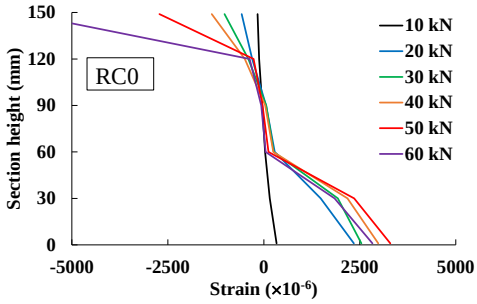

(a) Strain distribution of RC0

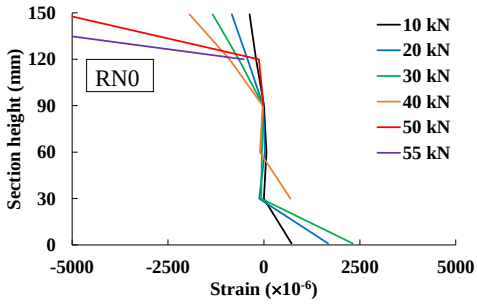

(b) Strain distribution of RN0

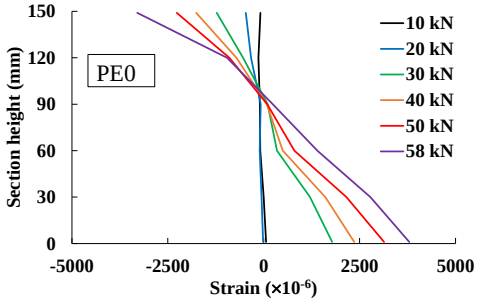

(c) Strain distribution of PE0

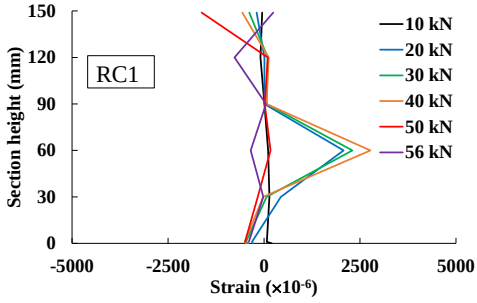

(d) Strain distribution of RC1

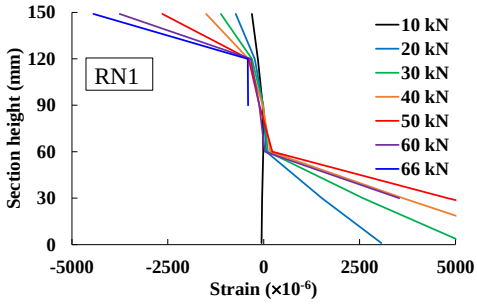

(e) Strain distribution of RN0

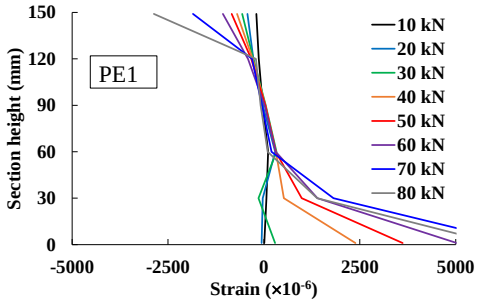

(f) Strain distribution of PE1

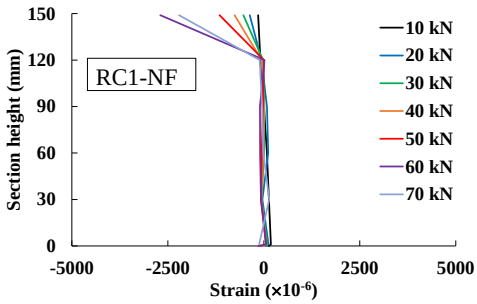

(g) Strain distribution of RC1-NF

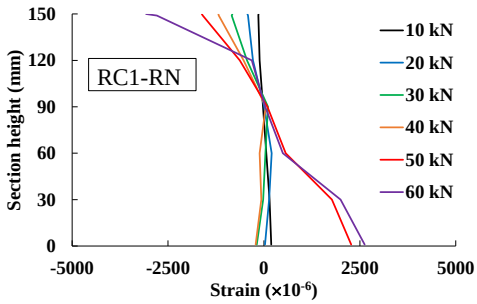

(h) Strain distribution of RC1-RN

Figure 2.17 Strain distributions at the midspan of RC beams.

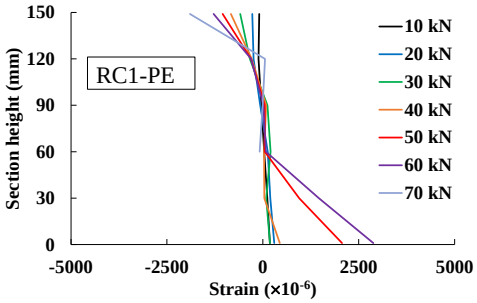

(i) Strain distribution of RC1-PE

Figure 2.17 Strain distributions at the midspan of RC beams (Cont.).

2.5.5 Crack openings

Crack openings at the bottom face of the beam were measured at the location of 35, 40, 45, 50, and 55 cm from the end-section of the beam as shown in Figure 2.9. Crack openings with respect to the load applied are shown in Figure 2.19. It should be note that for RC0, RN0, and PE0, the locations of pi-type gauge were at 25, 35, 45, 55, and 65 cm because those beams were experimented prior the other beams. Measurement locations were changed after that because of cracks tended to form at the center of the beams.

The beams that were sprayed with PCM-RN and PCM-PE showed smaller crack openings compared to RC0 and RC1. Crack widths of the PE0, PE1 and RN1-PE were relatively small with approximately 0.1 mm at the load of 50 kN as seen in Figure 2.18(c) and (i). RC beams sprayed with PCM-RN had slight wider cracks but still smaller than the non-repair beams (RN0, RN1). In addition, the increment of cracks openings seems to be limited for the beams sprayed with PCM-RN and PCM-PE compared to RC0 and RC1. Cracks in PE0 and PE1 enlarged slowly as load increased. For PCM-NF, an abruptly increasing in crack width were observed. Crack openings in RC1-NF were wider than those of RC0 and RC1.

It should be noted that cracks beyond the gauge length cannot be measured, which makes it difficult to evaluate the total increment rate of the crack opening. Test results concluded that adding fiber reduces crack width and delays the propagation of cracks.

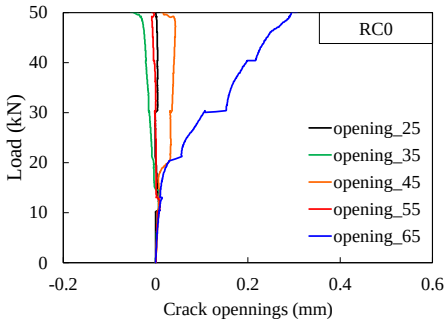

(a) Crack openings of RC0

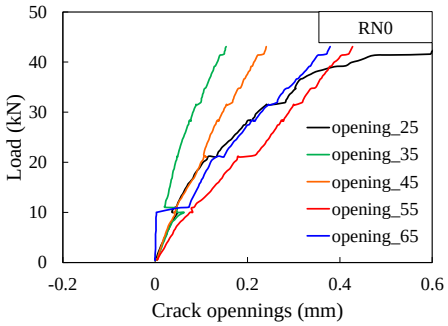

(b) Crack openings of RN0

Figure 2.18 Crack openings at the bottom face of the tested beams.

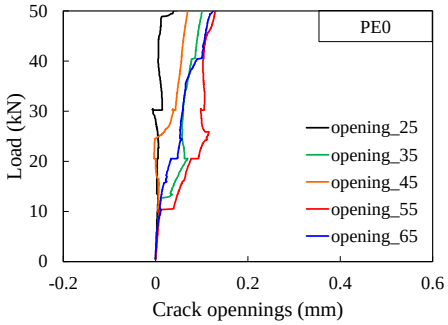

(c) Crack openings of PE0

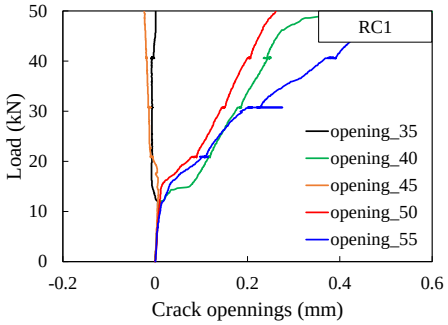

(d) Crack openings of RC1

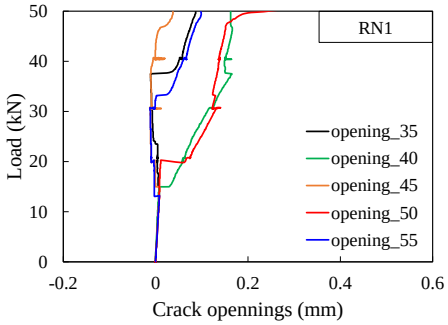

(e) Crack openings of RN1

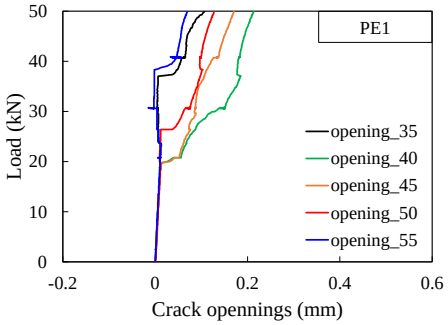

(f) Crack openings of PE1

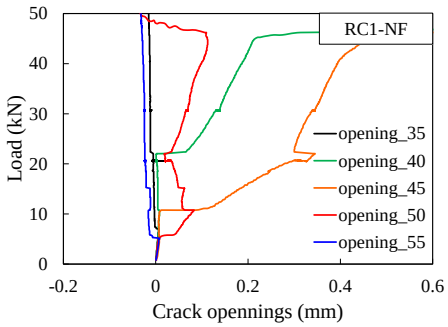

(g) Crack openings of RC1-NF

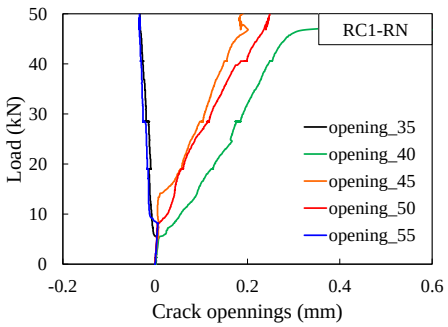

(h) Crack openings of RC1-RN

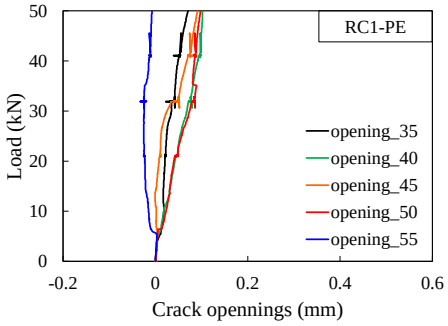

(i) Crack openings of RC1-PE

Figure 2.18 Crack openings at the bottom face of the tested beams (Cont.).

2.5.6 Cracks formation

After the flexural tests, final cracks pattern of the RC beams were carefully observed and drawn in Figure 2.19. Only visible cracks were count in this experiment. The beams sprayed with PCM-RN and PCM-PE had more distributed cracks comparing to the non-repaired beam (RC0 and RC1). Cracks in RC0 and RC1 were less distributed and concentrated at the center of the beams. Especially for PE0 and RC1-PE, many small cracks were observed and spread all over the span length as seen in Figure 2.19 (c) and (i). For RN0 and RC1-RN, cracks were widely distributed and spread towards the support rather than concentrated near the midspan of the beam (see Figure 2.19 (b) and (h)).

In contrast, cracks were observed to be most concentrated at the midspan for RC, RC1-NF and PE1. Many of small cracks found in PCM-RN and PCM-PE were corresponding to the smaller crack openings discussed earlier in section 2.5.5. It might conclude that adding fiber helps distributing stress in cement matrix and transferring stresses through cracks. Therefore, fibers prevent serious damage from wider cracks into many of small cracks.

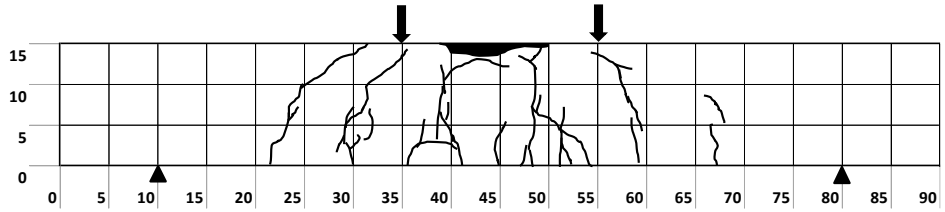

(a) RC0

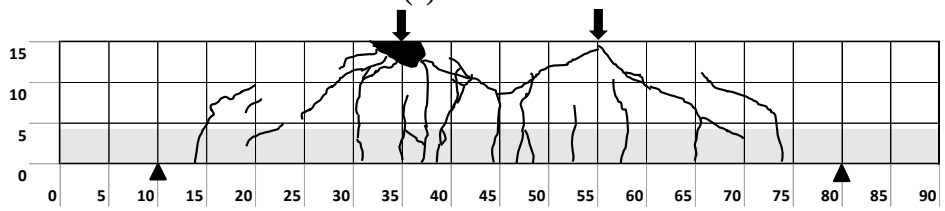

(b) RN0

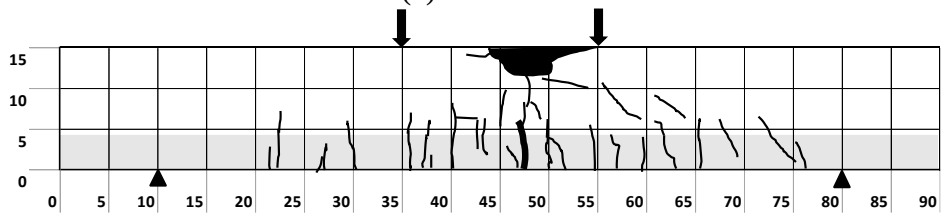

(c) PE0

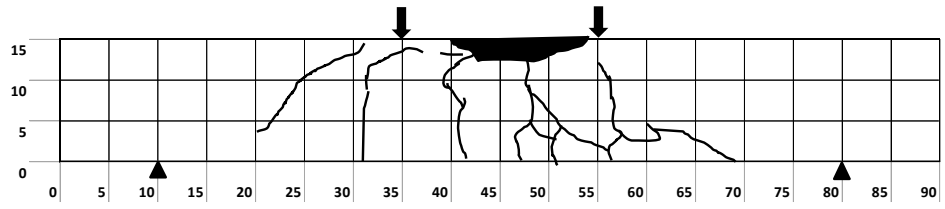

(d) RC1

Figure 2.19 Final crack formation of RC beams.
(unit shown are in centimeter)

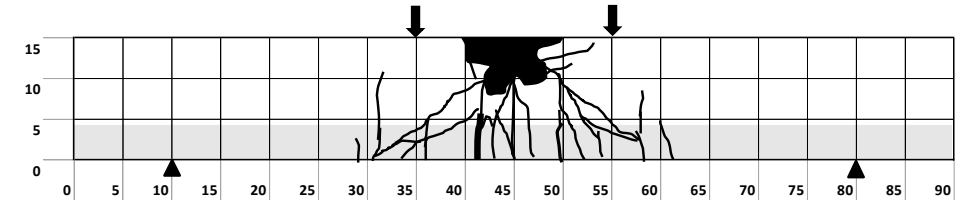

(e) RN1

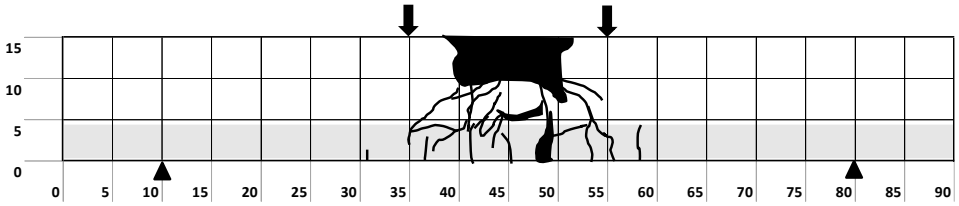

(f) PE1

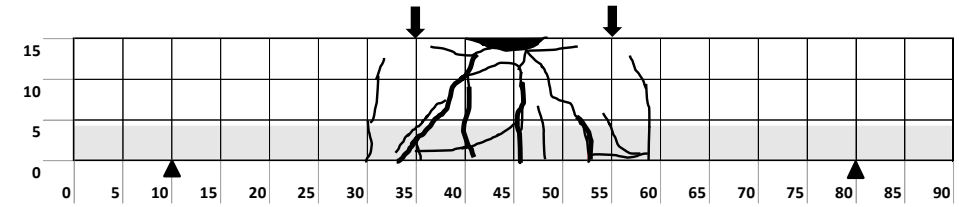

(g) RC1-NF

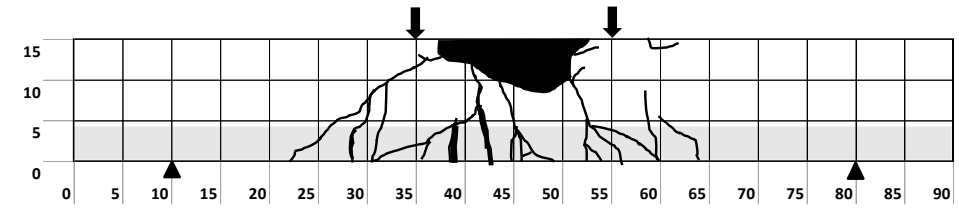

(h) RC1-RN

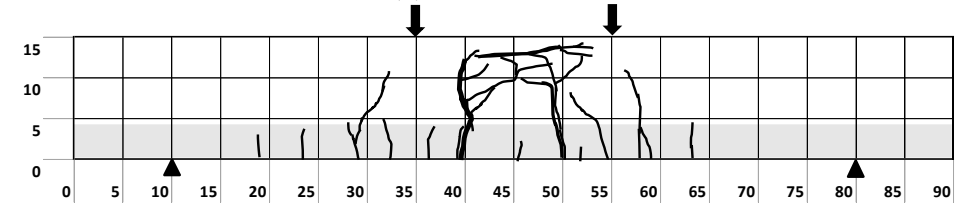

(i) RC1-PE

Figure 2.19 Final crack formation of RC beams (Cont.).
(unit shown are in centimeter)

2.5.7 Rebar mass loss

All RC beams were manually broken into pieces after the flexural tests, and the tensile rebars were collected from the beams carefully. The rebars were washed using diammonium hydrogen citrate solution, and the rebar mass losses were measured. The measured mass losses are given in Table 2.9. RC1 showed the highest mass loss rate up to 1.3% while the other exposed beams (group C) had 0.6 – 0.8%. RN1 and PE1 had lower mass loss rates of 0.8% comparing to RC1. Rusts were found mostly spread along the bottom side of the beam, and some rusts were found at the anchorage near end-section as shown in Figure 2.20. It is possible that the anchorage of steel bar was placed near the surface during concrete casting, the concrete cover near the end face of the beam may be less than that of the bottom face of the beam.

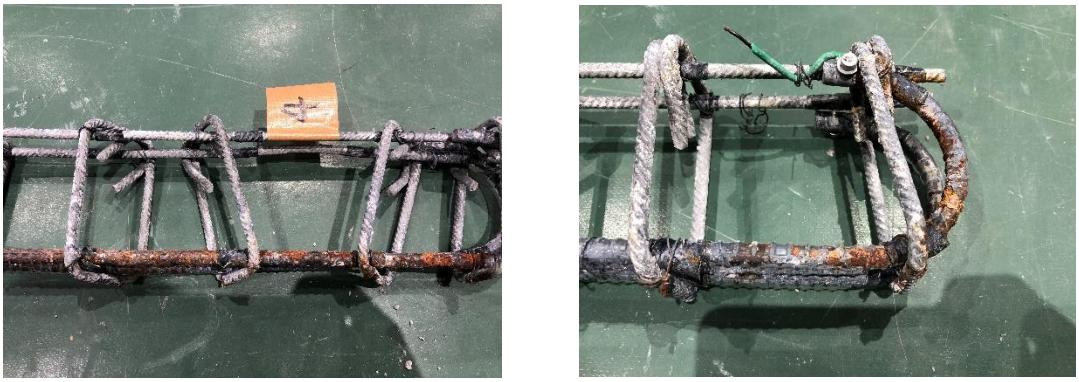

Figure 2.20 Rust formation in the tensile rebar.

2.6 RESULTS AND DISCUSSIONS: DURABILITY AND COMPATIBILITY

2.6.1 Chloride ion penetrability of PCM

Chloride ion penetration depths were measured on the PCM-PE cylinders to examine penetrability of chloride ion. The PCM-PE cylinders were exposed to the ocean tide for 231 and 377 days. Chloride ion content in hardened concrete was analysed corresponding to JIS A 1154 [15]. The appetent chloride diffusion coefficient was calculated as per JSCE G 573 [16] by fitting the following equation:

$$C(x,t) - C_i = C_{0s}\left\{1 - erf\left(\frac{x}{2\sqrt{D_{aps}\cdot t}}\right)\right\} \quad (1)$$

where x is the depth from surface (cm), t is the exposure time (year), $C(x,t)$ is the chloride ion concentration at depth x and exposed time t (kg/m^3), C_{0s} is the surface chloride concentration (kg/m^3), C_i is the initial chloride ion concentration (kg/m^3), D_{aps} is the apparent diffusion coefficient (cm^2/year) and erf is the error function described by:

$$\text{erf}(s) = \frac{2}{\sqrt{\pi}}\int_0^s e^{-\eta^2} d\eta \quad (2)$$

Omitting the initial chloride concentration (C_i), an apparent chloride ion coefficient can be calculated.

The chloride ion profiles of PCM-PE are shown in Figure 2.21. Chloride ion penetration depth was approximately 1 cm from the surface which did not reach the rebar yet. Apparent chloride diffusion coefficients of 231 and 377-days-exposed specimens were 0.28 and 0.09 cm^2/year, respectively. The low chloride ion penetration of PCM was due to low water-to-binder ratio, consequently the permeability of PCM was slightly lower than that of normal concrete. The low chloride ion penetrability of PCM layer might help mitigate the corrosion of steel bar.

Even though RN1 and PE1 were sprayed with PCM before the exposure, slight rebar corrosions were found especially at the end of the beams. It might possible that chloride ion penetrates through the interface of the PCM layer due to shrinkage. Even though the repair was conducted up to 20 mm over the tensile bar, uneven repair surfaces in actual construction work may cause some parts of the tensile bar got close to the interface; thus slight corrosion occurred. Another possible reason is that the corrosion of RN1 and PE1 were found near the end face of the beam. Since the anchorage of steel bar may be placed near the surface during concrete casting, the concrete cover near the end face of the beam may be less than that of the bottom face of the beam.

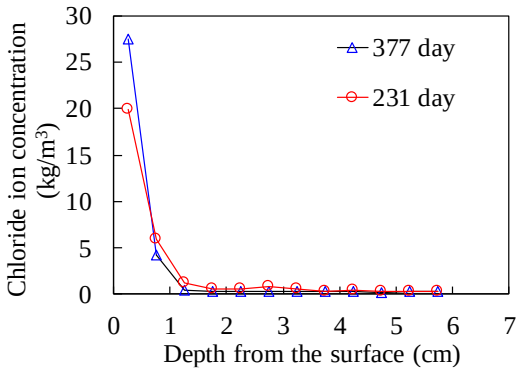

Figure 2.21 Chloride ion profiles in PCM-PE after 231 and 377 days of tidal exposure.

2.6.2 Deterioration of RN fibers

RN fibers were carefully taken from the PCM to investigate any sign of deterioration of fibers after 1 year. Surface of RN fibers were thoroughly observed using scanning electron microscope (SEM) and compared between stored RN fiber. SEM image of the RN fiber that was kept in laboratory and that was taken from RC beam are shown in Figure 2.22 and Figure 2.23 respectively. No sign of surface deterioration was observed on the RN fibers after spending 1 year in PCM. However, the smooth surface of RN fiber might cause poor bonding between fibers and the PCM substrate; therefore, the strength did not high as using PE microfibers.

It was also confirmed by Spadea et al, that recycled nylon fiber from waste fishing nets has adequate alkali resistance and able to apply in cementitious material without any harmful effect to environment [10]. In addition, RN fiber seems to have superior durability under high alkali environment than those of high-density polyethylene (HDPE) fiber fishing nets [17]. RN fibers showed a comparable surface condition as recycled PET-fibers in concrete environment [18]. It is concluded that RN fibers from waste fishing nets are durable under high alkalinity of cementitious material, and suitable for applying in PCM.

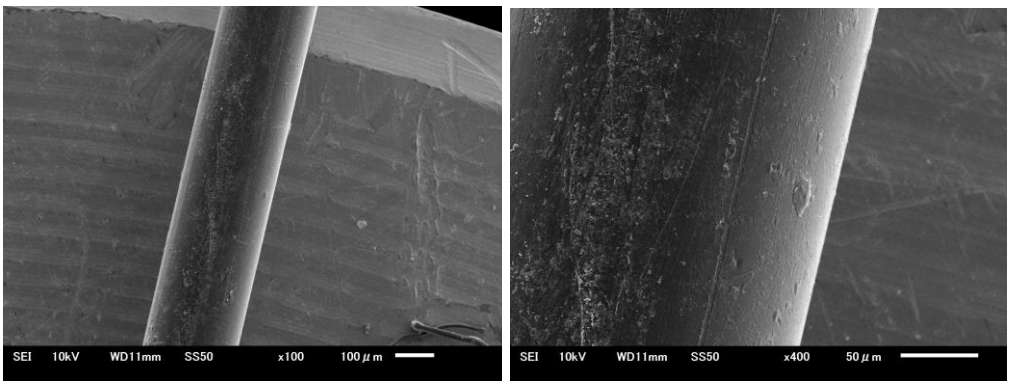

Figure 2.22 SEM image of RN fiber that was kept in the laboratory at (left) ×100 magnification and (right) ×400 magnification.

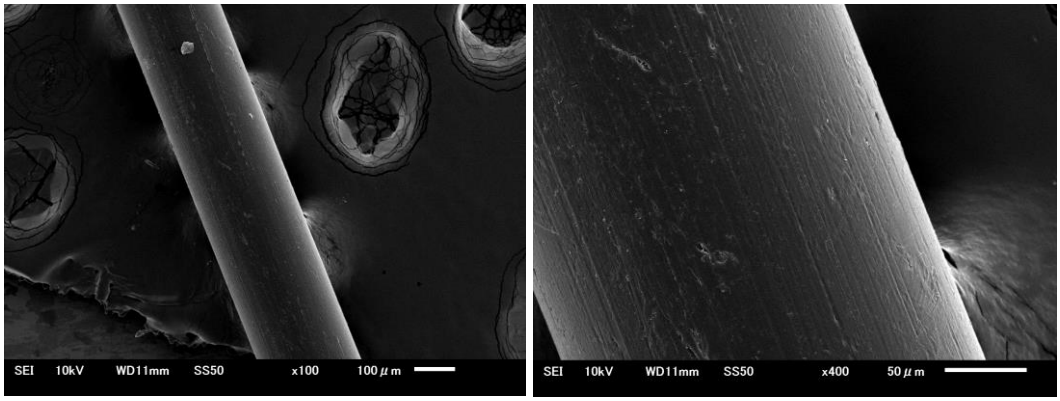

Figure 2.23 SEM image of RN fiber taken from RC beam at (left) ×100 magnification and (right) ×400 magnification.

2.7 REFERENCES

[1] S. Orasutthikul, D. Unno and H. Yokota, "Effectiveness of recycled nylon fiber from waste fishing net with respect to fiber reinforced mortar," *Construction and Building Materials,* vol. 146, pp. 594-602, 2017.

[2] ASTM C1557, "Standard test method for tensile strength and Young's modulus of fibers", ASTM International, Waste Conshohocken, PA, 2003.

[3] Corrosion criteria by half-cell potential method: Joint research report, Public Work Research Institute, Ibaraki, 2007.

[4] JIS A 1106, "Method of test for flexural strength of concrete", Japanese Standards Association, Tokyo, 2019.

[5] JIS A 1108, "Method of test for compressive strength of concrete", Japanese Standards Association, Tokyo, 2018.

[6] JIS R 5201, "Physical testing methods for cement", Japanese Standards Association, Tokyo, 2015.

[7] G. Lee, D. Han, M. C. Han, C. G. Han and H. J. Son, "Combining polypropylene and nylon fibers to optimize fiber addition for spalling protection of high-strength concrete," *Construction and Building Materials,* vol. 34, pp. 313-320, 2012.

[8] Y. Qin, X. Zhang and J. Chai, "Damage performance and compressive behavior of early-age green concrete with recycled nylon fiber fabric under an axial load," *Construction and Building Materials,* vol. 209, pp. 105-114, 2019.

[9] P. Zhang and Q. F. Li, "Effect of polypropylene fiber on durability of concrete composite containing fly ash and silica fume," *Composites Part B: Engineering,* vol. 45, no. 1, pp. 1587-1594, 2013.

[10] S. Spadea, I. Farina, A. Carrafiello and F. Fraternali, "Recycled nylon fibers as cement mortar reinforcement," *Construction and Building Materials,* vol. 80, pp. 200-209, 2015.

[11] O. B. Ozger, F. Girardi, G. M. Giannuzzi, V. A. Salomoni, C. E. Majorana, L. Fambri, N. Baldassino and R. Di Maggio, "Effect of nylon fibres on mechanical and thermal properties of hardened concrete for energy storage systems," *Materials and Design,* vol. 51, pp. 989-997, 2013.

[12] S. Lee, "Effect of Nylon Fiber Addition on the Performance of Recycled Aggregate Concrete," *Applied Sciences,* vol. 9, no. 4, p. 767, 2019.

[13] S. U. Khan and T. Ayub, "Modelling of the pre and post-cracking response of the PVA fibre reinforced concrete subjected to direct tension," *Construction and Building Materials,* vol. 120, pp. 540-577, 2016.

[14] C. Redon, V. C. Li, C. Wu, H. Hoshiro, T. Saito and A. Ogawa, "Measuring and modifying interface properties of PVA fibers in ECC matrix," *Journal of Materials in Civil Engineering,* vol. 13, no. 6, pp. 399-406, 2001.

[15] JIS A 1154, "Methods of test for chloride ion content in hardened concrete", Japan Standards Association, Tokyo, 2012.

[16] JSCE G 573, "Measurement method for distribution of total chloride ion in concrete structure", JSCE Guidelines for Concrete, Japan Society of Civil Engineers, Tokyo, 2005.

[17] I. Bertelsen and L. M. Ottosen, "Reuse of Waste Fishing Nets in Construction Materials," in *Circular Ocean Conference,* Ålesund, 2016.

[18] D. A. Silva, A. M. Betioli, P. J. Gleize, H. R. Roman, L. A. Gómez and J. L. Ribeiro, "Degradation of recycled PET fibers in Portland cement-based materials," *Cement and Concrete Research,* vol. 35, no. 9, pp. 1741-1746, 2005.

CHAPTER 3

SYNTHETIC AND RECYCLED FIBERS AS A REINFORCEMENT FIBER IN REPAIRING OF LIGHTLY CORRODED RC BEAMS

3.1 OUTLINE

This chapter investigates the effectiveness of the recycled nylon (RN) short fibers for reinforcing polymer cement mortar (PCM). Reinforced PCM is used for the repair of corroded reinforced concrete (RC) beams that were exposed to the natural deterioration environment. Materials and testing procedures are similar to those in Chapter 2 with the exposure duration for RC beams to be 2 years instead of 1 year. Two kinds of RN fibers having the same length, but different diameter were added in this study. Experimental procedures were modified.

Restorability of load-carrying capacity of the RC beams repaired with reinforced PCM is focused. In addition to the two types of RN fiber, manufactured polyvinyl alcohol (PVA) short fiber, and manufactured polyethylene (PE) microfiber were also used for comparing mechanical performances. The aim of this study is to evaluate effectiveness of the fiber reinforcement of the RN fibers and the manufactured fibers. Mechanical properties including load-carrying capacity, failure behavior and crack formation of the repaired RC beams were extensively investigated as well as the properties of the reinforced PCM.

3.2 TESTING MATERIALS

3.2.1 Fibers

There are 4 types of fibers used in this study: recycled nylon short fibers having the diameter of 0.24 (RNa) and 0.52 mm (RNb), manufactured PVA short fibers, and manufactured PE fibrillated microfibers as shown in Figure 3.1. RN fibers are the waste fishing nets for small fishes, and they are made from nylon 6-6. The RN fibers were processed by manually cut the fishing nets into designate length, and only the straight part of fiber was used for consistency of the shape of fibers. RNa and PE fibers are identical the fibers used in Chapter 2. Surface of RN fibers were observed using microscope as in Figure 3.2, and no noticeable sign of physical damage of fiber are found in the waste fishing net. The uniaxial tensile tests of RN fibers were conducted according to ASTM C1557 [1] with the constant crosshead displacement rate of 2 mm/min, and the properties of fibers are shown in Table 3.1.

Table 3.1 Properties of the fibers.

Fiber	Diameter (mm)	Length (mm)	Density (g/cm^3)	Tensile strength (MPa)
Recycled nylon type-A (RNa)	0.24	20	1.13	344
Recycled nylon type-B (RNb)	0.52	20	1.13	246
Polyvinyl Alcohol (PVA)	0.20	18	1.30	975
Polyethylene (PE)	0.01-0.1	9	1.05	n/a

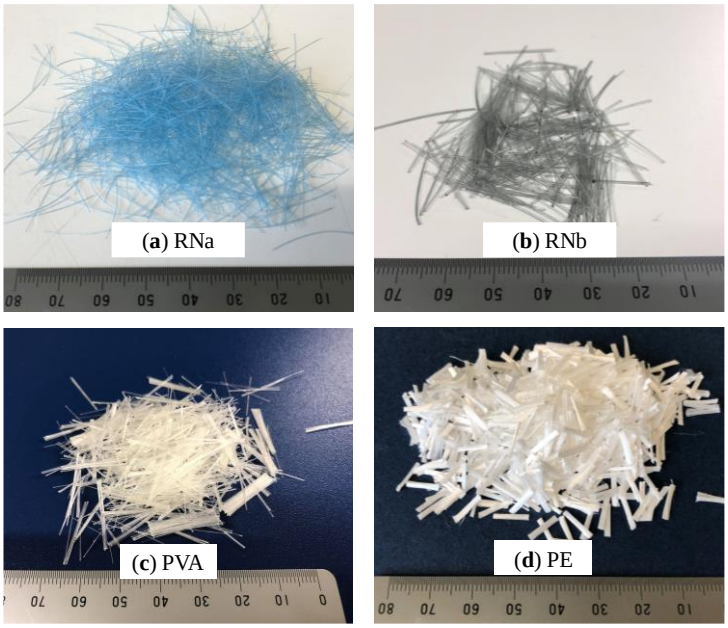

Figure 3.1 Types of fibers: (a) RNa, (b) RNb, (c) PVA, and (d) PE

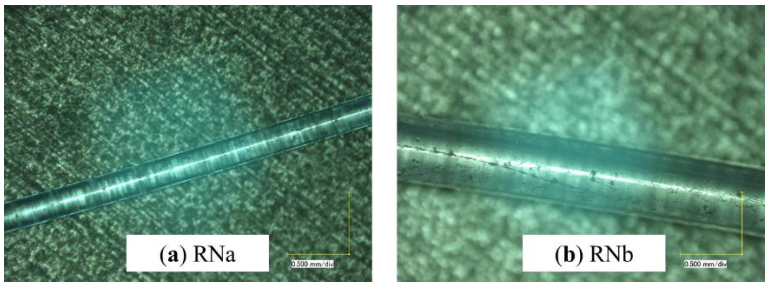

Figure 3.2 Microscope images (x100) of RN fibers: (a) RNa, (b) RNb

3.2.2 RC beams

RC beams tested in this chapter are made and thread in the same way as in Chapter 2. The beams having dimension of $900 \times 100 \times 150$ mm (length × width × height) were prepared. The beams were made using ordinary Portland cement (OPC) with the water-to-binder ratio of 0.5, and the design strength was 33 MPa. Galvanized coated steels were used as for the top reinforcement and the stirrups so that the corrosion concentrated on the bottom reinforcement. Test beams were transport to the exposure site to experience natural deterioration after curing for 7 days by wet towel.

3.2.3 Polymer cement mortar

PCM used in this chapter is the same type and was prepared in the same way as in Chapter 2. Five mixes of PCM were used: PCM with no fiber added (PCM-NF), PCM added with 0.24 mm-diameter RN (PCM-RNa), PCM added with 0.52 mm-diameter RN (PCM-RNb), PCM added PVA fiber (PCM-PVA), and PCM added with PE fiber (PCM-PE). The acrylic type PCM given from supplier in Japan was used as repair material, and the water-to-binder ratio was 0.2. Fiber fraction by volume of the reinforced PCMs were set to be 1.0% as indicated in the mix proportion of PCM in Table 3.2.

Table 3.2 Mix proportion of PCM for 25 kg batch.

Fiber	PCM (kg)	Water (kg)	Fiber (kg)	Fiber content by volume (%)
PCM-NF	25	4.93	-	
PCM-RNa	25	4.93	0.164	1.0
PCM-RNb	25	4.93	0.164	1.0
PCM-PVA	25	4.93	0.189	1.0
PCM-PE	25	4.93	0.160	1.1

3.3 EXPERIMENTAL PROGRAM

3.3.1 Exposure tests

Steel corrosion of the tested RC beams was induced by natural phenomenon. RC beams were placed in the tidal zone for 2 years, and the repair was taken place after completing the exposure. RC beams were repaired by removal of the bottom concrete cover 20 mm over the bottom reinforcement, and the removed section was sprayed with reinforced PCM. In addition, PCM specimens were also casted by directly sprayed in the 40×40×160 mm prism molds and the 50×100 mm cylinder molds for flexural and compressive tests respectively.

3.3.2 Repair operations

The tested RC beams were divided into 3 groups: control beams were stored in the laboratory room for 10 months and then tested; group A beams (upgraded RC beams) were exposed to the tidal zone for 2year; and group B beams (normal RC beams only) were repaired after the 2 year tidal exposure. The normal RC beam was directly exposed to the tide, and the repair was taken place after completing the exposure. The upgraded RC beams went through the repair operation before starting the exposure and was not further repaired even after the exposure. The details of the tested beams are listed in Table 3.3.

Exposed beams were lifted-up from the exposure side after completing exposed duration. Thereafter, repair operation of RC beams was conducted by removal of bottom surface cover up to 20 mm over the tensile rebar. After that, the removed section was then sprayed with different mixes of PCM. Repaired beams were leave in room temperature for 28 days before further tests.

Table 3.3 Name and conditions of the tested RC beams.

Specimen name	Condition	Exposure	Sprayed material
Control beam			
RC0	Normal RC	No	
Group A			
RNa2	PCM sprayed before exposure	2 years	PCM-RNa
PE2	PCM sprayed before exposure	2 years	PCM-PE
Group B			
RC2	Normal RC	2 years	
RC2-NF	Repair after exposure	2 years	PCM-NF
RC2-RNa	Repair after exposure	2 years	PCM-RNa
RC2-RNb	Repair after exposure	2 years	PCM-RNb
RC2-PVA	Repair after exposure	2 years	PCM-PVA
RC2-PE	Repair after exposure	2 years	PCM-PE

3.3.3 Loading tests

Four-point flexural tests were conducted on the RC beams following the JIS A 1106 [2]. Experimental setup is shown in Figure 3.3. Four linear variable differential transformers (LVDTs) were used for measuring deflection; 2 LVDTs at the mid-span and 2 LVDTs at each end supports. Strain gauge were also attached at the top and bottom surface at the midspan of the beam.

For PCM specimens, compressive strength tests and the three-point flexural tests were conducted in accordance with JIS A 1108 [3] and JIS R 5201 [4] respectively. A pi-type gauge was installed on the bottom surface of the prism PCM specimens to measure cracks opening during load application. Experimental setup for PCM specimens is shown in Figure 3.4. Those specimens were air cured for 28 days before testing.

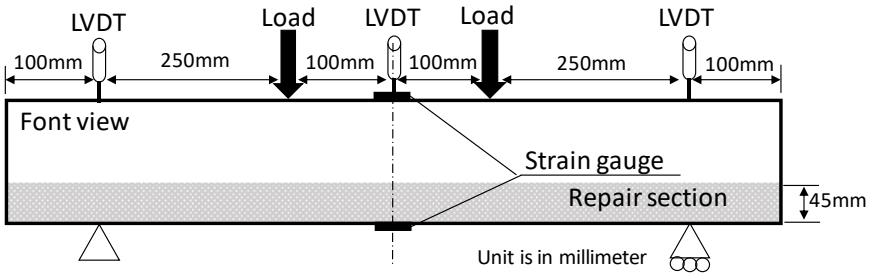

Figure 3.3 Experimental setup for RC beams.

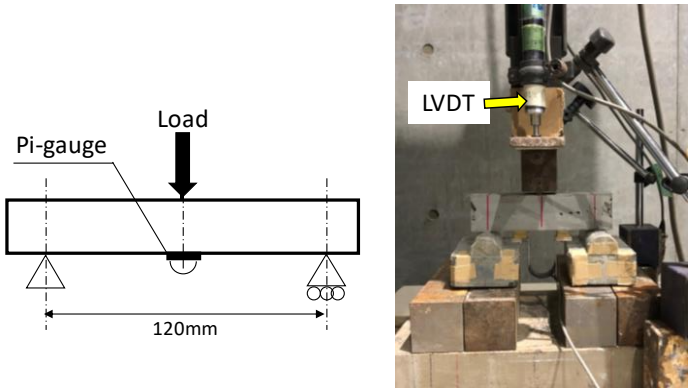

Figure 3.4 Experimental setup for PCM specimens.

3.4 RESULTS AND DISCUSSIONS

3.4.1 Flowability of fresh PCM

Flow diameter of PCM mixes were measured at the time of the spraying following JIS R 5201 [4]. Table 3.4 shows results of the flow diameter. Flow diameter of PCM-RNa and PCM-RNb reduced by approximately 1% while PCM-PE reduced by 24%. The addition of RNa, RNb and PVA fibers seemed to have neglectable effect on the flow diameter of fresh PCM except the PCM-PE that showed considerable reduction of flow diameter. The fibrillated characteristic of PE fibers and the relatively small in diameter and length of PE fibers may be the reason of lower flowability. Spadea et al. [5], and Orasutthikul et al. [6] also reported a slightly reduction of flow ability of fresh OPC mortar in the range of 5-10%; however, the smooth surface of RN fibers and the characteristic of PCM may affect the flowability. Further investigations are still needed.

Table 3.4 Flow diameters.

Specimen name	Flow diameter (mm)	%Δflow diameter
PCM-NF	165	-
PCM-RNa	164	-0.7
PCM-RNb	163	-1.4
PCM-PVA	170	2.7
PCM-PE	126	-23.7

3.4.2 Mechanical properties of PCM specimens

Compressive strength tests and the three-point flexural tests were conducted on PCM specimens, and the results are summarized in Table 3.5. Results shown in the table are the averaged of three specimens in each PCM mix.

The addition of fiber, regardless the fiber type, did not show clear influence on the compressive strength. PCM-PVA had slightly higher strength of 3.7% compared to PCM-NF. However, the addition of RNa, RNb and PVA fibers gave adverse effect to the flexural strength of reinforced PCM. Flexural strength of PCM-RNa, PCM-RNb and PVA reduced by 27%, 28% and 16%, respectively while only PCM-PE showed improvement of flexural strength at 37%. Karahan et al. suggested that fibers created voids inside the cement matrix and reduced modulus of elasticity [7]. Results showed that neither the addition of RN fibers nor the different in fiber diameter did not contribute to the improvement in compressive strength but rather diminish the flexural strength of mortar.

Table 3.5 Compressive strength tests and flexural strength tests results.

	Compressive strength tests			Flexural strength tests			
	f'_c (MPa)	*SD*	%Δ f'_c	P_{cr} (kN)	f_b (MPa)	*SD*	%Δ f_b
PCM-NF	43.6	4.95	-	3.50	9.84	0.30	-
PCM-RNa	43.9	3.33	0.7	2.56	7.19	0.43	-27.0
PCM-RNb	43.4	3.55	-0.4	2.53	7.11	0.21	-27.8
PCM-PVA	45.2	0.90	3.7	2.94	8.28	0.19	-15.9
PCM-PE	43.9	3.44	0.7	4.78	13.44	0.27	36.5

Note: f'_c is the compressive strength, *SD* is the standard deviation, %Δ f'_c is the percent difference in compressive strength compared to PCM-NF, P_{cr} is the maximum load, f_b is the flexural strength, and %Δ f_b is the percent difference in flexural strength compared to PCM-NF.

Load-midspan deflection curves of PCM specimens are shown in Figure 3.5. The load of PCM-NF, PCM-RNa, PCM-RNb suddenly dropped to zero after it reached the peak while PCM-PVA remain some of the post-peak loads at approximately of 0.5kN. For PCM-PE, the load dropped at approximately 3.4 kN and increased again to 4.8kN, then slowly dropped to zero. Adding RNa or RNb seems not contribute any post-peak loads, and stresses cannot transfer through the cracks via RN fibers. This behavior was supported by Orasutthikul et al. that recycled nylon fiber reinforced cement mortar gives only little amount of the post-peak load [6]. PVA and PE fibers help transferring stress even after the cracks occurred and provide additional strength after the peak load.

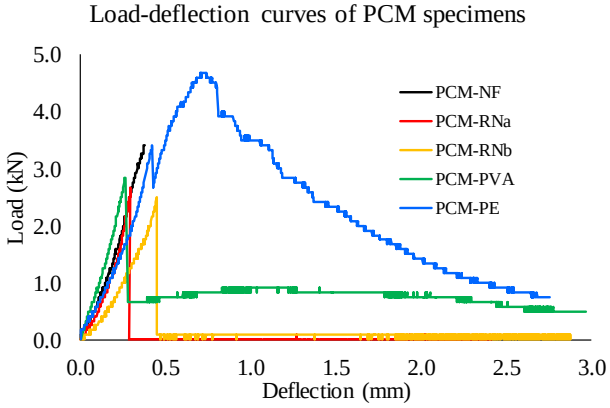

Figure 3.5 load-midspan deflection curves of PCM specimens.

3.4.3 Crack openings of PCM specimens

Crack openings was measured at the bottom of the PCM specimens during the load application as shown in Figure 3.6, and the cracks on the bottom surface of the specimens are shown in Figure 3.7. In all specimens, crack opening increased linearly until the peak. Cracks in PCM-NF increasing drastically after it reached the peak load. For PCM-RNa and PCM-RNb, crack opening increased rapidly while the load dropped to zero, however, PCM-PVA retain the post-peak load at about 0.6 kN. Crack opening in PCM-PE was found increasing as the post-peak load increased.

After the flexural test, PCM-NF split into 2 pieces while other PCM specimens remained together with large cracks observed on the side surface. PCM-RNa, PCM-RNb, and PCM-PVA had a single wide crack at the middle. Even though adding RNa, RNb and PVA fibers did not contribute to any pose-peak flexural load, the addition of fiber helps improve integrity and prevent abrupt failure of structure as in PCM-NF. On the contrary, PCM-PE had one wide crack at the middle with a few small cracks aside of the main crack. The damage to the structure was dispersed from one single wide crack into many of smaller cracks with the addition of PE fibers.

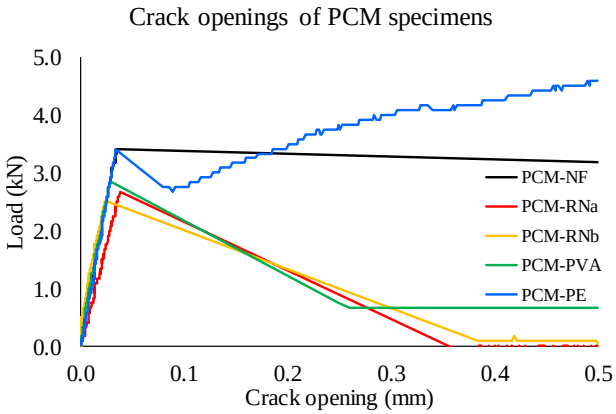

Figure 3.6 Crack openings of PCM specimens.

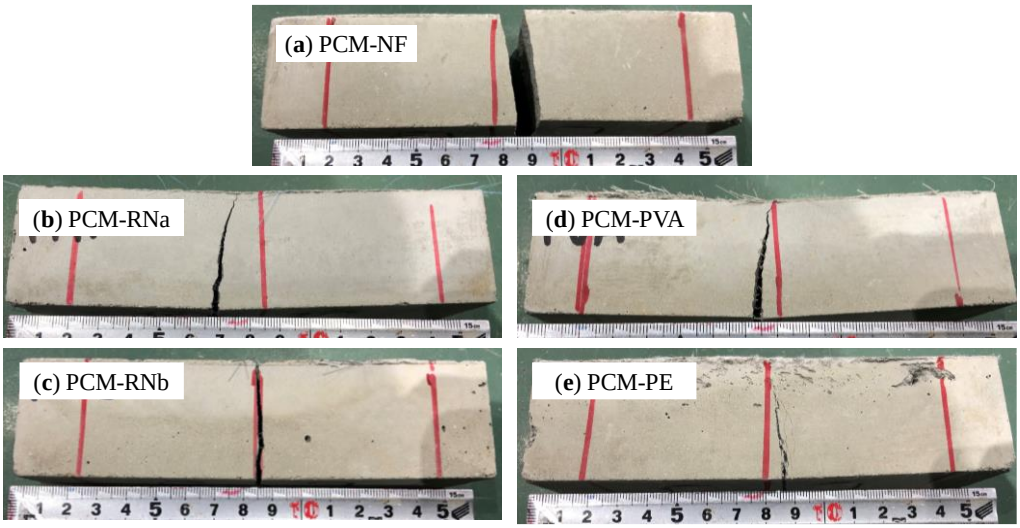

Figure 3.7 PCM specimens after the flexural tests.

3.4.4 **Load-carrying capacity of the RC beams**

Results from the four-point bending tests are summarized in Table 3.6 Four-points flexural test results and the load-midspan displacement curves are shown in Figure 3.8. The curves show only one beam in each testing condition since it was observed that the representative two beams with the same repair material having the identical behavior. Upgraded beams in group A showed improvement in the flexural capacity at 6% and 21% for RNa2 and PE2, respectively. PE fiber still gave superior performance than RNa fiber; however, the increase in flexural capacity of group A beam was attributed to the sprayed PCM.

For group B, RN2 gave slightly higher load-carrying capacity than the control beams (RC0) probably due to the longer curing period. RC2-PE showed the highest ultimate load followed by PCM-PVA, PCM-RNa, PCM-NF and PCM-RNb. RC beams that were sprayed with PCM-PE gave 27% higher flexural capacity than the control beams while other repaired beams (PCM-PVA, PCM-RNa and PCM-RNb) showed improvement in flexural capacity in the range of 8-17%. RC2-PVA had slightly higher flexural capacity than RC2-RNa, RC2-RNb because of the higher tensile strength of PVA fiber. RC2-RNb expressed marginally lower flexural capacity than that of the RC2-RNa. This phenomenon indicated that using larger diameter of RN fiber such as RNb does not improve flexural capacity of the mortar due to the fact that RNb has lower tensile strength than RNa. Results of the repaired beams are in agreement with the flexural strength of PCM material studied in section 3.4.2.

Table 3.6 Four-points flexural test results

Specimen name	P_y (kN)	P_u (kN)	$\%\Delta P_y$	$\%\Delta P_u$	Failure type	Mass loss of each tensile bar (%)	
Control beams							
RC0 (1)	49.1	59.6	-	-	Flexural	-	
RC0 (2)	48.1	60.9	-	-	Flexural	-	
Group A							
RNa2	49.43	63.6	1.7	5.6	Flexural	0.7	0.6
PE2	64.24	72.93	32.2	21.0	Flexural-shear	1.3	0.6
Group B							
RC2	43.79	60.86	-9.33	1.03	Flexural-shear	0.9	2.7
RC2	50.88	69.87	4.65	15.99	Flexural	1.3	1.7
RC2-NF (1)	49.91	67.94	2.66	12.79	Flexural-shear	0.9	0.5
RC2-NF (2)	52.31	67.91	7.59	12.74	Flexural-shear	0.2	0.3
RC2-RNa (1)	51.98	69.46	6.91	15.31	Flexural-shear	1.5	1.6
RC2-RNa (2)	51.54	67.69	6.01	12.82	Flexural-shear	0.9	1.6
RC2-RNb (1)	48.78	67.94	0.33	12.79	Flexural	1.2	0.9
RC2-RNb (2)	50.15	63.1	3.15	4.75	Flexural	1.0	0.9
RC2-PVA (1)	50.41	69.52	3.68	15.41	Flexural-shear	1.3	0.6
RC2-PVA (2)	60.06	71.72	23.53	19.06	Flexural-shear	0.9	0.9
RC2-PE (1)	60.86	70.84	25.18	17.60	Flexural	1.0	1.0
RC2-PE (2)	61.19	82.04	25.86	36.19	Flexural	0.8	1.1

Note) P_y is the yield load and P_u is the ultimate load and $\%\Delta P_y$ and $\%\Delta P_u$ are the percent difference in P_y and P_u compared to the average of RC0 (1) and RC0 (2), respectively.

Tested beams were demolished just after the tests. Bottom tensile rebars were carefully taken from the RC beams and washed with diammonium hydrogen citrate solution. Rebar mass losses were measured by comparing the weight of tensile rebar before and after the test, and the percentage of rebar mass losses are summarized in Table 3.6 Four-points flexural test results. All the exposed beams had an average rebar mass loss of 1-3% except for the PCM-NF that had lower than 1% mass loss. The lower mass loss of PCM-NF may be the reason for high flexural capacity of PCM-NF even though no reinforcement fiber. Overall, the exposed beams showed corresponding corrosion level.

Spraying reinforced PCM not only restore the load-carrying capacity of the beams to its original level but also increase the flexural capacity of the beams. Flexural capacity of the RC beams deteriorated by the corrosion of tensile rebars can be compensated with the sprayed PCM reinforced with fibers. The results conclude that RN fiber can be used as reinforcement material in cement mortar. Although effectiveness of the RN fibers still inferior than that of the PE fibers, RN fibers has a comparable performance to the manufactured PVA fibers.

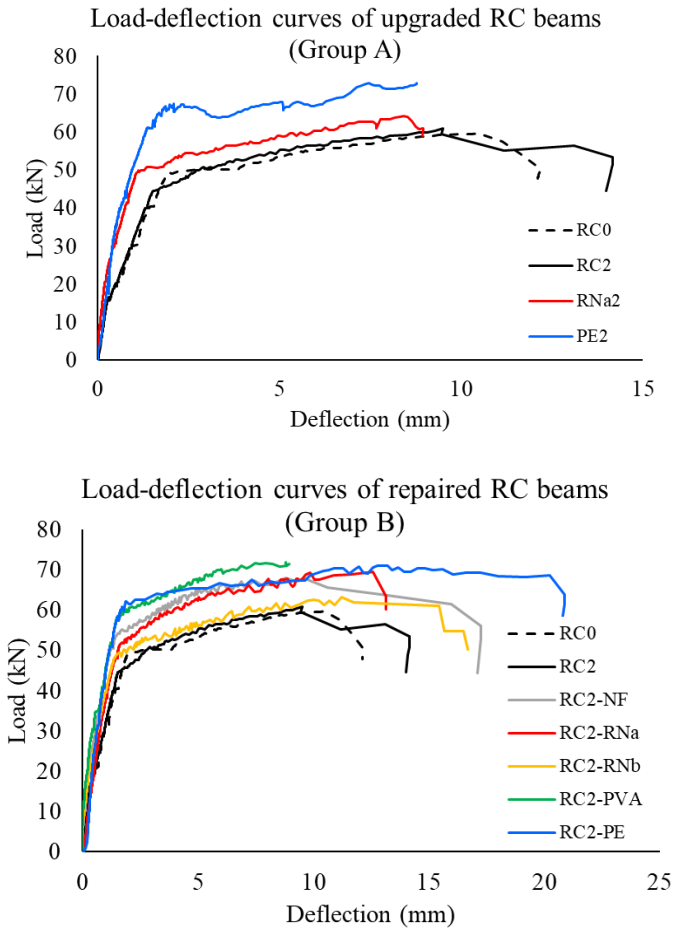

Figure 3.8 Load-deflection curves of RC beams.

3.4.5 Final crack formation

Figure 3.9 shows final crack patterns at the side surface of the beams after the test. Only a few cracks were observed on RC2 while the beams sprayed with PCM had many cracks. Especially, RC2-RNa cracks tend to spread through the end supports. Many of small vertical cracks were also observed on the beams sprayed with PCM-PE (PE2 and RC2-PE) with one or two wide cracks. PCM-NF expressed a brittle failure as the PCM layer spell of from the beam and the delamination of PCM was observed. Using PCM without reinforcement fiber is not recommend due to the brittle characteristic of the non-fiber PCM. Adding fibers, particularly PE fiber, helps distribute damage from large crack into many small cracks. It can be concluded that fibers improve integrity of the structure and prevent spalling of concrete during fracture.

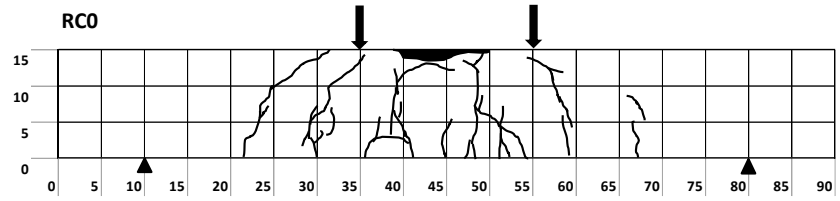

(a) RC0

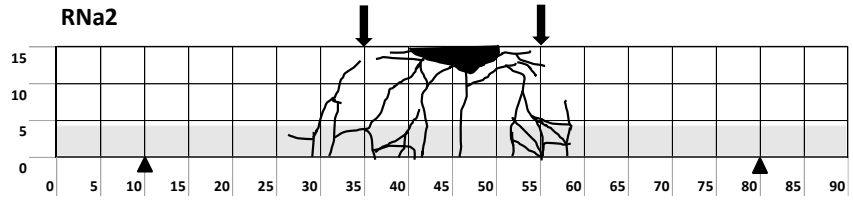

(b) RNa2

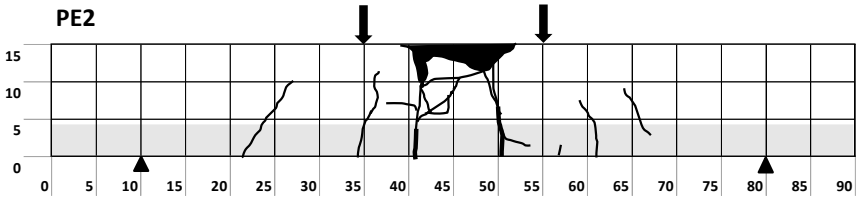

(c) PE2

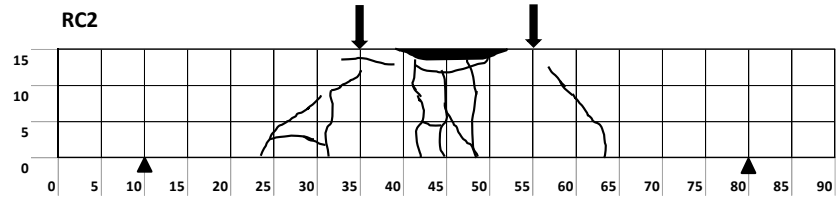

(d) RC2

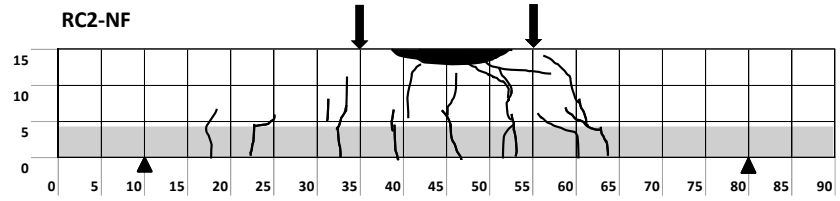

(e) RN2-NF

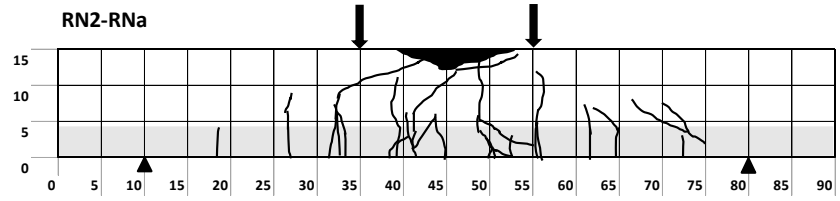

(f) RN2-RNa

Figure 3.9 Final crack formation of RC beams.

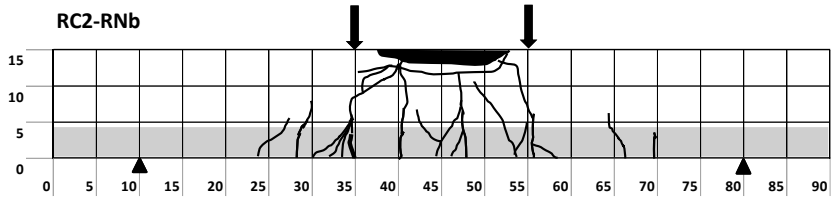

(g) RN2-RNb

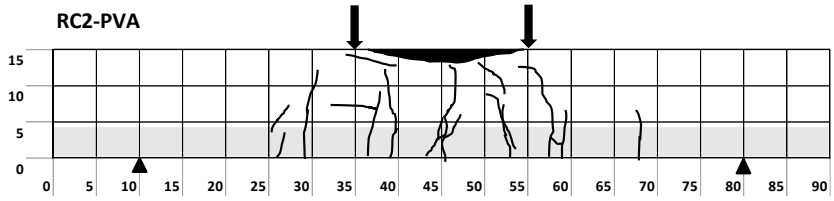

(h) RN2-PVA

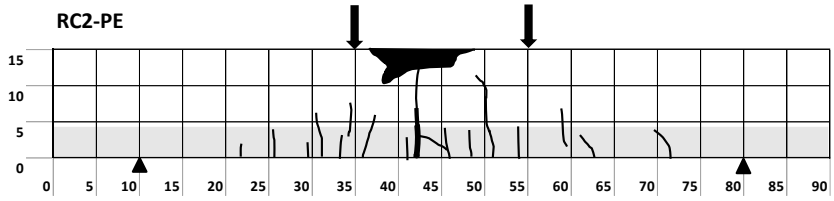

(i) RN2-PE

Figure 3.9 Final crack formation of RC beams. (cont.)
(unit shown are in centimeter)

3.5 REFERENCES

[1] ASTM C1557, "Standard Test Method for Tensile Strength and Young's Modulus of Fibers," American Society for Testing and Materials, 2003.

[2] JIS A 1106, "Method of test for flexural strength of concrete," Tokyo, Japan Standards Association, 2019.

[3] JIS A 1108, "Method of test for compressive strength of concrete," Tokyo, Japan Standards Association, 2018.

[4] JIS R 5201, "Physical testing methods for cement," Tokyo, Japan Standards Association, 2015.

[5] S. Spadea, I. Farina, A. Carrafiello and F. Fraternali, "Recycled nylon fibers as cement mortar reinforcement," *Construction and Building Materials,* pp. 200-209, 2015.

[6] S. Orasutthikul, D. Unno and H. Yokota, "Effectiveness of recycled nylon fiber from waste fishing net with respect to fiber reinforced mortar," *Construction and Building Materials,* pp. 594-602, 2017.

[7] O. Karahan and C. D. Atiş, "The durability properties of polypropylene fiber reinforced fly ash concrete," *Materials and Design,* pp. 1044-1049, 2011.

CHAPTER 4

EFFECTIVE DIFFUSION COEFFICIENT OF CHLORIDE ION IN MORTAR REINFORCED WITH RECYCLED FIBERS BY MIGRATION

4.1 OUTLINE

This chapter discusses the chloride ion resistivity of mortar that were reinforced with recycled nylon (RN) short fibers from the used fishing nets and the manufactured polyethylene (PE) microfibers. Two kinds of cementitious material were investigated which are ordinary Portland cement (OPC) and the polymer cement mortar (PCM). This study mainly focuses on the determination of the effective diffusion coefficient of the chloride ion using chloride migration tests. Test specimens were installed in migration cell. After running migration cell for a certain time, solution was collected, and the chloride ion concentrations were measured. The effective diffusion coefficient was then calculated and compared with various mixes. In addition, flowability of fresh mortar and the compressive strength were also investigated.

4.2 EXPERIMENTAL PROGRAMS

4.2.1 Sample preparation

Mortar cylinder specimens measuring 100 mm in diameter and 200 mm in height were casted. Two kinds of specimen were made, ordinary Portland cement (OPC) mortar and polymer cement mortar (PCM). For OPC, the water-to-cement ratio (W/C) was 0.5 and the sand-to-cement ratio (S/C) was set to be 3.0. Mix proportion of OPC specimens are shown in Table 4.1. PCM used in this study is the same type and same mix proportion as that used for spraying RC beams in Chapter 2 and 3. It should be noted that PCM was mixed using hand mixer and casted in a plastic mold instead of spraying through the nozzle (Figure 4.1). In addition, small cylinder specimens having diameter of 50mm and height of 100 mm were also casted for both OPC and PCM mixes to study compressive strength. All specimens were cure in water for 28 days before further experiments.

Table 4.1 Mix proportion of mortar specimen (per cubic meter).

Water (kg)	Cement (kg)	Sand (kg)	W/C	S/C
255	510	1500	0.5	3.0

Figure 4.1 Mixing of PCM.

Ten mixes of OPC and PCM were prepared. Recycled nylon (RN) short fiber obtained by manually cutting used fishing nets and the manufactured Polyethylene (PE) microfiber were introduced in the mix. RN and PE fiber used in this chapter is the same as RNa and PE in Chapter 2 and 3, respectively. Fiber content by volume was varied from 0.5% to 2.0%. Details in each mix are shown in Table 4.2. After 28 days of curing in water, specimens were cut with an automatic cutter into three dice specimens having 50 mm thick as shown in Figure 4.2. The top and bottom cap were removed, and the middle of three-disc specimens were used for the migration tests. The side of disc specimens was coated with epoxy resin to make one dimensional chloride ion migration.

Table 4.2 Name and condition of test specimens.

Name	Fiber	Fiber content (vol%)
OPC-NF	-	-
OPC-RN0.5%	RN	0.5
OPC-RN1.0%	RN	1.0
OPC-RN2.0%	RN	2.0
OPC-PE0.5%	PE	0.5
OPC-PE1.0%	PE	1.0
PCM-NF	-	-
PCM-RN1.0%	RN	1.0
PCM-PE1.0%	PE	1.0
PCM-PE2.0%	PE	2.0

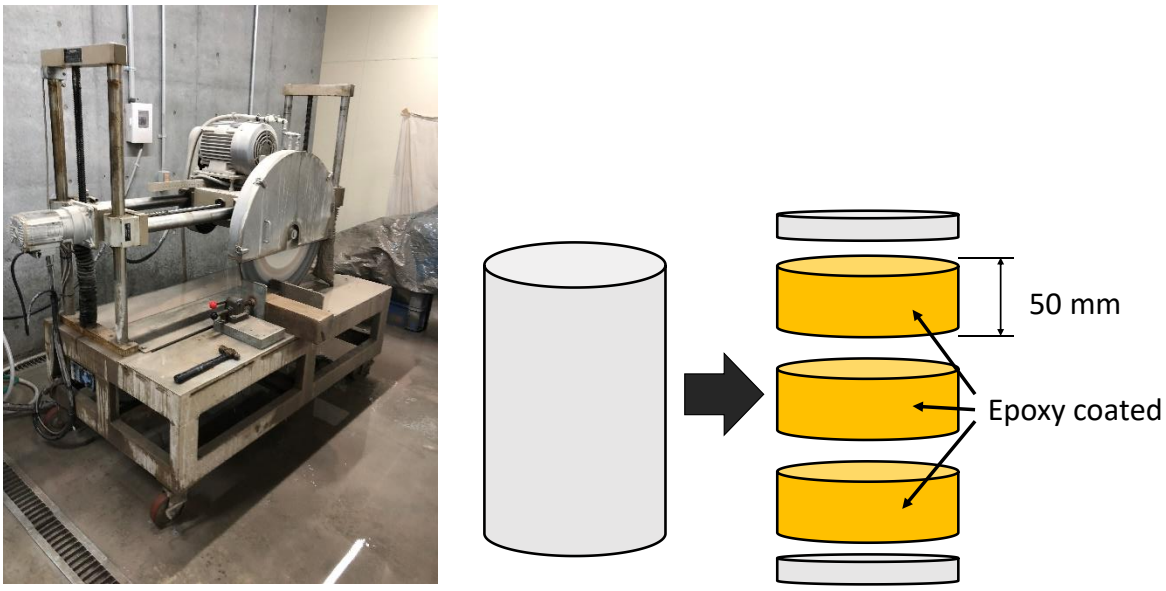

Figure 4.2 (Left) automatic cutter and (right) disc specimens.

4.2.2 Migration test

Chloride migration tests were conducted according to JSCE-G751-2003 [1]. Disc specimens were saturated in water under vacuum for 24 hours. Thereafter, test specimen was put in rubber block, then sealed with silicone. The block was subsequently installed in the migration cell. The migration cell comprised of the anode tank containing 0.3 mol/L of NaOH solution and the cathode tank having 0.5 mol/L NaCl solution as shown in Figure 4.3. Test specimen in rubber block was placed between two tanks so that it acts as a passing membrane. Titanium plate electrodes were installed in both tanks and connected with 15V constant DC source so that the chloride ions migrate into the pore solution of the concrete from cathode side to anode side through test specimen. Concentration of chloride ion in anode side were measured periodically to calculate chloride ion flux. Chloride ion concentrations were measured until the chloride ion flux reached steady state. Figure 4.4 shows experimental setup for migration test.

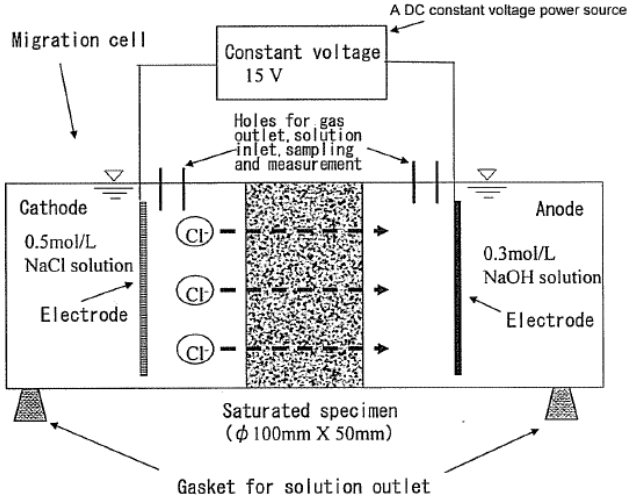

Figure 4.3 Drawing of migration cell.

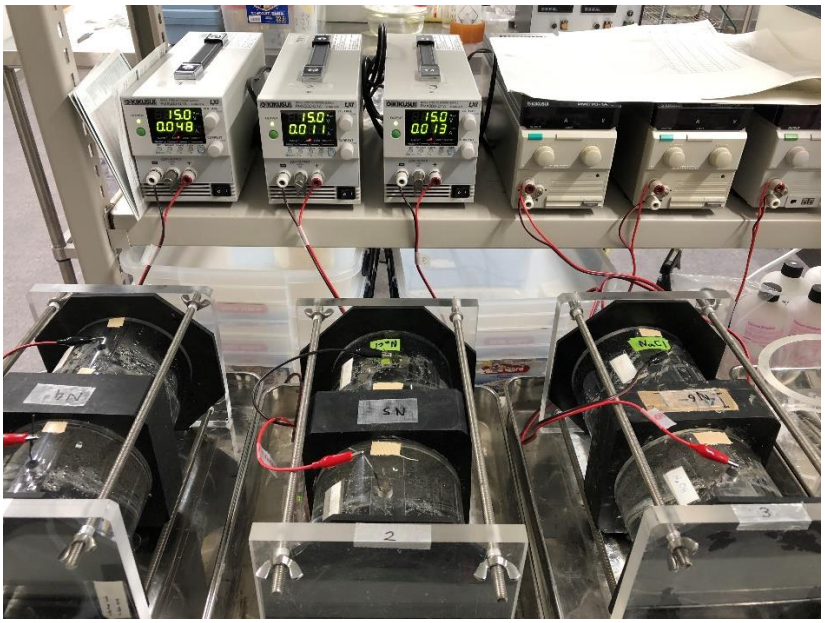

Figure 4.4 Experimental setup of migration cell.

4.2.3 Measurement procedure

Chloride ion concentrations in anode side were measured using potentiometric titrator (Figure 4.5). Silver nitrate ($AgNO_3$) solution of 0.1 Mol/L was used as a titrant. Supplied current, temperature and chloride ion concentration in cathode tank were also monitored periodically. The sampling interval was set at every 24 hours; however, sampling time may change to every 12 hours if the chloride ion concentration increased rapidly. Measurement data were carefully record during the testing period. The experiment ended when the increment of chloride ion concentration in anode tank become steady for the 5 consecutive measurements.

Figure 4.5 Potentiometric titrator.

4.2.4 Calculation of effective diffusion coefficient

Chloride ion concentration in anode tank were plotted against time. The flux of the chloride ions was calculated when the reaction reached steady state (i.e. the increasing of the chloride ion concentration in anode side become steady for 5 consecutive measurements as indicated in Figure 4.6) according to the following equation:

$$J_{cl} = \frac{V}{A}\frac{\Delta c_{cl}}{\Delta t}$$

Where, J_{cl} : Flux of chloride ions in steady state (mol/ (cm^2 year))

V : Volume of anode solution (L) (Neglect the deduction from sampling)

A : Cross section of the specimen (cm^2)

$\Delta c_{cl}/\Delta t$: Increment of chloride ion concentration in anode side ((mol/l)/year)

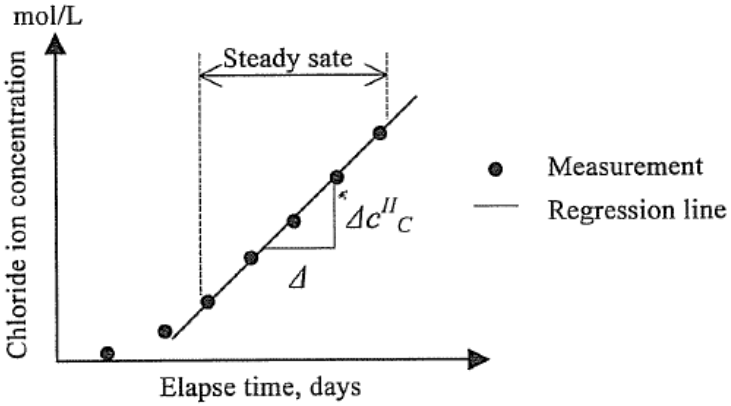

Figure 4.6 Plot of the chloride ion concentration in anode tank.

The effective diffusion coefficient of chloride ion in the tested samples were then calculate using the following equation:

$$D_e = \frac{J_{cl}RTL}{A|Z_{cl}|FC_{cl}(\Delta E - \Delta E_c)} \times 100$$

Where, D_e : Effective diffusion coefficient (cm^2 year)

R : Gas constant (= 8.31 J/ (mol K))

T : Absolute temperature (K)

Z_{cl} : Charge of chloride ion (= -1)

F : Faraday constant (= 96,500 C/mol)

C_{cl} : Measured chloride ion concentration in cathode side (mol/l)

$\Delta E - \Delta E_c$: Electrical potential difference between specimen surfaces (V)

L : Length of specimen (mm)

4.3 RESULTS AND DISCUSSIONS

4.3.1 Effective diffusion coefficient

Effective diffusion coefficient (D_e) obtained from the migration tests are shown in Figure 4.7. Error bars are also shown. It should be mentioned that results are averaged of 3 test samples. OPC specimens showed D_e at a range between 1.5 – 2.0 cm^2/year while PCM specimens showed an extremely low D_e at approximately 0.1 - 0.15 cm^2/year. Furthermore, during the experiment, OPC specimens took 5-7 days for reaching steady state, but PCM specimens took over 20 days. Adding fibers seems to lower D_e for the fiber content up to 1.0% for OPC and 0.5% for PE, respectively compared to plain mortar (OPC-NF). When fiber content is more than 1.0%, D_e tended to be increased. However, the effect of the type of fiber and the fiber content are still unclear, and type of mortar and the water-to-binder ratio still main factor govern the effective diffusion coefficient.

The decrease in D_e value when adding fibers was suggested by Ramezanianpour et al. that fibers reduce permeability and capillary porosity by pore blocking effect; therefore, ions penetration are reduced due to the reduction in inner pore connectivity [2]. On the contrary, the increase in D_e was probably due to the fact that high content of fiber increases porosity in cement matrix since fibers trap air in cement mixture [3, 4, 5].

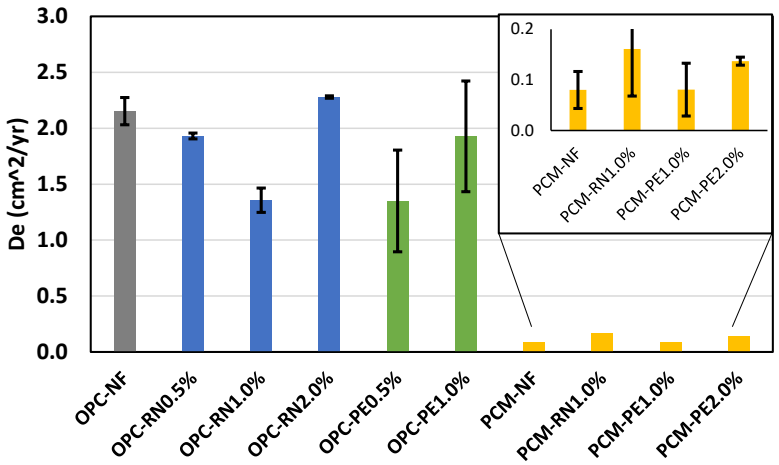

Figure 4.7 Results from migration tests.

4.3.2 Flowability of fresh mortar

Flow diameter in each mix were measured as per JIS R 5210 [6]. Flow diameter of fresh mortar and the changed in flow diameter compared with OPC-NF are shown in Table 4.3. Adding fiber reduced flowability of fresh mortar, especially at high fiber content. At 1.0% fiber content, PE caused further reduction of flowability than RN for both OPC and PCM mixes. The reduction in flowability was up to 37.4% for OPC and 21.1% for PCM with the addition of PE fiber at 1.0% by volume. Experimental results showed that applying PE fibers in OPC reduced flowability more than those of using PCM. On the other hand, at 1.0% fiber content, adding RN fiber reduce flowability about 2.0% for both OPC and PCM mixes, and the effect is considered negligible. It is concluded that RN fibers does not affect to the flowability of fresh mortar and PCM because of the smooth surface of fiber.

The reduction in flowability with the addition of fibers was reported by Spadea et al. that applying fibers reduced flowability especially with fibers that have high aspect ratio [7]. It is possible that when fiber fraction increased the number of fiber per unit volume mortar become larger, so it increase obstructive effect of fibers [4]. In addition, Orasutthikul et al. reported the fiber ball effect that fibers in cement mix formed a fiber cluster causing the reduction of flow ability [8]. Since PE fiber had exceedingly small diameter and had lower density than RN, more amounts of PE fiber are needed to comprise the same fiber fraction compering to RN. Therefore, PE has greater surface area and more easily to be dispersed in the mix. PE fiber may act as a mesh to cover all over the mortar surface, thus adding friction in the flow.

Table 4.3 Compressive strength and flowability of tested specimens.

Name	f'_c (MPa)	*SD*	$\%\Delta f'_c$	Flow diameter (mm)	%Δflow
OPC-NF	38.6	3.97	-	169	
OPC-RN0.5%	51.2	4.92	32.5	187	10.5
OPC-RN1.0%	45.5	5.19	17.7	166	-1.7
OPC-RN2.0%	37.2	0.09	-3.7	152	-10.0
OPC-PE0.5%	31.5	3.97	-18.5	141	-16.5
OPC-PE1.0%	28.5	2.81	-26.2	106	-37.4
PCM-NF	41.5	5.82	7.5	167	-1.3
PCM-RN1.0%	38.5	10.29	-0.3	169	-0.4
PCM-PE1.0%	44.6	6.23	15.4	134	-21.1
PCM-PE2.0%	50.2	1.47	29.9	120	-29.0

Note: f'_c is the compressive strength, *SD* is the standard deviation, $\%\Delta f'_c$ is the percent difference in compressive strength compared to OPC-NF, %Δflow is the percent different in flow diameter compared to OPC-NF.

4.3.3 Compressive strength

Compressive strength tests as per JIS A 1108 were conducted on cylinder specimens [9]. Three cylinder specimens were experimented in each mix and results are shown in Table 4.3. Adding fiber was found both improvement and diminishment in compressive strength. For OPC mixes, adding RN fiber increased compressive strength of mortar up to 32.5% for OPC-RN0.5%, but for PE fiber, the reduction of compressive strength was observed at 26.2% for PCM-PE1.0%. However, for PCM mixes, adding PE fiber seems to have positive effect since PCM-PE2.0% showed increasing in compressive strength at 29.9%, but for PCM-RN1.0%, compressive strength seems to be unchanged.

The effect of fibers to the compressive strength of mortar is still unclear. Many researchers reported the decreasing [8, 7], increasing [10, 11] and no changed [12, 13, 14] of the compressive strength of mortar. It is possible that fiber improves lateral tensile strength by forming fiber networks in mortar, so the compressive strength is increased [10, 15, 16]. However, adding fiber may increase voids in cement mix and reduce modulus of elasticity of mortar [8, 10]. In addition, it was observed during the mixing of OPC-PE1.0% that PE fibers absorb water in the mix, and it is difficult to form in the mold. Therefore, OPC with more than 1.0% PE fiber cannot be made.

4.3.4 Failure after compressive tests

Test specimens experiencing compressive tests were carefully examined to study failure behavior. Figure 4.8 shows cylinder specimens after the compressive tests. OPC-NF and PCM-NF expressed a quite brittle failure that some parts of mortar spalled-off. Test specimens that reinforced with RN and PE fibers showed a more ductile failure with some lateral cracks. Cracks seem to spread into many of small cracks in OPC-PE2.0% and PCM-PE2.0%. Test specimens with reinforced fiber remain together in one piece after the test. It was also reported that adding fibers improves integrity of the mortar because fiber formed a reinforcement networks that hold the specimen together even cracks occurred [17]. This phenomenon was observed in the case of OPC-RN2.0% that fiber prevented spalling of mortar as shown in Figure 4.9.

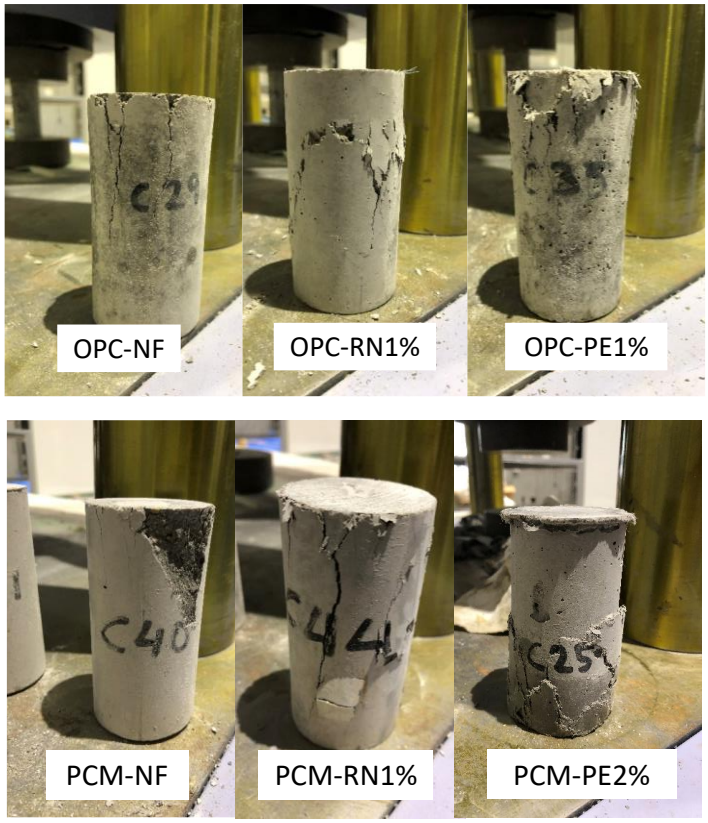

Figure 4.8 Cylinder specimens after the compressive tests.

Figure 4.9 Failure plane of OPC-RN2.0%.

4.4 REFERENCES

[1] JSCE G571, “Test method for effective diffusion coefficient of chloride ion in concrete by migration”, Japan Society of Civil Engineers, Tokyo, 2003.

[2] A. A. Ramezanianpour, M. Esmaeili, S. A. Ghahari and M. H. Najafi, "Laboratory study on the effect of polypropylene fiber on durability, and physical and mechanical characteristic of concrete for application in sleepers," *Construction and Building Materials,* vol. 44, pp. 411-418, 2013.

[3] G. Lee, D. Han, M. C. Han, C. G. Han and H. J. Son, "Combining polypropylene and nylon fibers to optimize fiber addition for spalling protection of high-strength concrete," *Construction and Building Materials,* vol. 34, pp. 313-320, 2012.

[4] P. Zhang and Q. F. Li, "Effect of polypropylene fiber on durability of concrete composite containing fly ash and silica fume," *Composites Part B: Engineering,* vol. 45, no. 1, pp. 1587-1594, 2013.

[5] R. Siddique, J. Khatib and I. Kaur, "Use of recycled plastic in concrete: A review," *Waste Management,* vol. 28, no. 10, pp. 1835-1852, 2008.

[6] JIS R 5201, “Physical testing methods for cement”, Japanese Standards Association, Tokyo, 2015.

[7] S. Spadea, I. Farina, A. Carrafiello and F. Fraternali, "Recycled nylon fibers as cement mortar reinforcement," *Construction and Building Materials,* vol. 80, pp. 200-209, 2015.

[8] S. Orasutthikul, D. Unno and H. Yokota, "Effectiveness of recycled nylon fiber from waste fishing net with respect to fiber reinforced mortar," *Construction and Building Materials,* vol. 146, pp. 594-602, 2017.

[9] JIS A 1108, “Method of test for compressive strength of concrete”, Japanese Standards Association, Tokyo, 2018.

[10] O. B. Ozger, F. Girardi, G. M. Giannuzzi, V. A. Salomoni, C. E. Majorana, L. Fambri, N. Baldassino and R. Di Maggio, "Effect of nylon fibres on mechanical and thermal properties of hardened concrete for energy storage systems," *Materials and Design,* vol. 51, pp. 989-997, 2013.

[11] Y. Qin, X. Zhang and J. Chai, "Damage performance and compressive behavior of early-age green concrete with recycled nylon fiber fabric under an axial load," *Construction and Building Materials,* vol. 209, pp. 105-114, 2019.

[12] D. A. Silva, A. M. Betioli, P. J. Gleize, H. R. Roman, L. A. Gómez and J. L. Ribeiro, "Degradation of recycled PET fibers in Portland cement-based materials," *Cement and Concrete Research,* vol. 35, no. 9, pp. 1741-1746, 2005.

[13] L. A. Pereira De Oliveira and J. P. Castro-Gomes, "Physical and mechanical behaviour of recycled PET fibre reinforced mortar," *Construction and Building Materials,* vol. 25, no. 4, pp. 1712-1717, 2011.

[14] S. Yin, R. Tuladhar, J. Riella, D. Chung, T. Collister, M. Combe and N. Sivakugan, "Comparative evaluation of virgin and recycled polypropylene fibre reinforced concrete," *Construction and Building Materials,* vol. 114, pp. 134-141, 2016.

[15] S. Lee, "Effect of Nylon Fiber Addition on the Performance of Recycled Aggregate Concrete," *Applied Sciences,* vol. 9, no. 4, p. 767, 2019.

[16] S. U. Khan and T. Ayub, "Modelling of the pre and post-cracking response of the PVA fibre reinforced concrete subjected to direct tension," *Construction and Building Materials,* vol. 120, pp. 540-577, 2016.

[17] Y. Qin, X. Zhang and J. Chai, "Damage performance and compressive behavior of early-age green concrete with recycled nylon fiber fabric under an axial load," *Construction and Building Materials,* vol. 209, pp. 105-114, 2019.

CHAPTER 5

CHLORIDE ION PENETRABILITY IN MORTAR REINFORCED WITH RECYCLED FIBERS UNDER SEAWATER EXPOSURE BY EPMA

5.1 OUTLINE

This chapter studies the chloride ions penetrability of the mortar reinforced with recycled nylon (RN) short fibers from the used fishing nets and the manufactured polyethylene (PE) microfibers. Ordinary Portland cement (OPC) and the polymer cement mortar (PCM) mixes were introduced. OPC and PCM were mixed with RN and PE fibers, then exposed to seawater for the duration of 3 months (92 days) and 1 year (408 days). After that, spatial distribution of chloride ions in mortar were analyzed using electron probe microanalyzer (EPMA). Moreover, chloride ion profiles in different mix were plotted and the effective diffusion coefficients were then calculated using non-linear fitting.

5.2 THEORETICAL BACKGROUND OF EPMA

The electron probe micro analyzer (EPMA) is an instrument used for analyzing element composition. The electron beams irradiated onto the surface of substance so that the characteristic X-ray is emitted. EPMA can be used to perform element analysis, observation, and area analysis as large as 10 cm square. The application of EPMA appears in many fields such as steel, minerals, semiconductors, ceramics, textiles, medical and dental materials, medicine, and biology, as well as for application research and product quality management [1].

In concrete engineering EPMA is widely used for determining material transportation in cementitious material. It can be effectively used for the quantitative evaluation of chloride ions ingress into concrete. Spatial distribution of chloride ions in concrete can be evaluated, and the chloride ion profile can be constructed. It can also accurately estimate diffusion coefficient in concrete. The chloride ion concentrations obtained with EPMA were equivalent to that of obtained with conventional slicing and grinding methods [2]. In Japan, JSCE G574-2005 specifies test method for chemical element distribution in concrete using EPMA [3].

5.2.1 Configuration and mechanism of EPMA

Figure 5.1 shows typical configuration of EPMA. Current EPMA devices usually equip with 4 – 5 wavelength-dispersive spectroscopy (WDS) spectrometers for the simultaneous analysis of several elements. An electron probe emitted from the source is accelerated at a certain voltage under cavum and irradiated onto the surface of specimen. The characteristic X-ray spectrums corresponding to elements composting on surface are emitted and detected by WDS. By analyzing wavelength and the intensity of the characteristic X-ray, chemical composition of the sample can be quantified.

Mapping image of the element compositions and concentration of elements can be obtained by scanning the probe on specified area of the sample. In general, a specimen was fixed on the stage, and the stage is moved so that the electron probe irradiate on the designated point or area. Two methods are mainly used, a stage scan for a sample size in the order of 1cm, and the beam scan for the analysis area less than 100 μm. EPMA can perform area analysis with spatial resolution of 0.1 – 1 μm depending on the type of machine. The emitted x-ray intensities are counted by x-ray detectors which the concentration of elements is represented in the color band of the mapping image. Each analysis point represents one pixel of mapping image.

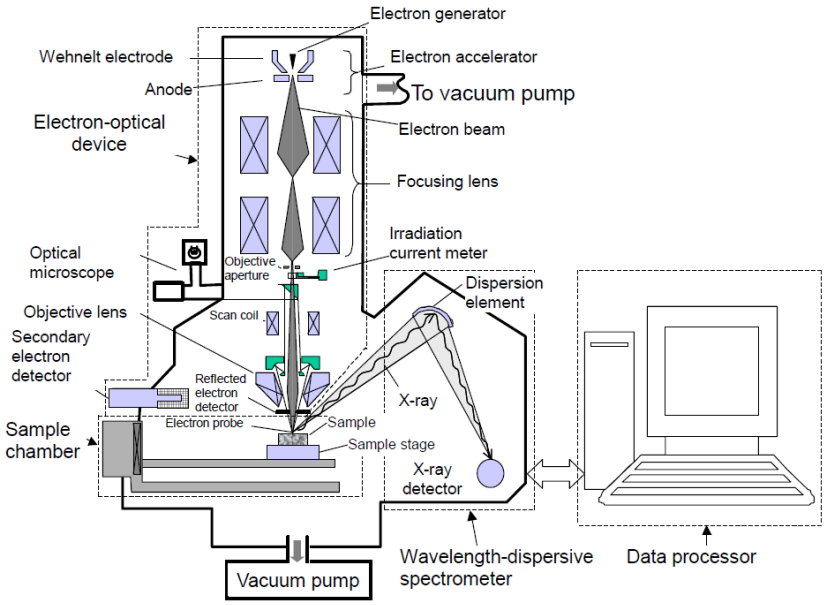

Figure 5.1 Configuration of EPMA.

5.2.2 Sample preparation

Preparation for the EPMA analysis of concrete sample usually undergo cutting and grinding process. When water is used for the cutting some water-soluble materials may leach out from the concrete lead to the inhomogeneous distribution [4]. Another consideration in sample preparation is that the resin impregnation. Concrete is a brittle and porous material, and it emits gases under high vacuum in the electron chamber. Therefore, homogeneous impregnation and the contamination of some elements in resin should be concerned. Especially when chloride in concrete is the target material, a chloride free epoxy should be used. Considering the ease of analysis, a sample size of 4 to 10 cm in width or length, and the thickness of 1 to 2 cm is recommended to prevent deformation from drying. However, it should be considered that bigger size of sample requires longer time to be vacuumed. In addition, the analysis face of the sample must be as parallel as possible as well as the four adjoining sides must be cut perpendicular to one another to ensure homogeneous detection ability of characteristic x-ray intensity.

5.2.3 Analysis of elements using EPMA

Target elements and analysis conditions should be decided before performing analysis. Elements associated with the cement hydration and material transportation in concrete such as Ca, Si, S, Na, and Cl are used. Analysis conditions are depending on the required data to be obtained from the analysis and the limitation of the sample such as accelerating voltage, probe diameter, probe current, characteristic x-ray wavelength and the type of dispersion element. Some of elements such as Na, K, Cl and S may damage by the electron probe irradiation and cause errors in the analysis, so analysis conditions should appropriately selected. JSCE-G574 specifies standard measurement conditions for the analysis of EPMA as shown in Table 5.1. It should be noted that values in table are recommend values, and the analysis conditions may be adjusted according to the analysis objective and characteristic of sample.

Table 5.1 Standard measurement conditions of area and point analysis using EPMA.

	Area analysis: Small area (cement paste and aggregate)	Area analysis: Large area (concrete and mortar sections)	Point analysis
Measuring range	0.4×0.4 to 4 × 4 mm	4×4 to 80×80 mm	Ø0.1-10 μm
Pixel size	0.1-10 μm	10-100 μm	-
Accelerating voltage	15 kVA		15 kVA
Probe current	10-50 nA	50-300 nA	5-50 nA
Probe diameter	0.1-10 μm	10-100 μm	0.1-10 μm
Unit measuring time	30-50 ms		10-20 s
Movement of analysis point	Movement of sample stage		Fixed
Number of pixels (analysis point)	200×200 to 800×800		-

Area analysis is performed by a moving of sample stage, and the sample is continuously scanned by keeping the position of the sample surface at the same height. Characteristic x-rays corresponding to the target element as well as x-ray intensity that emitting from the sample are detected and counted by the x-ray detector, respectively. X-ray intensity is then transferred to computer and converted into color band in the mapping image. Measurement location is changed by the movement of sample stage when the measurement finished. In general, the measurement time is set to be 30 ms with 0.1 mm interval between each point. Data obtained from the measurement consists of the position information and the x-ray intensity of the target elements in 0.1×0.1mm square of the sample surface. In the machine with multiple EDS, several characteristic x-rays and the x-ray intensity can be simultaneously measured.

In phase analysis of concrete, an attention should be paid on the contamination of data which is unavoidable. Since probe diameter (e.g. 0.1 mm) is bigger than the microstructure of concrete, it is possible that data from difference phases are mixing in the same measurement point. It was suggested by Mori and Yamada that point analysis is required because of reducing probe diameter causes excessively increment in total measuring point and measuring time which is no applicable in real practice [4]. In point analysis, designated points in analysis area can be picked and analyzed with higher resolution. In this case, graphical image is not obtained but phase analysis with high spatial resolution is possible.

5.2.4 Quantification methods

Element concentration obtained from the characteristic x-ray intensity can be calculated using several theories. The ratio method specified by JSCE converts characteristic x-ray intensity of the target sample based on the characteristic x-ray intensity and the element concentration obtained in the standard sample. This method assumes that the characteristic x-ray intensity of the target element in the sample is proportional to the element concentration in sample. However, this assumption is not valid when the chemical compositions in the standard sample and the target sample are very different [4]. In addition, different standard samples may cause scatter data in the quantification.

Another method that is more reliable is using calibration curve from the standard sample that have the same chemical composition similar to that of the target sample. If chloride is measured in cement paste, several cement paste samples which the chloride concentration is known from conventional slicing or

grinding methods are used for constructing calibration curve as shown in Figure 5.2. With this method all factors affecting characteristic x-ray intensity can be omitted.

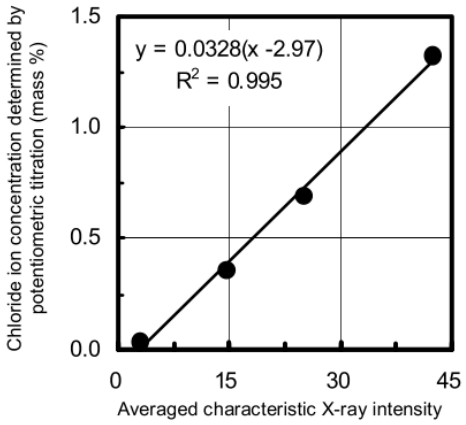

Figure 5.2 Example of calibration line (JSCE G574-2005).

5.3 EXPERIMENTAL PROGRAMS

5.3.1 Testing specimens

Mortar specimens having the dimension of 100 mm × 100 mm × 400 mm were prepared. Recycled nylon (RN) short fibers from used fishing nets and the manufactured polyethylene (PE) microfiber were mixed in ordinary Portland cement (OPC) mortar and polymer cement mortar (PCM). Mix design of OPC and PCM mixes are the same as that casted in chapter 4 (See section 4.2.1), and name and condition of test specimens are shown in Table 5.2. It should be noted that RN fiber used in this chapter is the same as that of RNa I Chapter 2 and 3. After 28 days of curing in water, prism specimens were cut into 4 cube specimens as shown in Figure 5.3, and the side and the bottom surfaces of cube specimen were coated with epoxy so that the specimen has only one expose surface. Cube specimens were then transported to exposure site.

Table 5.2 Name and condition of test specimens.

Name	Fiber	Fiber content (vol%)
OPC-NF	-	-
OPC-RN1.0%	RN	1.0
OPC-PE0.5%	PE	0.5
OPC-PE1.0%	PE	1.0
PCM-NF	-	-
PCM-RN1.0%	RN	1.0
PCM-PE1.0%	PE	1.0
PCM-PE2.0%	PE	2.0

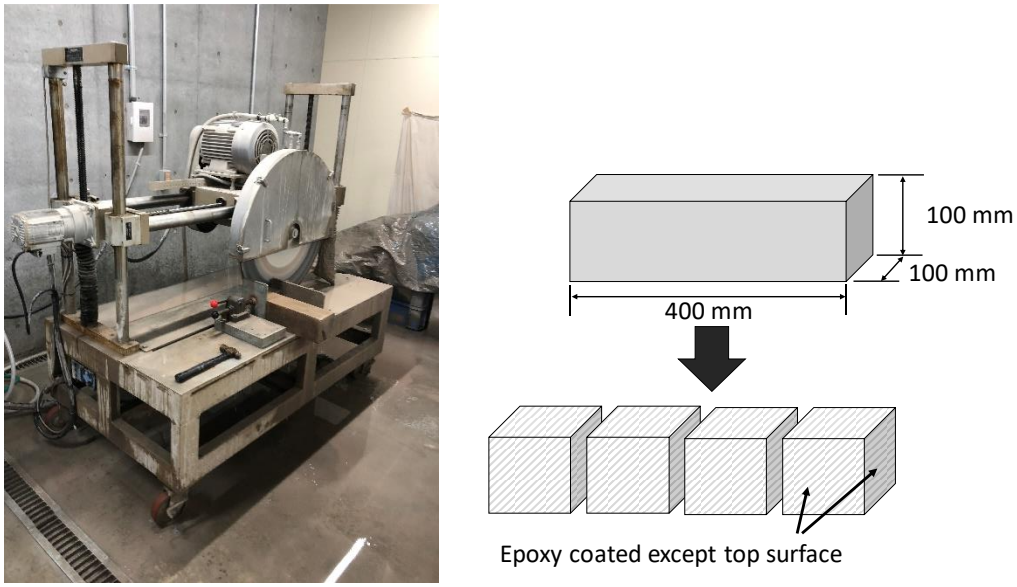

Figure 5.3 (Left) Automatic cutter and (right) cut specimens.

5.3.2 Seawater exposure

Cube specimens were sprayed with seawater for 2 times a day, 3 hours each, for the duration of 3 months (92 days) and 1 year (408 days). Figure 5.4 shows testing specimens at the exposure site.

Figure 5.4 Testing specimens at the exposure site.

5.3.3 EPMA analysis

After completing the exposure duration, specimens were cut using dry cutter, and the middle portion was taken. That middle portion was then cut again into 40 mm×40 mm square slice. Figure 5.5 shows preparation of EPMA sample. The prepared samples were impregnate with resin to prevent gases emission during the test and to prevent deformation under vacuum. In this study, a chloride-free polyester resin [5] is used for the impregnation. Specimens were attached onto glass plate then sliced into thin section having the thickness of 0.2 mm then coated again using same resin. Finally, carbon deposition was performed on the surface of the sample to improve conductivity of the sample during the test.

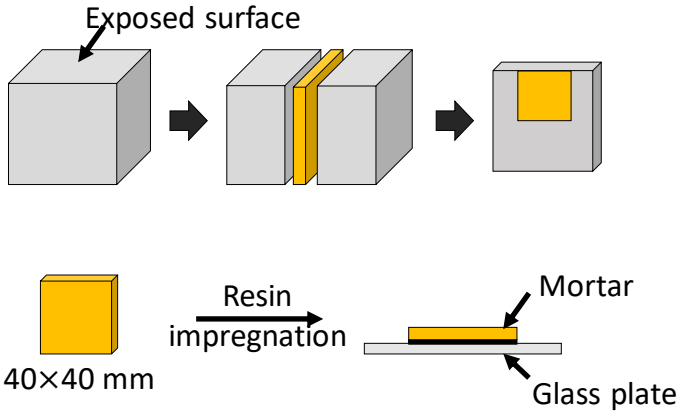

Figure 5.5 Specimen preparation for EPMA.

EPMA machine model JEOL JXA-8900R with 3 WDS spectrometers was used for analyzing spatial distribution of chloride ions in mortar. Figure 5.6 shows sample stage and the EPMA device. Analysis was performed following the JSCE G574-2005 [3] and the measurement conditions are shown in Table 5.3.

Figure 5.6 (Left) Testing sample on sample stage and (Right) EPMA device.

Table 5.3 Measuring conditions.

Measuring range	400×400 mm
Pixel size	100×100 mm
Accelerated voltage	15 kV
Probe current	100 nA
Probe diameter	50 μm
Unit measuring time	40ms
Number of pixels	400×400 pixels
Movement of analysis point	Movement of sample stage
Target elements	Cl, Ca, Si
Standard elements	Halite (Cl), Wallastonite (Ca, Si)
Total measuring time	Approximately 3 hours

5.4 RESULTS AND DISCUSSIONS

5.4.1 Spatial distribution of chloride ions

Figure 5.7 and Figure 5.8 show mapping image of spatial distribution of chloride ions from EPMA analysis of the test specimens having 3-months and 1-year of exposure, respectively. Top side is the exposed surface, and color bands represent characteristic x-ray intensity irradiated from the surface of test specimen. It is considered that characteristic x-ray intensity is equivalent to chloride ions concentration in the test sample; therefore, area that has high concentration of chloride ions is shown in green and yellow while the area that has relatively low chloride ion concentration is shown in blue or black. Each specimen has the size of 40 mm × 40 mm square except that the OPC-NF in Figure 5.7 (a) that has the size of 40 mm × 20 mm rectangle.

Chloride ion distribution of the 3-months exposure specimens were identical with the chloride penetration depth at about 1-2 cm from the surface. OPC-NF and OPC-PE1.0% seem to have higher chloride ion concentration near the surface, however the difference is negligible. The effect of fiber cannot be judged because the exposure time is too short so that the differences cannot be seen. Therefore, only OPC mixes were analyzed. High concentration spots (light-blue and green spots) were observed in and at the borders of the tested samples. It is possible that the epoxy coating has some chlorides and the contamination occurred. The coating was then changed to a chloride-free polyester resin as mentioned earlier in section 5.3.3.

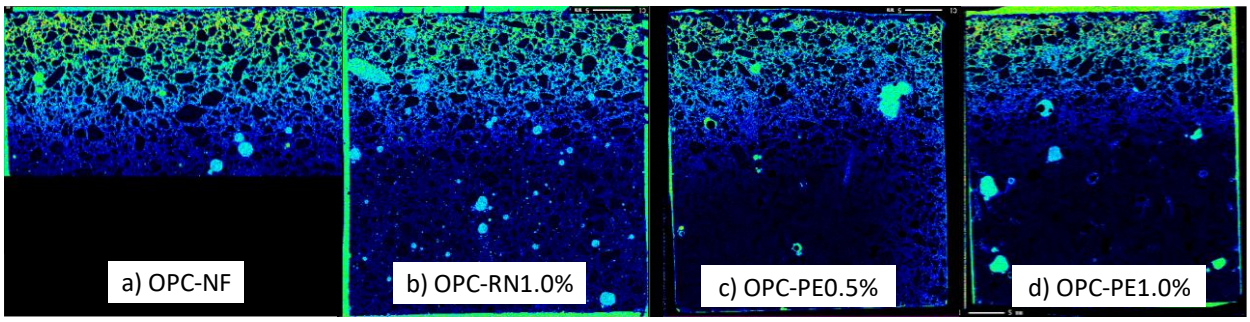

Figure 5.7 Spatial distribution of chloride ions of 3-months exposed specimens.

Spatial distribution of chloride ion in 1-year exposed specimens are shown in Figure 5.8. OPC specimens had the chloride ion distribution at approximately 3 cm from the surface while PCM mixes had less than 1 cm of chloride ion penetration. PCM showed extremely low chloride ion penetration due to low the water-to-binder ratio of 0.2 compared to OPC that has water-to-binder ratio of 0.5. Comparing between OPC-NF and OPC-RN1.0%, no difference of chloride ion distribution was found. Therefore, adding RN does not mitigate the chloride ion ingression. For the mix containing PE fiber, no noticeable difference in chloride ion distribution was observed. Changes in chloride ion distribution can be seen only from the difference mortar type (i.e. OPC mix or PCM mix). Based on the results, adding RN fiber does not change the chloride ion distribution.

It should be noted that OPC-PE0.5% and OPC-PE1.0% had lower chloride ion concentration compared to the OPC-NF and OPC-RN1.0. It is believed that this phenomenon resulted from errors during the sample preparation. It is possible that water was used for the cutting and grinding process and chloride ions were washed. It was suggested by Mori and Yamada [4] that when water is used for the grinding and cutting for excessively long time, it can cause non-homogeneous distribution of water soluble materials such as chloride; therefore, kerosene should be used for the grinding solvent. Even tough non-homogeneous distribution occurred in OPC-PE0.5% and OPC-PE1.0%, the relative trend between different mixes can be judge. It is concluded that adding fiber shows negligible effect to the chloride ion distribution regardless the RN or PE.

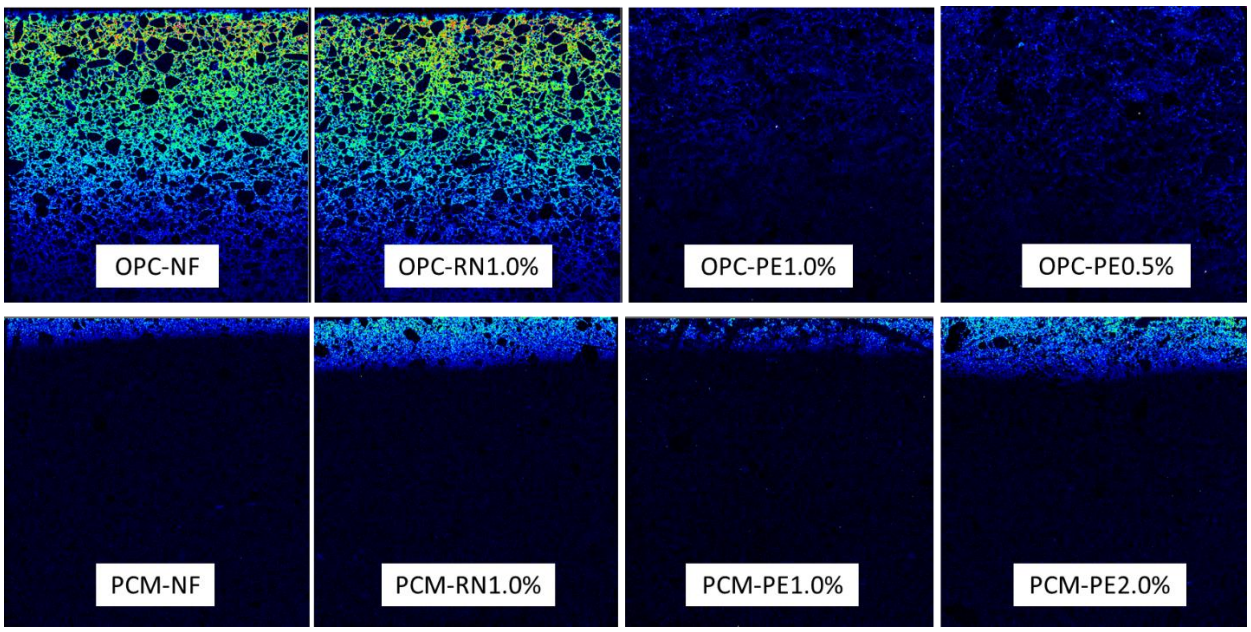

Figure 5.8 Spatial distribution of chloride ions of 1-year exposed specimens.

5.4.2 Chloride ion distribution near RN fiber

Mapping analysis of chloride ion distribution was performed in the area adjacent to the RN fiber. The probe size was set at 1 μm and the pixel size was set at 1 $\mu m \times 1$ μm with the probe current of 10 nA. Analysis was perform for the material distribution of Si, Ca, Cl simultaneously as shown in Figure 5.9 which RN fiber represents in a circular shape in the image. Based on the result, no accumulation of chloride ion was found near the interface between fiber and cement paste. Therefore, fiber interface does not provide a transportation channel for the chloride ions. Chloride ion concentrations were found mainly on the cement paste part. It is possible that the area of fiber is relatively small compared to the cement paste where chloride ion can penetrate. This might be the reason why there is no difference in chloride ion distribution between OPC-NF and OPC-RN1.0%

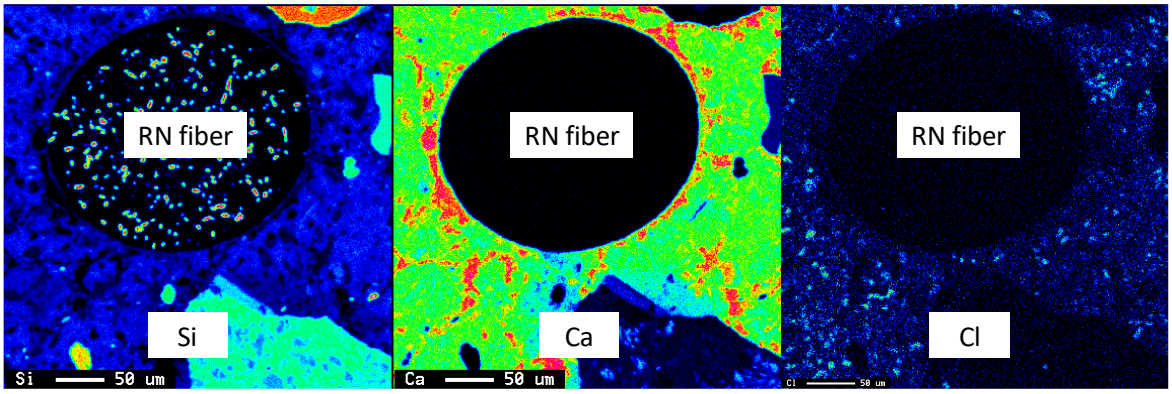

Figure 5.9 Mapping analysis of the area near RN fiber.

5.4.3 Chloride ion profile

X-ray intensity in each pixel of the image were averaged, and the x-ray intensity profile was constructed. Since the characteristic x-ray intensity is increased proportionally with the concentration of the chloride ion; therefore, chloride ions concentration profile can be constructed based on the x-ray intensity data. Each point in Figure 5.10 represents the averaged of characteristic x-ray intensity from 3800 data points in each of 0.1 mm depth from the surface. The effect of aggregate and mortar can be neglected when the when the averaged data are more than 750 points [2].

Chloride ion profile of the 3-months and 1-year exposed specimens are shown in Figure 5.10 and Figure 5.11 , respectively. Chloride penetration depth of OPC specimens having 3-months exposure were approximately 20 mm while the 1-year expose specimens showed approximately 30-40 mm depth as for the case of OPC-NF and OPC-RN1.0%. PCM specimens expressed extremely low chloride penetration depth at less than 10 mm. Results confirmed corresponding to the mapping analysis in section 5.4.1 that no observable difference in the chloride ion profile, and the effect of adding RN and PE fibers cannot be concluded.

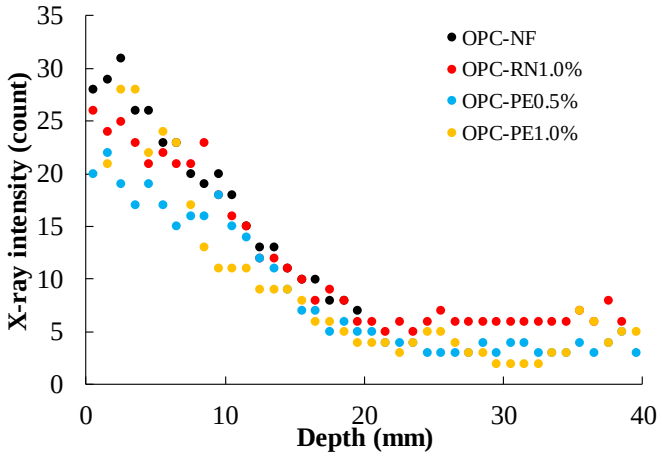

Figure 5.10 X-ray intensity profile of the 3-months exposed specimens.

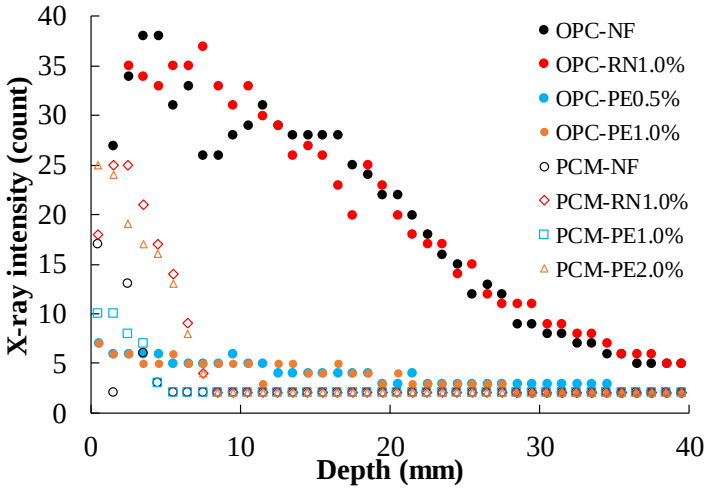

Figure 5.11 X-ray intensity profile of the 1-year exposed specimens.

5.4.4 Effective diffusion coefficient

The effective diffusion coefficient (apparent diffusion coefficient) of chloride ions was calculated based on x-ray intensity profiles obtained from EPMA. Although the calculated value does not represent the actual effective diffusion coefficient, the relative trend can be judged based on the x-ray intensity profile. The calculation was performed in accordance with JSCE G573 [6] by fitting the following equation:

$$C(x,t) - C_i = C_{0s}\left\{1 - erf\left(\frac{x}{2\sqrt{D_{ap}\cdot t}}\right)\right\}$$

Where, x: Depth from the exposed surface (cm)

t: Exposure time (year)

$C(x,t)$: Chloride content at depth x and the exposure time t

C_{0s}: Surface chloride content

C_i: Initial chloride content in cementitious mixture

D_{ap}: Apparent diffusion coefficient

erf: Error function described by:

$$erf(s) = \frac{2}{\sqrt{\pi}}\int_0^s e^{-\eta^2} d\eta$$

From the chloride ion concentration profiles in Figure 5.10 and Figure 5.11, x-ray intensity and depth from surface were defined as $C(x,t)$ and x, respectively. Non-linear fitting was performed by fixed C_i, and C_{0s} and D_{ap} are variables. C_i was chosen according to the lowest intensity found in each sample. It is assumed that the innermost part of sample was not affected from the chloride ion ingress by seawater, and it can be judged as the initial chloride content in the mixture. Some of regression points near exposed surface were omitted to reduce bias from the chloride ions that were washed away near the surface. Results from calculation are shown in Table 5.4 and the x-ray intensity profile with regression curves (shown as "Eqn") are shown in Figure 5.12 and Figure 5.13.

D_{ap} in the 3-months specimens were in the range of 1.9 – 2.0 cm^2/year except for the OPC-PE1.0% that had D_{ap} of 2.7 cm^2/year. OPC-RN1.0% and OPC-PE0.5% seems to have lower D_{ap} but the difference cannot be judged because of the short exposure duration.

For the case of 1-year exposure. OPC mixes had D_{ap} in the range of 1.6 – 3.0 cm^2/year while PCM mixes had the D_{ap} lower than 0.2 cm^2/year. OPC-NF showed the highest D_{ap} among all the OPC mixes at 3.0 cm^2/year. Adding RN and PE fibers seem to lower the D_{ap} value with the OPC-PE1.0% had lowest D_{ap} followed by OPC-PE0.5% and OPC-RN1.0%, respectively. The effect of adding fiber in PCM mixes still unclear. However, the effect adding fiber to the effective chloride ion coefficient cannot be concluded due to the error in OPC-PE0.5% and OPC-PE1.0%.

Table 5.4 Fitting results

Name	C_i	C_{0s}	D_{ap}	R^2
3-months exposure				
OPC-NF	5	49.04	2.036	0.98
OPC-RN1.0%	5	49.04	1.880	0.93
OPC-PE0.5%	3	52.35	1.909	0.97
OPC-PE1.0%	2	31.70	2.756	0.85
1-year exposure				
OPC-NF	2	37.70	3.024	0.89
OPC-RN1.0%	2	40.96	2.704	0.96
OPC-PE0.5%	2	4.50	2.018	0.92
OPC-PE1.0%	2	4.50	1.658	0.88
PCM-NF	2	13.65	0.038	0.67
PCM-RN1.0%	2	26.18	0.161	0.89
PCM-PE1.0%	2	10.44	0.057	0.94
PCM-PE2.0%	2	27.26	0.127	0.97

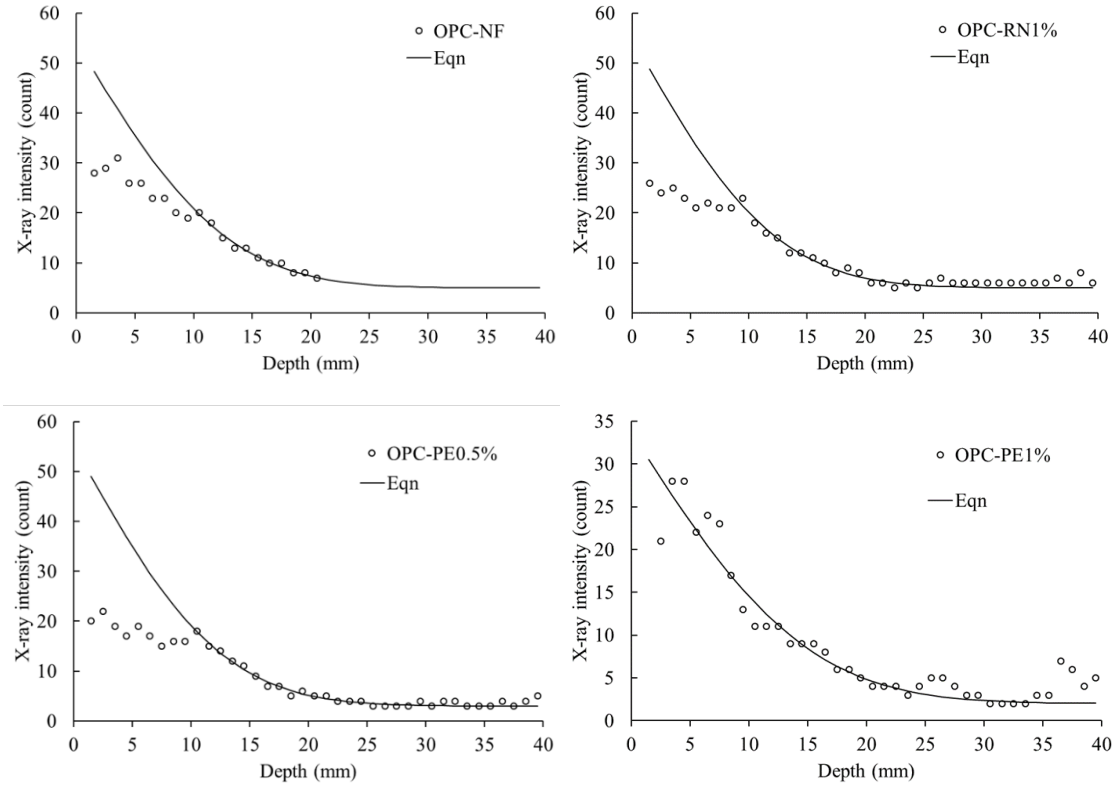

Figure 5.12 X-ray intensity profile with regression curve of 3-months exposed specimens

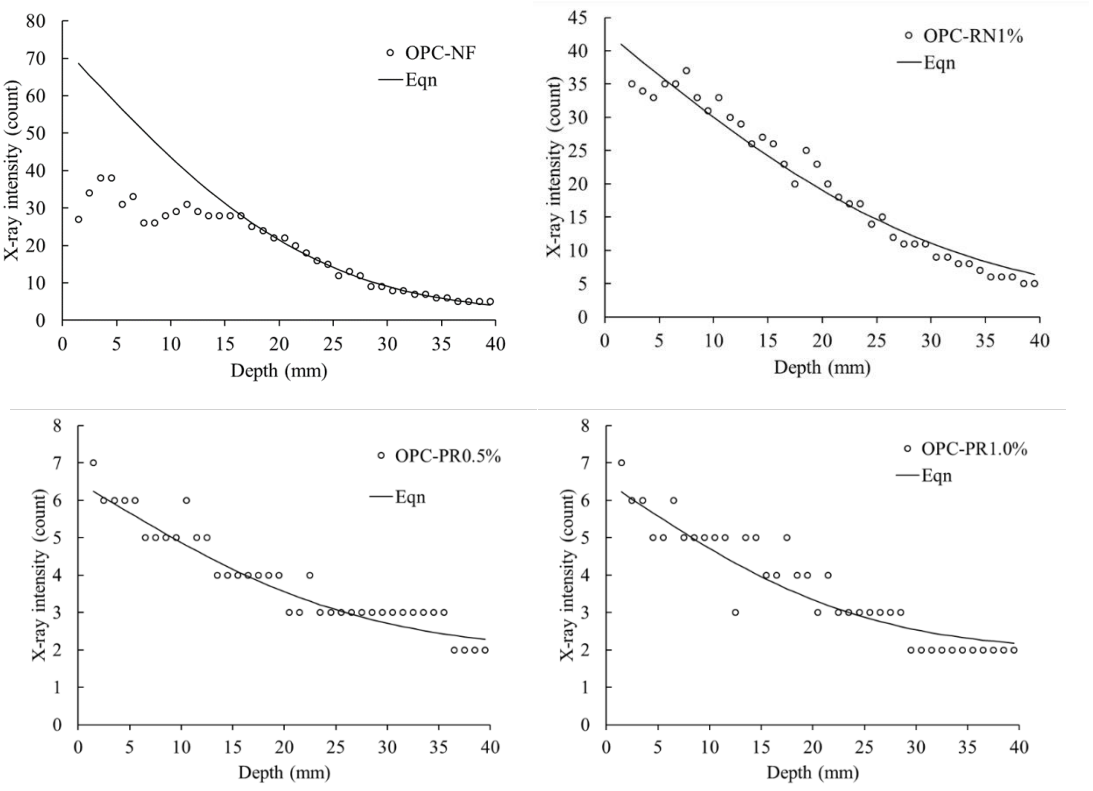

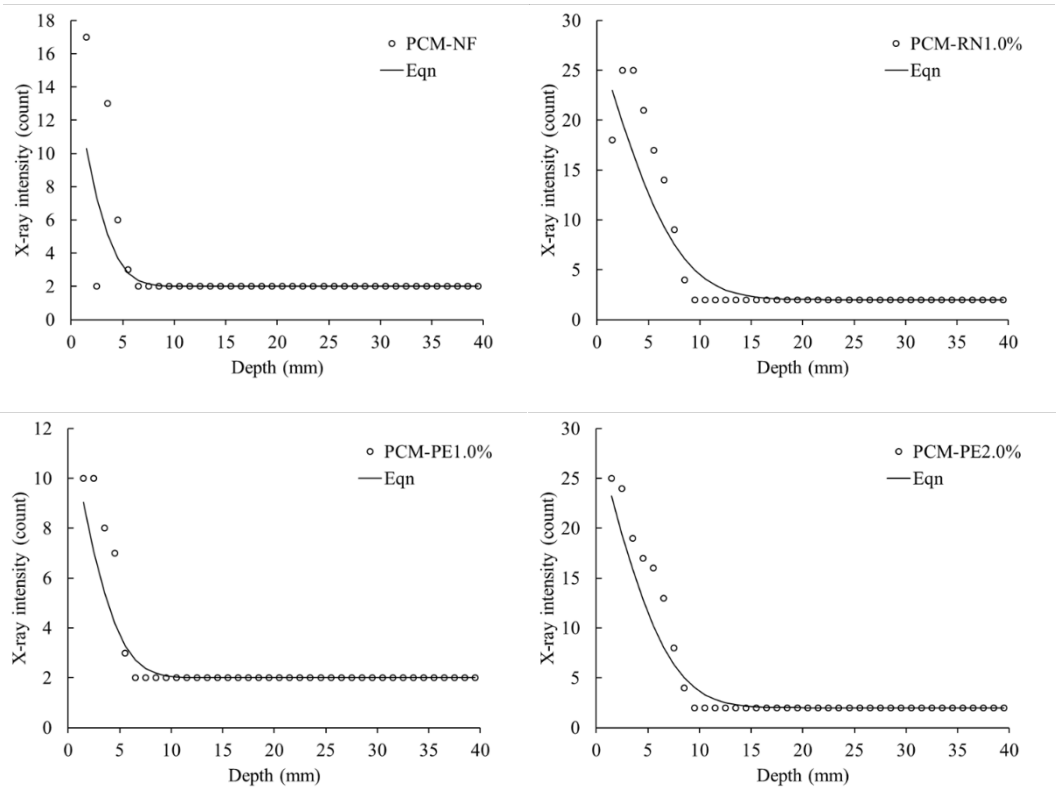

Figure 5.13 X-ray intensity profile with regression curve of 1-year exposed specimens

5.5 REFERENCES

[1] Electron Probe Micro Analyzer, JEOL, [Online]. Available: https://www.jeol.co.jp/en/science/epma.html. [Accessed 28 5 2020].

[2] D. Mori, K. Yamada, Y. Hosokawa and M. Yamamoto, "Applications of Electron Probe Microanalyzer for Measurement of Cl Concentration Profile in Concrete," *Journal of Advanced Concrete Technology,* vol. 4, no. 3, pp. 369-383, 2006.

[3] JSCE G574, “Test method for chemical element distribution in concrete using EPMA”, Japan Society of Civil Engineers, Tokyo, 2005.

[4] D. Mori and K. Yamada, "A Review of Recent Applications of EPMA to Evaluate the Durability of Concrete," *Journal of Advanced Concrete Technology,* vol. 5, no. 3, pp. 285-298, 2007.

[5] 5-1-3　ポリエステル樹脂･MMA 樹脂, マルトー, [Online]. Available: http://www.maruto.com/products/5-1-3/index.html. [Accessed 29 5 2020].

[6] JSCE G 573, “Measurement method for distribution of total chloride ion in concrete structure”, JSCE Guidelines for Concrete, Japan Society of Civil Engineers, Tokyo, 2005.

CHAPTER 6

CONCLUSIONS

6.1 OUTLINE

This chapter concludes the application of recycled nylon (RN) fibers from used fishing nets in mortar from the viewpoint of the repair application of corroded reinforced concrete (RC) beams using reinforced polymer cement mortar (PCM) and the long-term durability against chloride ion ingress. The study on the repair of corroded RC beams emphasizes on the restorability of flexural capacity of RC beams subjected to natural chloride ion ingress to induce steel corrosion. The long-term durability under chloride rich environment of the reinforced PCM used for repairing RC beams was investigated which focus on the resistibility of chloride ion ingress and spatial distribution of chloride ions. New findings from each chapter are concluded into 3 major perspectives which are mechanical properties of reinforced PCM, restorability of corroded RC beams using reinforced PCM, and durability against chloride ion ingress of the mortar reinforced with recycled fibers.

6.2 CONCLUSIONS

6.2.1 Mechanical properties of PCM specimen

PCM reinforced with RN fiber, manufactured polyvinyl alcohol (PVA) fiber and manufactured polyethylene (PE) fibers were used for the repair of corroded RC beams. Mechanical properties of reinforced PCM were studied, for instance, flowability of fresh PCM, compressive and flexural strength of reinforced PCM and the failure behavior. Following conclusions were drawn:

1. The addition of RN does not have adverse effect to the flowability of fresh PCM. However, the addition of PE fiber results in a reduction of flowability of PCM up to 23.7% due to the geometry and surface property of PE fiber.

2. Neither adding RN fibers nor using larger diameter of RN fiber contribute to the improvement in compressive strength but rather diminish the flexural strength of mortar. Adding fibers regardless the fiber type does not show clear influence on the compressive strength; however, flexural strength of PCM seem to be reduced except for the case of PE fiber.

3. The addition of RN short fiber does not contribute to the post-peak load due to the weak bonding between fiber and mortar; however, RN fiber help prevent abrupt failure of the beams. On the contrary, the addition of PVA and PE fibers enables the PCM to sustain more flexural loads after the peak. PCM-PVA retains a stable post-peak load of approximately 23% of the yield load. Adding PE fiber leads to an increase in the load after the yield point.

4. Adding RN fiber as well as PVA and PE fibers help preventing sudden collapse of the structure after the failure. The damage to the structure was disperse from wide crack into many small cracks with the addition of PE fibers.

6.2.2 Restorability of corroded RC beams using PCM reinforced with fibers

Experimental study on recycled fiber reinforced mortar for the repair of corroded RC beams reveals that recycled nylon fibers from used fishing nets have great potential for the effective repair and upgrading RC structures. RN fiber shows performance comparable to the manufactured PVA and PE. As such, application of recycled nylon fiber for civil engineering is a possible way of utilizing waste fishing nets. From this study, the following points were drawn:

1. RN, PVA and PE fibers can be used as a reinforcement material for the repair of lightly corroded RC beams. Spraying PCM reinforced with those fibers can compensate the flexural

capacity that deteriorated due to the corrosion of tensile rebar. The effectiveness of the RN fibers is comparable to PVA fibers but still inferior to that of PE fibers.

2. RN fiber helps distributing stresses throughout the beam under the bending load. Short fibers such as RN fiber and PVA fiber help transfer stresses through wide cracks and spreads the cracks toward the support of the beams. Microfibers such as PE fiber prevents severe damage of the beams by distributing damage from a wide crack to many small cracks.
3. Adding RN fibers in PCM reduces the rate of crack openings the RC beams. The beams that were repaired with PCM-PE exhibit the lowest crack opening and the rate of crack openings, followed by PCM-RN.
4. Spraying PCM can enhance the durability of the RC beams because PCM has very low chloride ion penetrability.
5. RN fibers are stable under high alkalinity of cementitious material with no visible sign of deterioration to the fiber; however, the smooth surface of RN fibers may cause poor bonding between fiber and cement substrate.

6.2.3 Long-term durability against chloride ion ingress

The addition of RN fiber and PE fibers in cement mortar reveals interesting behavior on durability and mechanical behaviors. The addition of RN fiber shows sign of improvement in durability against chloride ion ingress; however, special attention should be paid on the negative effect of adding fibers. Based on the experimental studies, following conclusion were drawn:

1. Adding RN fibers in mortar seems to improve the chloride ion resistivity based on the chloride migration test, but the tendency is still unclear. The type of mortar mix (e.g. OPC or PCM) and water-to-binder ratio are still dominant factors to govern the effective diffusion coefficient of mortar.
2. Adding RN fibers slightly decrease the flowability of fresh mortar and the effect may negligible. On contrary, adding PE fiber considerably reduces flowability of mortar for both OPC and PCM mixes, especially at higher fiber content.
3. Compressive strength of OPC increases with the addition of RN fiber but decreases with the addition of PE fibers. For the PCM mix, compressive strength improves with the addition of PE fibers instead of RN fibers.
4. Adding RN fiber improves ductility and integrity of mortar during load application, and fibers prevent spalling of mortar after the failure.
5. Based on EPMA analysis, adding fiber does not show noticeable effect to the chloride ion distribution in mortar. Changes in chloride ion distribution and the chloride penetration depth between different types of fiber and fiber contents cannot be judged.

6.3 FUTURE POTENTIALS AND RECOMMENDATIONS

Recycled nylon fibers from used fishing nets has been proven its potential in reinforcing cementitious materials with a comparable effectiveness to manufactured fibers. Based on the experimental results obtained from this research, further studies can be made to extend understanding and limits of using recycled fibers. The application of recycled fiber reinforced mortar gives advantage to concrete structure such as improvement in flexural capacity, stress transfer, integrity and ductility. However, adding fiber also has adverse effects such as reduction in flowability and compressive strength. Such trade-off between advantages and drawbacks should be carefully considered.

The study on the repair application of corroded RC beams confirms that RN fiber helps transferring stress through wide cracks while PE fiber promotes stress distribution and improve integrity of the structure. Combination of two fibers is possible to combine benefits from both fibers. The repair using reinforced PCM may extend to a moderate and heavily corroded RC beams. Prediction model on the

bending behavior of the fiber reinforced concrete can be made to optimize the strengthening performance.

Detail studies may conduct on the bond strength and rupture mechanics of the fibers in mortar. Bonding between fibers and cement substrate is the main factors for providing additional strength to structure. Since RN fiber is hydrophilic material, bond strength mainly comes from the surface friction during the pull-out. Whether improve physical or chemical bonding are necessary to increase efficiency of the reinforcement. Moreover, various kinds of fishing nets can be applied such as twisted bundle fishing nets or PE type fishing nets.

EPMA analysis is a powerful measurement method for evaluating material transportation in cementitious materials such as chloride ion. However, sample preparation can be time consumed and costly. A chloride free epoxy coating should be used for coating and impregnation of sample. In addition, water should not be used for the cutting and grinding of sample since it caused uneven distribution of Cl during the analysis. Size and thickness of the specimen are factors affect to the measurement time because thick sample require longer time for the vacuum. Further investigations are needed on the factors relating to long-term durability such as permeability and pore structure in mortar.

Finally, for RN fibers, pre-treatment and quality control of the recycled fibers should be developed. At the experimental scale, RN fibers were prepared by manually cut by hand, which is time consumed and not suitable for real applications. Processing machines need to be developed for mass production of RN fibers. Pre-treatment of fiber is also necessary to improve bond between fibers and the cement substrate. Based on mechanical properties and durability of the reinforced mortar, lifecycle cost of the reinforced structures using recycled fibers can be estimated for selecting suitable strengthening and repair procedure.